Geometric continuity for surfaces and scalar fields

Ahmed Blidia

UNIVERSITÉ CÔTE D'AZUR

ÉCOLE DOCTORALE
SCIENCES FONDAMENTALES ET APPLIQUÉES

THÈSE DE DOCTORAT

Continuité Géométrique pour les surfaces et les champs scalaires

Ahmed Blidia

AROMATH, INRIA Sophia-Antipolis Méditerranée

Présentée en vue de l'obtention du grade de docteur en Mathématiques Appliqués d'Université Côte d'Azur
Dirigée par : Bernard Mourrain
Soutenue le : 08/04/2020

Devant le jury, composé de :
Stefanie Hahmann, Professeur, INRIA – Laboratoire Jean Kuntzmann,
Chandrajit Bajaj, Professeur, Oden Institute of Computational Engineering and Sciences,
Abdelghani Zeghib, Professeur, Ecole Normale Supérieure de Lyon,
Ioannis Z. EMIRIS, Professeur, National Kapodistrian University of Athens,
Boniface Nkonga, Professeur, Université de Nice Sophia-Antipolis,
Nelly Villamizar, Maître de conferences, Université de Swansea,
Bernard Mourrain, Directeur de recherche, INRIA Sophia Antipolis Méditerranée,

Marie Skłodowska-Curie Actions
ARCADES

Résumé

Dans les systèmes de CAO, une fonction polynomiale par morceaux se trouve derrière toute représentation de courbe, de surface ou de champ scalaire. Ainsi, il est important d'analyser les propriétés des espaces des fonctions polynomiales par morceaux. Dans cette thèse, nous étudions des outils d'algèbre commutative qui peuvent être utilisés pour analyser la dimension d'espaces polynomiaux par morceaux et pour en construire des bases. Nous testons les méthodes que nous produisons pour modéliser des surfaces de forme libre et pour des calculs d'analyse numérique.

La principale motivation du concept de continuité géométrique est la construction de surfaces multi-patchs et de champs scalaires. Le principal défi dans ce type de surfaces est de gérer les zones de la surface autour des sommets avec un certain nombre de patchs voisins différents de 4 (que nous appelons sommets extraordinaires). Dans ces régions, les méthodes de collage habituelles provoqueront l'apparition de singularités. La continuité géométrique est un moyen spécial de coller deux patchs de surface 3D le long de leur bord commun dans une surface multi-patchs, et qui produit des surfaces lisses même autour de sommets extraordinaires.

La condition de collage de continuité géométrique est exprimée en termes de relations linéaires entre les paramétrisations des surfaces le long des bords de jonction. Les coefficients de ces relations sont appelés les données de collage, et le choix est crucial pour la régularité de la surface résultante. Les données de collage que nous proposons sont des fonctions splines qui respectent la contrainte de lissage telle que la contrainte d'enceinte de sommet. Nous expliquons notre choix en fournissant une formule que les données de collage doivent respecter à chaque sommet extraordinaire.

Nous exigeons que la spline géométriquement continue (Nous appelons Gsplines les splines géométriquement continues) que nous produisons pour pouvoir interpoler n'importe quelle position donnée des sommets de son maillage correspondant. C'est ce que nous appelons la condition de séparabilité. Nous décrivons les conditions sur les données de collage qui permettent à l'espace d'être séparable, et donnons une liste d'exemples de telles données de collage. Le manuscrit décrit également un «schéma d'assemblage» qui permet de produire une base pour l'espace des Gsplines.

Nous avons abordé la possibilité d'étendre les méthodes d'homologie existantes pour analyser la dimension de l'espace spline avec des conditions de continuité géométrique. Ces extensions fournissent de nombreuses formules qui expriment les dimensions de nos espaces splines au moyen d'autres groupes d'homologie.

Notre analyse de cet espace conduit à trois applications: La première est un algorithme qui, étant donné un maillage, produit une surface lisse qui s'en rapproche. Cet algorithme est basé sur la projection de la surface approximative catmull-clark sur l'espace des splines que nous produisons. Les deux autres tests portent sur la reconstruction de surfaces lisses et l'analyse IsoGeoemtric.

Abstract

In CAD systems, a piecewise polynomial function is behind any curve, surface or scalar field representation. Thus, it is important to analyse the properties of the spaces of piecewise polynomial functions. In this thesis, we study commutative algebra tools that can be used to analyze the dimension of piecewise polynomial spaces, and to construct bases for them. We test the methods that we produce to model free form surfaces and for numerical analysis computations. The main motivation for the concept of geometric continuity is the construction of multi-patches surfaces and scalar fields. The main challenge in this kind of surfaces is to handle areas of the surface around vertices with a number of neighboring patches different from 4 (that we call Extraordinary vertices). In this regions, the usual gluing methods will cause the appearance of singularities. Geometric continuity is a special way to glue two 3d surface patches along their common edge in a multi-patch surface, and that produces smooth surfaces even around extraordinary vertices.

The geometric continuity gluing condition is expressed in terms of linear relations between the parametrizations of the surfaces along there junction edges. The coefficients of those relations are called the gluing data, and there choice is crucial for the smoothness of the resulting surface. The gluing data that we propose are spline functions that respect smoothness constraint such as the vertex enclosure constraint. We explain our choice by providing a formula that the gluing data have to respect at each extraordinary vertex.

We require that the Geometrically continuous spline(We call Gsplines the Geometrically continuous splines) spaces that we produce to be able to interpolate any given positions of the vertices of its corresponding mesh. This is what we call the separability condition. We describe conditions on the gluing data that allows the space to be separable, and give a list of examples of such a gluing data. The manuscript also describe a "piecing scheme" that allows to produce basis for the space of Gsplines.

We have addressed the possibility of extending the existing homology methods to analyse the dimension of spline space with geometric continuity conditions. These extensions provide many formulas that expresses the dimensions of our spline spaces by means of other homology groups.

Our analyse of this space leads to three applications: The first one is an algorithm that given a mesh, produces a smooth surface that approximates it. This algorithm is based on the projection of the Approximate catmull-clark surface on the space of splines that we produce. The two other tests are on smooth surfaces reconstruction and IsoGeometric analysis.

Acknowledgement

I would like to thank and express my sincere gratitude to my advisor Pr. Bernard Mourrain for his interest in my work and his encouragement during my project. His guidance and his immense knowledge helped me to elaborate my research and prepare this thesis. He is an example of seriousness and mastery of work. Without him I would not have done this work.

I would like also to thank all members of my thesis comity for reading my thesis and for all their valuable comments and questions.

I benefited from speaking with many professors from my field, especially thanks to the Nelly Villamizar for her continuous interest and valuable advices.

My thanks go to all the members of the ARCADES network, students and professors with who I have had great experiences.

Many people have influenced my mathematical career, I would like to thanks my high school teacher Belkacem Benmbarek. Many thanks to professor Zeghib Abdelghani for his enormous efforts toward us.

Last but not the least, I would like to thank my Parents, Hadia, Ikram, Abdelhamid and all members of my family for all what they have done for me. Their presence and their affection have always helped me overcome difficulties. I express to them a lot of appreciation with love. I am grateful to my friends Hassan, Mohamed, Khlifa, Mehdi and Khaled for their moral support.

Contents

Chapter 1

Introduction

In CAD systems, a piecewise polynomial function is behind any curve, surface, or scalar field representation. Thus, it is important to analyse the properties of the spaces of piecewise polynomial functions. In this thesis, we study commutative algebra tools that can be used to analyse the dimension of piecewise polynomial spaces, and to construct bases for them. We particularly focus on the concept of geometric continuity, by adapting to it the homological techniques used before in parametric continuity.

1 Presentation

1.1 Spline spaces

Standard CAD framework proposes to use piecewise polynomial functions to model smooth surfaces and scalar fields. We do that by choosing a subdivision of a polygonal region of the plane and define a basis for the space of piecewise polynomial functions defined over it, that have a fixed maximal degree, and a fixed minimal order of regularity. This is what we call the space of bivariate splines.

One of the most commonly used models are the tensor product splines, that are defined over a rectangular domain of the plane, subdivided using horizontal and vertical lines through that rectangle, with the possibility of reducing the regularity of the space functions along those lines. A special instance of this basis is the Bézier-Bernstein [1] tensor product functions that form a basis for the space of polynomials with fixed maximal degree. More generally, tensor product bsplines form a basis for the space of piecewise polynomials with respect to the chosen subdivision of the plane using horizontal and vertical lines, with a fixed maximal degree, and minimal regularity.

Thanks to the good properties of these functions, one can model efficiently any surface that is diffeomorphic to a region from the plan. In CAD software, a 3d spline surface is controlled using points that corresponds to the coefficients

[1] The polynomials $\binom{n}{i} x^i (1-x)^{n-i}$ are called Bézier-Bernstein polynomials. Indeed, these polynomials have been used the first time to prove the Weierstass theorem by Sergei Natanovich Bernstein [1]. Then Forrest showed that the Bézier curves, who where initially defined as the intersection of two elliptical cylinders, can be expressed using Bernstein polynomials [2].

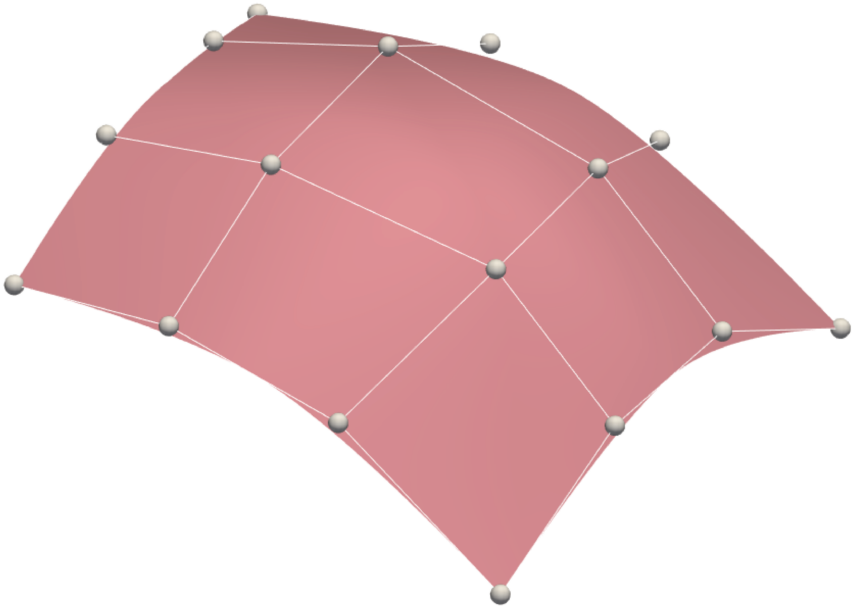

Figure 1.1: Bézier surface with appearing control points

of the surface in the chosen spline basis (See Fig. 1.1). One good property of the tensor product bspline basis functions is the positivity over their domain of definition, so the surface lies on the convex hull of its control points [3].

Many studies analyse spline spaces, by counting their dimension, and producing bases for them. Preferred bases are those which elements have high regularity, positive values and local supports. High degree polynomials will slow down the evaluating process. This make the splines space unusable for instance in interactive applications. In the same time, low degree polynomials provide less degrees of freedom on the surfaces, that makes the space less efficient in interpolation. The tradeoff can also move towards reducing regularity by adding more subdivisions. This corresponds in tensor product bsplines to "knots insertion". Regularity defect can be recovered, by imposing "fairness" constrained on the splines during the modelling process.

In [4], Gilbert Strang mentioned for the first time the question: Given a triangulation of the plane, a fixed maximal polynomial degree and a fixed minimal regularity, what is the dimension of the corresponding space of spline functions?

Since then, many works on counting the dimension of this space have appeared. Some of the works describe explicitly the degrees of freedom, by describing explicitly a minimal determining set (see Section 6 of Chapter 2 for the definition of determining set) using barycentric coordinates polynomials representations (eg. [5, 6]). This approach allows to provide general formulas for the dimension of the space of splines over simplicial complexes. But this formulas are not all ways valid for low polynomial degree space of splines.

Other works study the space of splines as an $\mathbb{R}$-module using homological tools (eg. [7, 8]). This approach is able to provide general dimension formulas for spline spaces over polyhedral complexes. This formulas are valid only for a polynomial degree that is enough large. In the other hand, the homological approach allows us to understand that the dimension in low polynomial degree depend on

the geometry of the complex. It can even give some dimension formulas that are valid for any polynomial degree, but only for particular geometries.

1.2 Surfaces with complex topologies

CAD models have often complex topologies and require the use of more than a single spline patch. Nowdays, CAD software offer the possibility of creating multi-patch surfaces with useful properties that are suitable for applications in architecture, computer aided manufacturing, medical animation, game development tools, surface reconstruction...

State of the art includes many models generation processes with different input/output. We mention for instance: algorithms that interpolate the vertices of a given mesh [9, 10], algorithms for interpolating a network of curves (eg. [11, 12]), algorithms for reproducing a surface given a sampling cloud of points of it [13, 14].

Subdivision surfaces

A subdivision scheme is an iterative algorithm that can be applied to a coarse mesh with complex topology and that converges "at infinity" to a C^0, C^1 or higher regularity surface, depending on some parameters of the scheme. The resulting surface is called a subdivision surface.

One goal of studying the subdivision surfaces is to analyse the behaviour of the surface around extraordinary vertices (EVs)[2]. We know for instance that for a regular meshes (ie. meshes without EVs), the Catmull-Clark surface is a standard b-spline surface continuous in tangent and curvature[15]. If the mesh contains an EV, then a subdivision surface can be represented locally using an infinite number of b-spline patches. In the other hand, the degree of smoothness around an EV of a subdivision surface is related to the values of the eigenvalues of the subdivision matrix[16].

The algorithm in [17] combines fast contract subdivision algorithms with Geometric continuity around EV. This allows have a finite number of patches around an EV, and good smoothness properties in the same time.

Multi-patch 3d shapes

Our manuscript studies multi-patches surfaces and scalar fields with smoothness conditions along the junctions between the spline patches. A major bottleneck in multi-patch constructions is to find an efficient way to stitch patches around an EV. For instance gluing 5 Bézier surfaces around a single vertex by using standard junctions [3] will enforce all the partial derivatives at the vertex to vanish (see Chapter 3), and thus will produce a cuspidal singularity.

Several constructions are used to solve this problem, for instance T-splines are NURBS [18] surfaces with an extra row of control points that doesn't traverse

[2] An extraordinary vertex is an internal vertex with a number of neighbouring patches different from 4, or a boundary vertex with a number of neighbouring patches different from 2

[3] Equality along any junction edge of the partial derivative of the two neighbouring patches

the entire surface. This allows us to have local refinement around extraordinary vertices.

In this thesis we focus on the Geometric continuity for multi-patches surfaces and scalar fields. It is a special way to glue two patches along their common edge in a multi-patch surface, that produces smooth surfaces around EV. In G^k-junction (Geometrically continuous junction of order k), the two glued patches have the same partial derivatives of order at most k along the junction edges after a smooth change of coordinates. More intuitively, in the G^1-junction case, the partial derivatives of the two glued patches are enforced to be coplanar, and thus will generate the same tangent space to the surface along the gluing edge. The standard gluing between patches is different since it requires that the partial derivatives are exactly the same [4]. Using this approach we will create a special space of splines that we call Gsplines of order G^k that is used to parametrise smooth surface and define smooth scalar fields on them.

1.3 Splines for Isogeometric analysis

Finite element method (FEM) is a numerical method that is used to find approximate solutions for linear differential equations over physical domains. Spline spaces are often used to represent these approximate solutions. The more regular are the spline, the more accurate is the solution.

In the early stage, the physical domains in FEM were approximated using polygonal geometries. The use of inaccurate domain representations necessarily induce errors on FEM solutions. Although geometry processing systems are able to improve the representations by a remeshing process, the computational cost is relatively high. Isogeometric Analysis (IgA) was created to address this shortage. The idea of IgA is to use the same spline space to parametrise the physical domain and to represent the PDE solution, and thus, the error of domain approximation is eliminated [19].

G^k-spline spaces offers an advantage in that context. Indeed, if the test functions and the surface parametrisations are from the same G^k- splines space, then the composition of the first with the inverse of the second is a C^k-function [20].

2 Overview

The goal of the thesis is to explore commutative algebra techniques that can be used to analyse the Gspline space by counting its dimension and describing a basis for it.

We start this manuscript by a chapter on computing the dimension of spline spaces. In this chapter, we consider only parametric continuity. Most of the techniques that we mention are based on the homology theory.

In the third Chapter we define the geometric continuity and give an example of basis construction based on the Syzygies modules μ-basis. Indeed, the construction of a G^1-spline basis requires first to determine the degrees of freedom of simple topologies composed of only two patches. The G^1 gluing conditions

[4] We call the space of splines with standard gluing the "parametric splines space"

in that case (see equation (3.4)) are given by a syzygy equation of a module. It has been proposed in [21] to use that fact to determine all the possible degrees of freedom of the G^1-spline space that can be generated. The method described in [21] is applicable only for G^1-splines with polynomial elements. We show in this manuscript how to generalise this method for bspline patches with knots. In particular, we define exact sequences that allows to compute the dimension of a Syzygy module over the ring of piecewise polynomial functions, and show how to compute a basis of it as a vector space.

Next we describe a general new piecing scheme for generating G^1-splines over quad meshes. Compared with other piecing schemes such as [22, 23] which extract the gluing data from an existing bilinear parametrisation, our scheme use predefined gluing data that depend only on the topology of the mesh. We use this algorithm to produce base for many gluing data fun. They will be tested on solving fitting problems and IgA in chapter 5.

In Sections 8 and 9 of Chapter 3 we give a new algebraic characterisation of a G^k-junction. Based on that characterisation we provide several homological constructions that lead to define the space of G^k-splines as a homology space of an chain complex as in (3.45), or a term of an exact sequence as in (3.50). This allows to express the dimension of the space of G^k splines in terms of dimension of other spaces.

In the Fourth chapter, we give an example of how to construct a multi-patch 3d shape that approximate a given mesh, this is what we call a mesh smoothing algorithm. We explain in particular the vertex enclosure problem. One way of looking at this problem is to write the constraints of the G^k-junctions in terms of the bspline coefficient of the patches. This generates a series of equations for each junction. When the system is solved for each edge apart, some bspline coefficients may interfer in the equations of two different junctions, and induce overlaping of solutions. This happens for instance with the first layer of coefficients around a vertex in the G^1 constrains. This kind of overlapping makes it impossible to solve the constraints of each junctions independently of the other, and makes it necessary to consider a new order while resolving the G^1-constrains. In the G^1-junction case, we do that by regrouping together all the equations that include the bspline coefficients of the first layer around a given vertex in the same system. This system will be called the vertex enclosure system. Most of the Gspline multi-patches shapes generators start by solving this vertex enclosure system at each vertex and then move to the others equations. The algorithm we are proposing in the fourth chapter follows the same scheme, and the resulting surface will be an approximation of the Catmull-Clark surface. The scheme that we present is described using explicit formulas for the bsplines coefficients that determine the final G^1-surface.

The same smoothing scheme can be used also to generate basis for a space of G^1-splines as we will see in Section 3.3 of the Chapter 4. More precisely, we fix the topology of the mesh, then we apply the smoothing scheme to the canonical base of the space of one dimensional meshes of the same topology as the initial one. The resulting set of splines will span a space of splines that is suitable for fitting. We have tested that base for a medical data fitting in lung model reconstruction (Chap. 5).

In the Chapter 5 we test the Gspline basis constructions in data fitting and IgA problems. We test in the first section of Chapter 5 a method of 3d smooth surface reconstruction, based on the G^1-spline basis that we have constructed. The input is a cloud of points with their normals, and the output is a smooth surface representing the initial surface. The method is performed in two main steps. First we apply a marching Triangles algorithm to produce a mesh that approximates the cloud. We have chosen the algorithm [24] to do that. Then a simplification process is applied to generate a quad mesh with less number of patches by combining the Catmull-Clark subdivision and a progressive edge collapse decimation algorithm. The second step is the regression step, where we minimise a quadratic expression using a least squares method. The expression is composed of a distance term and a fairness term that minimises the value of the partial derivatives. Multiple basis are tested in that section, and a comparison between some of them is given.

In the second part of the application chapter, we test a bi-quintic basis in IgA computations.

Chapter 2

Computing the dimension of the space of splines

1 Parametric Splines

In this chapter we explain the homology tools used to compute the dimension of the spline space. We begin by giving basic definitions.

Let Δ be a polyhedral complex in the euclidean space of dimension d, this means that there is a region Ω from that space and Δ is a subdivision of it using polyhedrons. The polyhedrons of Δ are called maximal faces or the set of faces of dimension d, the vertices of Δ are called the minimal faces or the faces of dimension 0, any sub face of a polyhedron from Δ who's linear span is of dimension k is called a k dimension sub face of Δ. We will denote by:

- Δ_k the set of sub faces of dimension k.
- we denote by $\overset{\circ}{\Delta}_k \subset \Delta_k$ the set of k-dimensional internal faces, ie. the faces $\sigma \in \Delta_k$ such that $\sigma \not\subset \partial\Delta$.
- By $\mathcal{S}(\Delta)$ the space of splines over Δ. In other words, $\mathcal{S}(\Delta)$ is the set of real functions who's restriction to any polyhedron of Δ is polynomial.
- $\mathcal{S}(\Delta)_{\leqslant m} := \{f \in \mathcal{S}(\Delta) | \text{degree}(f_{|\sigma}) \leqslant m \text{ for any } \sigma \in \Delta_d\}$
- $\mathcal{S}(\Delta)_m := \{f \in \mathcal{S}(\Delta) | \text{ degree}(f_{|\sigma}) = m \text{ for any } \sigma \in \Delta_d\}$
- $\mathcal{S}(\Delta)^r := \{f \in \mathcal{S}(\Delta) | f \in C^r\}$
- $\mathcal{S}(\Delta)^r_m := \mathcal{S}(\Delta)^r \cap \mathcal{S}(\Delta)_m$
- $\mathcal{S}(\Delta)^r_{\leqslant m} := \mathcal{S}(\Delta)^r \cap \mathcal{S}(\Delta)_{\leqslant m}$

For each $d-1$-face τ the linear form whose affine space supports τ is denoted by l_τ, the ideal generated by this form is denoted I_τ.

For each d-dimensional polyhedral complex Δ, we define the homogenisation $\hat{\Delta}$ of Δ, to be the complex build from Δ in the following way: we embed Δ in the hyperplane x using the map $p : (x_0, x_1, \ldots, x_d) \mapsto (1, x_1, \ldots, x_d)$, and for each face

$\sigma \in \Delta_d$ we consider the cone $\hat{\sigma}$ formed by $p(\sigma)$ and the point $(0,\dots,0)$, the set of all polyhedrons $\hat{\sigma}$ will form the complex $\hat{\Delta}$, the utility of this complex consist in the fact that the two spaces $\mathcal{S}(\hat{\Delta})^r_m$ and $\mathcal{S}(\Delta)^r_{\leqslant m}$ are isopmorphic through the dis-homogenisation map $p^* : \mathcal{S}(\hat{\Delta})^r_m \to \mathcal{S}(\Delta)^r_{\leqslant m}$, with $p^*(f(\mathbf{x})) = f(p(\mathbf{x}))$ for any $\mathbf{x} = (x_0, x_1, \dots, x_d)$, so if we compute the Hilbert polynomial of $\mathcal{S}(\hat{\Delta})^r$ the we get the dimension of $\mathcal{S}(\Delta)^r_{\leqslant m}$ for each m. The Homogenisation map (the inverse of p^*) is given by $p^{*-1}(f(\mathbf{x})) = x_0^{deg(f)} f(\frac{x_1}{x_0}, \dots, \frac{x_d}{x_0})$.

Now we state an important characterisation of the C^r continuity over piecewise polynomial functions.

Proposition 1.1 ([25]). *Let Δ be a polyhedral complex. Then for any $f \in \mathcal{S}^r(\Delta)$ we have: $f \in \mathcal{S}(\Delta)^r$ if and only if for each $\sigma_1, \sigma_2 \in \Delta_n$ such that there exists $\tau = \sigma_1 \cap \sigma_2$, $\tau \in \Delta_{n-1}$ and l_τ devides $f_{|\sigma_1} - f_{|\sigma_2}$.*

2 A chain complex for computing the dimension of $\mathcal{S}(\Delta)^r_m$

The main method used in this chapter to compute the dimension of $\mathcal{S}(\Delta)^r_m$ is to build a chain complex such that one of his homology groups is $\mathcal{S}(\Delta)^r_m$, then use the Euler characteristic to form a formula for the dimension, in this section we explain how to build the chain complex. There are two types of complexes that we use, one of them uses the ideals I_τ generated by the linear equation of the hyperplane supporting the subface τ in Δ. The other type uses the ideal $I_{\hat{\tau}}$, generated by the linear equation of the hyperplane supporting the subface $\hat{\tau}$ in $\hat{\Delta}$.

Let Δ be a d-dimensional complex, $\mathbb{R}[\mathbf{x}] = \mathbb{R}[x_1, \dots, x_d]$ and $\mathbb{R}[\hat{\mathbf{x}}] = \mathbb{R}[x_0, \dots, x_d]$. For any ring R, an R-complex $\mathcal{C}$ consists of the following data:

- An R-module $\mathcal{C}(\sigma)$ for each $\sigma \in \Delta$.
- An R-module morphism $\partial_k : \sum_{\sigma\in\Delta_k} \mathcal{C}(\sigma) \to \sum_{\tau\in\Delta_{k-1}} \mathcal{C}(\tau)$ for each $k \in d \dots 1$, such that $\partial_{k-1} \circ \partial_k$.

The complexes can be written in the following way:

$$\mathcal{C} : \mathcal{C}^d \xrightarrow{\partial_d} \mathcal{C}^{d-1} \xrightarrow{\partial_{d-1}} \dots \xrightarrow{\partial_2} \mathcal{C}^1 \xrightarrow{\partial_1} \mathcal{C}^0$$

with $\mathcal{C}^i = \oplus_{\sigma\in\Delta_i} \mathcal{C}(\sigma)$ for $i \in d \dots, 0$. Two types of complexes are going to be used in this chapter, we denote them by $\mathcal{C}$, $\hat{\mathcal{C}}$ and define them in the following way:

with:

$$\begin{aligned}
\mathcal{C}(\sigma) &= \mathbb{R}[\mathbf{x}] && for\, \sigma \in \Delta_d \\
\mathcal{C}(\sigma) &= \mathbb{R}[\mathbf{x}]/I(\sigma) && for\, \sigma \in \Delta_i,\ i < d-1 \\
\hat{\mathcal{C}}(\sigma) &= \mathbb{R}[\hat{\mathbf{x}}] && for\, \sigma \in \Delta_d \\
\hat{\mathcal{C}}(\sigma) &= \mathbb{R}[\hat{\mathbf{x}}]/J(\hat{\sigma}) && for\, \sigma \in \Delta_i,\ i < d-1 \\
J(\tau) &= I_{\hat{\tau}}^{r+1} && for\, \tau \in \Delta_{d-1} \\
I(\tau) &= I_{\tau}^{r+1} && for\, \tau \in \Delta_{d-1} \\
J(\gamma) &= \sum_{\gamma \in \tau} I_{\hat{\tau}}^{r+1} && for\, \tau \in \Delta_i,\ i < d-1 \\
I(\gamma) &= (\sum_{\gamma \in \tau} I_{\tau})^{r+1} && for\, \tau \in \Delta_i,\ i < d-1
\end{aligned}$$

with ∂_i, in both of the two complexes, a differential map similar to the one we use in relative homology of a simplicial complex $\Delta/\partial\Delta$.

In the complex $\hat{\mathcal{C}}$, since we are quotiening by homogeneous ideals, all the terms of the complex are graded, and more over all the maps of this complex are graded maps, so it is convenient to denote by $\hat{\mathcal{C}}_m$ the sub complex of $\hat{\mathcal{C}}$ of elements of degree m. In the same times we will use $\mathcal{C}_m$ to denote the the sub complex of elements in $\mathcal{C}$ of degree at most m.

The complex $\hat{\mathcal{C}}$ have been studied in [26], earlier works such as [25] used the ideal $I(\gamma) = (\sum_{\gamma \in \hat{\tau}} I_\tau)^{r+1}$ instead of $J(\hat{\gamma}) = \sum_{\gamma \in \tau} I_\tau^{r+1}$ the difference is that we use the power of the sum instead of the sum of powers. The main use of this complex is that it allows to compute the dimension of the space of splines because we know that for $m \geqslant 0$ and $r \geqslant 0$ we have from [26] and [25]:

$$H^d(\mathcal{C}_m) \simeq \mathcal{S}(\Delta)^r_{\leqslant m} \simeq \mathcal{S}(\hat{\Delta})^r_m \simeq H^d(\hat{\mathcal{C}}_m)$$

This property besides of the Euler formula allows us to "approximate" the dimension of the space of splines. Let $\mathcal{C}_m$ be the complex obtained from $\mathcal{C}$ after bounding the degree of the polynomials, then the Euler formula can be written:

$$dim(H^d(C_m)) = \chi(\mathcal{C}_m) - \sum_{i=0,..,d-1} (-1)^i dim(H^i(C_m)) \tag{2.1}$$

where $\chi(\mathcal{C}_m)$ is the Euler characteristic.

Both of the ideals $I(\sigma)$ and $J(\sigma)$ have been used in approximation theory to prove interesting results, however they don't have the same properties. Lemma 2.2 illustrates the difference between them, but before stating it we need to define the Krull dimension.

Definition 2.1. *The Krull dimension of a ring R is the length n of the longest possible chain of primes in R:*

$$P_0 \nsubseteq P_1 \nsubseteq \ldots \nsubseteq P_n$$

If M is an R-module then the Krull dimension of M is by definition the Krull dimension of the ring:

$$R/Ann(M)$$

where

$$Ann(M) = \{a \in R \mid am = 0 \ for \ all \ m \in M\}$$

is the annihilator of M.

For example, in algebraic geometry, if an ideal I is generated by a set of polynomials $f_1, \ldots, f_n$ in the ring of polynomials R, then the Krull dimension of R/I is the dimension of the algebraic set defined by $f_1, \ldots, f_n$.

Lemma 2.2. *[26] If Δ corresponds to the embedding of a d-dimensional ball in the d-dimensional euclidean space then for all $i < d$, $H_i(\hat{\mathcal{C}})$ has the Krull dimension $\leqslant i - 1$.*

It means in particular that for a planar simplicial complex isomorphic to a disk, the two homology groups $H_i(\hat{\mathcal{C}})$ for $i = 1, 0$ have dimension zero. As illustrated in the example 3.5 of [27], this property doesn't hold for $I(\sigma)$.

In the following sections we will show some interesting results on dimension using both of the two constructions.

3 A dimension formula for generic embeddings

The following result is a formula of dimension for $\mathcal{S}(\Delta)^1$ in the case of a planar simplicial complex embedded generically in the two dimensional euclidean space. By generic embedding we mean that the set of vertex positions for which the formula is valid is given by the complement of some algebraic set. The ideal $I(\sigma)$ is used in this construction.

Theorem 3.1 ([25])**.** *For a generic embedding Δ of a planar simplicial complex in $\mathbb{R}^2$, we have:*

$$dim\, \mathcal{S}(\Delta)^1_m = \binom{m+2}{2} |\Delta_2| - (2m+1)|\mathring{\Delta}_1| - 3|\mathring{\Delta}_0|$$

the word generic comes from the rank of a matrix that is called "spline matrix" and that has full rank if the vertices positions are generic.

The proof will follow from the formula (2.1) if we show that $H^i(C_m) = 0$ for $i = 0, 1$.

To show that $H^0(\mathcal{C}_m) = 0$ we define the following exact sequence of complexes:

$$0 \to \mathcal{I} \to \mathfrak{R} \to \mathcal{C} \to 0$$

that is given by:

$$
\begin{array}{ccccc}
 & 0 & 0 & 0 \\
 & \downarrow & \downarrow & \downarrow \\
\mathcal{I}: & 0 & \longrightarrow \oplus_{\tau\in\Delta_1} I_(\tau) & \longrightarrow \oplus_{\gamma\in\Delta_0} I(\gamma) \\
 & \downarrow & \downarrow & \downarrow \\
\mathfrak{R}: & \oplus_{\sigma\in\Delta_2}\mathbb{R}[\mathbf{x}] & \longrightarrow \oplus_{\tau\in\overset{\circ}{\Delta}_1}\mathbb{R}[\mathbf{x}] & \longrightarrow \oplus_{\gamma\in\Delta_0}\mathbb{R}[\mathbf{x}] \\
 & \downarrow & \downarrow & \downarrow \\
\mathcal{C}: & \oplus_{\sigma\in\Delta_2}\mathbb{R}[\mathbf{x}] & \longrightarrow \oplus_{\tau\in\overset{\circ}{\Delta}_1}\mathbb{R}[\mathbf{x}]/I(\tau) & \longrightarrow \oplus_{\gamma\in\overset{\circ}{\Delta}_0}\mathbb{R}[\mathbf{x}]/I(\gamma) \\
 & \downarrow & \downarrow & \downarrow \\
 & 0 & 0 & 0
\end{array}
$$

By the zigzag lemma [28], the following sequence:

$$\ldots \to H^0(\mathcal{I}) \to H^0(\mathfrak{R}) \to H^0(\mathcal{C}) \to 0$$

We know from the universal-coefficient theorem [29] that $H^0(\mathfrak{R}) = 0$, thus $H^0(\mathcal{C}) = 0$.

The vanishing of $H^1(C_m)$ is shown using another construction based on the quotient of the two complexes $\mathcal{C}_{m+1}$ and $\mathcal{C}_m$, after simplifications of the quotient complex, we get the following complex when $r = 1$:

$$\mathcal{C}_{m+1}/\mathcal{C}_m : \oplus_{\sigma\in\Delta_2} R_{m+1}/R_m \to \oplus_{\sigma\in\overset{\circ}{\Delta}_1} R_{m+1}/R_m \to 0 \tag{2.2}$$

where R_m is the set of bivariate polynomials of degree less or equal to m. The form of the terms of the complex follows from the three isomorphism theorems [30] , the last term of that complex vanish only because we are using the $I(\sigma)$ ideal, the same doesn't hold for the ideal $J(\sigma)$([25] .

At the same time by considering the exact sequence of complexes:

$$0 \to \mathcal{C}_m \to \mathcal{C}_{m+1} \to \mathcal{C}_{m+1}/\mathcal{C}_m \to 0$$

taking into account the fact that $H^0(\mathcal{C}_m) = 0$, we deduce, again by the zigzag lemma, the long exact sequence of homologies:

$$\ldots \to H^1(\mathcal{C}_m) \to H^1(\mathcal{C}_{m+1}) \to H^1(\mathcal{C}_{m+1}/\mathcal{C}_m) \to 0$$

From this, We have the two homological properties (cf. [25]):

A) $H^1(\mathcal{C}_m) = 0$ implies $H^1(\mathcal{C}_{m+1}) \simeq H^1(\mathcal{C}_{m+1}/\mathcal{C}_m)$.

B) If $H^1(\mathcal{C}_{m+1}/\mathcal{C}_m) = 0$ then $dim\, H^1(\mathcal{C}_{m+1}) \leqslant dim\, H^1(\mathcal{C}_m)$.

It is shown in [31] that the matrix of the map in the complex 2.2 has full rank when the positions of the vertices are generic. Thus for a generic embedding of a simplicial complex in the plan we have $H^1(\mathcal{C}_{m+1}/\mathcal{C}_m) = 0$ for $m \geqslant 2$. If Δ is a disk then by proposition 4.8 in [25] we have that $H^1(\mathcal{C}_r) = 0$ when the degree m

is the same as the regularity r, and by applying the properties A) and B) several times we get that $H^1(\mathcal{C}_m) = 0$ when Δ is a disk. The result for general complexes follows from the the following proposition proved in [25] by recursion on the genus of Δ.

Proposition 3.2. *If $H^1(\mathcal{C}_2) = 0$ for generic embeddings of 2-disks in the plane, then it holds also for generic embeddings of any 2-manifold*

4 About the freeness of $\mathcal{S}(\hat{\Delta})^r$

The freeness of the space of splines is a question that has been addressed in several works before ([32], [33], [26], [34], [27]). In most of this works, the freeness of the space $\mathcal{S}(\hat{\Delta})^r_d$ is analysed instead of $\mathcal{S}(\Delta)^r_{\leqslant d}$ since this two spaces are isomorphic. In this section we will see that free spline space gives, in some cases, facilities in computing the dimension.

4.1 Freeness for bivariate case

We mention in this section results on the freeness of the space $\mathcal{S}(\hat{\Delta})^r$ in the bivariate case. For the beginning, we will use the ring of polynomials $\mathbb{R}[\mathbf{x}] = \mathbb{R}[x, y, z]$ to study the bivariate case. The results of this section are from [27].

We consider the following chain complex:

$$\hat{\mathcal{C}} : \oplus_{\sigma\in\Delta_2}\mathbb{R}[\mathbf{x}] \to \oplus_{\tau\in\overset{\circ}{\Delta}_1}\mathbb{R}[\mathbf{x}]/J(\tau) \to \oplus_{\gamma\in\overset{\circ}{\Delta}_0}\mathbb{R}[\mathbf{x}]/J(\gamma) \to 0 \tag{2.3}$$

The ideal $J_\tau \subset \mathbb{R}[\mathbf{x}]$ is generated using the linear form corresponding to τ in $\hat{\Delta}$, and $J(\gamma)^r = \sum_{\gamma\in\tau} J^r_\tau$. In the same way we define the two complexes:

$$\hat{\mathfrak{R}} : \oplus_{\sigma\in\Delta_2}\mathbb{R}[\mathbf{x}] \to \oplus_{\tau\in\overset{\circ}{\Delta}_1}\mathbb{R}[\mathbf{x}] \to \oplus_{\gamma\in\overset{\circ}{\Delta}_0}\mathbb{R}[\mathbf{x}] \to 0,$$

$$\hat{\mathcal{J}} : 0 \to \oplus_{\tau\in\overset{\circ}{\Delta}_1}\mathbb{R}[\mathbf{x}]/J(\tau) \to \oplus_{\gamma\in\overset{\circ}{\Delta}_0}\mathbb{R}[\mathbf{x}]/J(\gamma) \to 0.$$

We get the following exact sequence of complexes:

$$0 \to \hat{\mathcal{J}} \to \hat{\mathfrak{R}} \to \hat{\mathcal{C}} \to 0$$

and by using the zig-zag lemma and the fact that $H^0(\hat{\mathfrak{R}}) = 0$ we deduce the following exact sequence of graded maps:

$$0 \to H^2(\hat{\mathfrak{R}}) \to H^2(\hat{\mathcal{C}}) \to H^1(\hat{\mathcal{J}}) \to H^1(\hat{\mathfrak{R}}) \xrightarrow{d_1} H^1(\hat{\mathcal{C}}) \xrightarrow{d_2} H^0(\hat{\mathcal{J}}) \to 0 \tag{2.4}$$

and that

$$H^0(\hat{\mathcal{C}}) = 0.$$

This sequence has the property of being graded. At the same time we have that $H^1(\hat{\mathcal{J}}) \subset \oplus_{\tau\in\overset{\circ}{\Delta}_1} J_(\tau)$. It means that the elements of $Im(d_1) = ker(d_2)$ are of degree

at least $r+1$. Besides of that, according to the universal-coefficient theorem, if $H^1(\hat{\mathfrak{K}}) \neq 0$ then $H^1(\hat{\mathfrak{K}})$ contains degree zero elements, this says that:

$$H^1(\hat{\mathfrak{K}}) \neq 0 \;\; implies \;\; \partial_1 \neq 0 \;\; implies \;\; H^1(\hat{\mathcal{C}}) \neq 0 \tag{2.5}$$

On the other hand, we know from standard results of algebraic topology (see for example [35]) that a planar simplicial complex has first homology group equal to zero if and only if the genus (that is the number of holes in the complex δ) is equal to zero, by the universal coefficient theorem we get that genus$\neq 0$ implies $H^1(\hat{\mathfrak{K}}) \neq 0$. By collecting all the arguments we have:

$$genus \neq 0 \;\; implies \;\; H^1(\hat{\mathcal{C}}) \neq 0 \tag{2.6}$$

Theorem 4.1 ([27]). *$S^r(\hat{\Delta})$ is free if and only if $H^1(\hat{\mathcal{C}}) = 0$.*

This theorem and the previous discussion imply that the only planar topology Δ that can produce a free module $S^r(\hat{\Delta})$ is the simply connected one. So in the remainder of the section we focus on the simply connected cases, we will relate in particular the freeness of the module with the generic dimension of $S^r(\hat{\Delta})$ that we will define in the following.

Since the topology is equivalent to the disk, then $H_1(\hat{\mathfrak{K}}) = 0$, this produce the sequence:

$$0 \to H^2(\hat{\mathfrak{K}}) \to H^2(\hat{\mathcal{C}}) \to H^1(\hat{\mathcal{J}}) \to 0 \tag{2.7}$$

and the isomorphism:

$$H^1(\hat{\mathcal{C}}) \simeq H^0(\hat{\mathcal{J}}) \tag{2.8}$$

the short exact sequence above induces the isomorphism:

$$S^r(\hat{\Delta}) = H^2(\hat{\mathcal{C}}) \simeq H^2(\hat{\mathfrak{K}}) \oplus H_1(\mathcal{J}) = \mathbb{R}[\mathbf{x}] \oplus H_1(\mathcal{J}) \tag{2.9}$$

where the last equality comes from the universal-coefficient theorem. Furthermore, the complex $\hat{\mathcal{J}}$ induces the exact sequence:

$$0 \to H^1(\hat{\mathcal{J}}) \to \oplus_{\tau \in \overset{\circ}{\Delta}_1} J(\tau) \to \oplus_{\gamma \in \overset{\circ}{\Delta}_0} J(\gamma) \to H^0(\hat{\mathcal{J}}) \to 0$$

We gather all the formulas and sequences below in the following:

$$dim\, \mathcal{S}(\hat{\Delta})^r_m = dim\, \mathbb{R}[\mathbf{x}]_m + dim\, H_1(\hat{\mathcal{J}})_m \tag{2.10}$$

$$= dim\, \mathbb{R}[\mathbf{x}]_m + \sum_{\tau \in \overset{\circ}{\Delta}_1} dim\, (J^{r+1}_\tau)_m - \sum_{\gamma \in \overset{\circ}{\Delta}_0} dim\, (J(\gamma))_m + dim\, H^0(\hat{\mathcal{J}})_m \tag{2.11}$$

$$= dim\, \mathbb{R}[\mathbf{x}]_m + \sum_{\tau \in \overset{\circ}{\Delta}_1} dim\, (J^{r+1}_\tau)_m - \sum_{\gamma \in \overset{\circ}{\Delta}_0} dim\, (J(\gamma))_m + dim\, H^1(\hat{\mathcal{C}})_m \tag{2.12}$$

$$\tag{2.13}$$

It is proved in [27] that the modules $H^1(\hat{\mathcal{C}})$ and $H^0(\hat{\mathcal{J}})$ has finite length for any topology Δ. Since these modules are graded we deduce that they have finite

dimension, in particular for a degree m that is sufficiently high, the dimension of the Splines module is exactly the generic dimension that is defined by :

$$g(\Delta, r, m) := dim\, \mathbb{R}[\mathbf{x}]_m + \sum_{\tau \in \overset{\circ}{\Delta}_1} dim\, (J(\tau))_m - \sum_{\gamma \in \overset{\circ}{\Delta}_0} dim\, (J(\gamma))_m \tag{2.14}$$

It's shown in [5] that this quantity is the exact dimension for $m \geqslant 4r + 1$.

4.2 Freeness and generic embedding

Another important aspect that the formula (2.12) reveals is that for a simply connected planar simplicial complex we have that $\mathcal{S}(\hat{\Delta})^r$ is free if and only if $dim\, \mathcal{S}(\hat{\Delta})^r_m = g(\Delta, r, m)$ for all m. On the other hand, by using the the formula (2.11) we deduce a simpler formulation:

$$\mathcal{S}(\hat{\Delta})^r \textit{ is free if and only if } dim(\mathcal{S}(\hat{\Delta})^r_{r+1}) = g(\Delta, r, r+1) \tag{2.15}$$

Indeed the first implication is deduced from Theorem 4.1, and the reverse implication holds since $H^0(\hat{\mathcal{J}})$ is generated by elements of degree $r+1$, so $H^0(\hat{\mathcal{J}})_{r+1} = 0$ implies $H^0(\hat{\mathcal{J}})_m = 0$ for all m.

Now we want to compare $g(\Delta, 1, m)$ with the formula in Theorem 3.1. The terms of $g(\Delta, 1, m)$ can be computed in the following way:

$$dim\, \mathbb{R}[\mathbf{x}]_m = \binom{m+2}{2},\ dim\, J_\tau^{r+1} = dim \mathbb{R}[\mathbf{x}]_{m-r-1} \tag{2.16}$$

$$\tag{2.17}$$

For the dimension of $J(\gamma)_1$ we distinguish two cases, the first one is when there is exactly two slopes supporting the edges around the vertex γ, in that case by a linear and homogeneous change of coordinates $J(\gamma) = (x, y)^2$, the dimension of that ideal is computed by using the exact sequence:

$$0 \to J(\gamma) \to \mathbb{R}[\mathbf{x}] \to \mathbb{R}[\mathbf{x}]/J(\gamma) \to 0 \tag{2.18}$$

and we get: $dim\, J(\gamma)_1 = \binom{m+2}{2} - 3$. Otherwise, by a linear change of coordinates we have the ideal $J(\gamma)_1 = (x^2, y^2)$, and we get: $dim\, J(\gamma)_1 = \binom{m+2}{2} - 4$. This distinction is mentioned in [27]page 538, we will adopt the same terminology of that paper by saying that the vertex γ is singular if $J(\gamma)/I(\gamma) \neq 0$. By replacing all that in Formula 2.14 and by using the Euler characteristic formula:

$$|\Delta_2| - |\overset{\circ}{\Delta}_1| + |\overset{\circ}{\Delta}_0| = 1$$

we get :

$$\begin{aligned} g(\Delta,1,m) &= \binom{m+2}{2} + |\overset{\circ}{\Delta}_1|\binom{m}{2} - \sum_{\gamma\in\overset{\circ}{\Delta}_0}[\binom{m+2}{2} - 3 - s(\gamma)] \\ &= \binom{m+2}{2} + |\overset{\circ}{\Delta}_1|\binom{m}{2} - |\overset{\circ}{\Delta}_0|\binom{m+2}{2} + |\overset{\circ}{\Delta}_0|3 + \sum_{\gamma\in\overset{\circ}{\Delta}_0} s(\gamma) \\ &= |\Delta_2|\binom{m+2}{2} - |\overset{\circ}{\Delta}_1|(2m+1) + 3|\overset{\circ}{\Delta}_0| + s \end{aligned}$$

where $s = \sum_{\gamma\in\overset{\circ}{\Delta}_0} s(\gamma)$ and $s(\gamma)$ is 1 if the vertex is singular, and 0 otherwise. If we have no singular vertex, the generic dimension $g(\Delta,1,m)$ is the same as the one mentioned in Theorem 3.1, this means that if the embedding is generic then $S^1(\hat{\Delta})$ is free.

Now we want to give a geometric condition that induce freeness. We say that an edge τ in a planar simplicial complex Δ is pseudo boundary if there exists a set of interior edges $\tau_1,\ldots,\tau_n$ such that the union $(\cup_{i=1\ldots,n}\tau_i)\cup\tau$ is a line segment $[a,b]$ such that $a\in\partial\Delta$ or $b\in\partial\Delta$, this line segment will be denoted L_τ, denote by: s_τ the maximal number of slopes of a vertex lying on L_τ, and by $s(\Delta) := min\{s_\tau, \tau\in\overset{\circ}{\Delta}_1\}$.

Theorem 4.2 ([27])**.** *Let Δ be a simply connected planar simplical complex, then we have:*

- *If every edge of Δ is pseudo boundary, then $\mathcal{S}(\hat{\Delta})_r$ is free for each r.*
- *If Δ has at least one edge that is not pseudo boundary, then for $r\geqslant s(\Delta)-2$, $\mathcal{S}(\hat{\Delta})_r$ is not free.*

The bound in the second point is not sharp, see example [27] . The following theorem proved in [36] helps to understand more the freeness of our space.

Theorem 4.3. *Let Δ be a simply connected simplicial complex. If $\mathcal{S}(\hat{\Delta})_r$ is free then $\mathcal{S}(\hat{\Delta})_{r-1}$ is also free.*

Example 4.4. *The complex in Fig. 2.1 is an example of simplicial complex in which all the edges are pseudo boundary. According to the Theorem 4.2, the dimension is equal to the generic dimension given by the expression* (2.14)*. In particular, the generic dimension for a degree 2 for the polynomials, and regularity $r=1$, will be equal to 6.*

In the same time it have been proved in [37] that the dimension of the same space over the Morgan-Scott simplicial complex (see Fig. 2.2) is equal to 7.

This example shows that the homology in fact depend on the geometry of the complex.

It is shown in [32] that the space $\mathcal{S}(\Delta)^0$ for Δ a simplicial complex, is isomorphic to the face ring of the complex Δ. This property has been used in the same reference to show that $\mathcal{S}(\Delta)^0$ is free if and only if Δ is simply connected. The same is not true for general polyhedral complexes, as the example provided in [34] shows that the freeness in polyhedral complexes depends on the embedding.

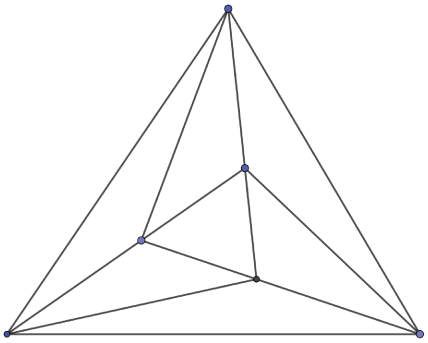

Figure 2.1: Example of a simplicial complex where all the edges are pseudo-boundary

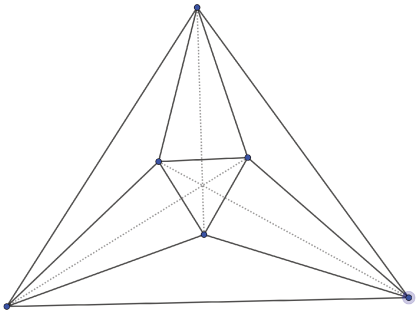

Figure 2.2: Example of a simplicial complex where none of the edges is pseudo-boundary, here the three doted lines doesn't belong to the simplicial complex, and intersects in the same point at the centre of the figure

4.3 Freeness for higher dimensional complexes

The constructions above have been generalised to higher dimensional complexes. We will see that freeness of the space of splines make easier to compute the dimension of the space of the splines in some cases, indeed, it implies that the homology groups of $\hat{\mathcal{C}}$ are equal to zero as we will see. For a simplicial complex of dimension d we define the following chain complex:

$$\hat{\mathcal{C}} : \oplus_{\sigma\in\Delta_d}\mathbb{R}[\mathbf{x}] \xrightarrow{\partial_d} \ldots \to \oplus_{\tau\in\Delta_1^\circ}\mathbb{R}[\mathbf{x}]/J(\tau) \xrightarrow{\partial_1} \oplus_{\gamma\in\Delta_0^\circ}\mathbb{R}[\mathbf{x}]/J(\gamma) \to 0$$

for $\mathbb{R}[\mathbf{x}] = \mathbb{R}[x_0, \ldots, x_d]$. We define in the same way the two complexes: $\hat{\mathcal{J}}$, $\hat{\mathfrak{R}}$ and get the exact sequence:

$$0 \to \hat{\mathcal{J}} \to \hat{\mathfrak{R}} \to \hat{\mathcal{C}} \to 0$$

The main results mentioned in [26] are the following:

Theorem 4.5. *If Δ is a d-dimensional simplicial complex with $H^i(\mathfrak{R}) = 0$ for each $i < d$ then $\mathcal{S}(\Delta)_r$ is free if and only if $H_i(J) = 0$ for all $i < d-1$.*

Theorem 4.6. *For all $i < d$, $H_i(\mathcal{C})$ has Krull dimension less or equal to $i-1$.*

Unlike the bivariate case, having a generic embedding of the simplicial complex of dimension > 2 doesn't mean that the spline space is free according to examples given in [26]

5 The Hilbert polynomial of the space of splines

The Hilbert function h_M of a graded module $\oplus_{n\in\mathbb{N}}M_n$ associate to each $n \in \mathbb{N}$ the dimension of the space of M_n. We know that there exists a polynomial p_M such that for a sufficiently large $n \in \mathbb{N}$ we have that $h_M(n) = p_M(n)$, the degree of that polynomial is equal to the Krull dimension of M.

Now we want to define an exact sequence to compute the Hilbert polynomial of a spline space. The dual graph $G(\Delta)$ of a d-dimensional polyhedral complex is a graph whose vertices correspond to maximal faces of Δ, and whose edges corresponds to $d-1$-dimensional faces of Δ. The (signed) incidence matrix $\partial = \partial(G)$ of an oriented graph $G = (V, E)$ where V is the set of vertices and E is the set of edges is a matrix of dimension $|V| \times |E|$, indexed in rows by the edges and in columns by vertices, such that at the coefficient $c_{e,v}$ corresponding to the edge e and the vertex v is equal to 1 (resp. -1) if e emanates from (resp. head to) v and 0 otherwise. In the following we choose a random orientation of the dual graph of the complex Δ. Suppose we are given a polyhedral complex Δ, then for any codimension 2-linear subspace $\mathfrak{s}$ of $\mathbb{R}^d$ we denote by $G_{\mathfrak{s}}(\Delta)$ the subgraph of $G(\Delta)$ where we consider only the vertices corresponding to a maximal face σ containing a $d-1$-sub-face whose linear span contain $\mathfrak{s}$.

The star of a face σ in Δ is the union of all the faces of Δ containing σ. We will say that Δ is hereditary if the dual graph of the star of any face of Δ is connected.

Let Δ be a d-dimensional polyhedral complex, $r \in \mathbb{N}$ and $R = \mathbb{R}[x_0, \ldots, x_d]$. We define the following map:

$$L : R^{|\Delta_d| + |\mathring{\Delta}_{d-1}|} \to R^{|\mathring{\Delta}_{d-1}|}$$

given by the left multiplication by the matrix:

$$\begin{pmatrix} \partial & \begin{vmatrix} l_1^r & & \\ & \ddots & \\ & & l_{|\Delta_{d-1}|}^r \end{vmatrix} \end{pmatrix}$$

l_i is the linear form whose vanishing set is supporting the $d-1$ face of the i^{th} row of ∂. This induce the following exact sequence:

$$0 \to M \to R^{|\Delta_d| + |\mathring{\Delta}_{d-1}|} \xrightarrow{L} R^{|\mathring{\Delta}_{d-1}|} \to N \to 0 \tag{2.19}$$

where L is the map defined above, $M = ker(L)$ and $N = coker(L)$. The star of a face σ in Δ is the union of all the faces of Δ containing σ. We will say that Δ is hereditary if the dual graph of the star of any face of Δ is connected.

Proposition 5.1 ([7]). *For any hereditary polyhedral complex we have $ker(L) \simeq \mathcal{S}(\Delta)^r$.*

So to describe the Hilbert polynomial of the space of splines, we need to find the Hilbert polynomial of N. It is shown in [7] that for $d \leqslant 2$ the codimension of N is larger than 2, thus the degree of the Hilbert polynomial of N is at most $d-2$.

We need some definition before stating the formula of the Hilbert polynomial. An R-module E is called prime if for any sub-module E' of E we have that $Ann(E) = Ann(E')$, the annihilator of a module is always prime. An ideal $P \in R$ is said to be associated to the module E if there exists a sub-module F of E such that $P = Ann(F)$. Let $\mathcal{P}$ be the set of all minimal associated primes of N, and $N(Q) = \{n \in N | Ann(n) \subset Q\}$.

Theorem 5.2 ([38]). *The two Hilbert polynomials of the modules N and $\bigoplus_{Q \in \mathcal{P}} N(Q)$ have the same degree and the same leading monomial coefficient.*

For any graph G, let $\mathcal{C}(G)$ denote the set of cycles of G.

Theorem 5.3 ([38]). *For any codimension 2 associated prime of N whose vanishing set is denoted by s, we have:*

$$N(Q) \simeq \bigoplus_{c \in \mathcal{C}(G_s(\Delta))} R/I_c$$

where $I_c := \{l_\tau^{r+1} | \tau \in \Delta_d - 1, \tau \in e(c)\}$ and $e(c)$ is the set of edges of c.

It is shown [38] that any codimension two ideal I_c for $c \in \mathcal{C}$ that is minimally generated by $I_1^{r+1}, \ldots, I_n^{r+1}$ admits an exact sequence of the form:

$$0 \to R(-r-1-\alpha(c))^{s_1} \oplus R(-r-2-\alpha(c))^{s_2} \to R(-r-1) \to R \to R/I_c \to 0 \tag{2.20}$$

where $\alpha(c) = \lfloor \frac{r+1}{k+1} \rfloor$, $s_1 = (n-1)\alpha(c) + n - r - 2$, $s_2 = r + 1 - (n-1)\alpha(c)$. $R(t)$ denote the same module R with shifted grading: $R(t)_m = R_{t+m}$. By applying all this to the bivariate case we get the following:

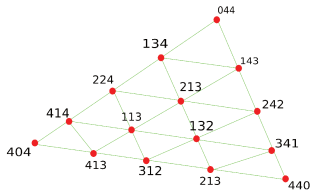

Figure 2.3: Barycentric coordinates grid for a polynomial in the degree 4 Bézier Bernstein representation

Theorem 5.4 ([38]). *Let Δ be a planar hereditary simplicial complex, then:*

$$p_{\mathcal{S}(\hat{\Delta})^r}(k) = \frac{|\Delta_2|}{2}k^2 + \frac{3|\Delta_2| - 2(r+1)|\overset{\circ}{\Delta_1}|}{2}k + |\Delta_2| + (\binom{r}{2} - 1)|\overset{\circ}{\Delta_1}| + \sum_{c\in\mathcal{C}} t_c$$

with $t_c = \binom{r+2}{2} + \frac{\alpha(c)}{2}(2r + 3 + \alpha(c) - n(1 + \alpha(c)))$.

6 A dimension formula for the space of splines of smoothness r and degree $d \leqslant 4r + 1$

One of the main contribution in the field of approximation theory is the dimension formula described in [5] , it describes the dimension of the space $\mathcal{S}_d^r(\Delta)$ for $d \leqslant 4r + 1$ and Δ is a triangulation of a polygonal domain.

The proof of this formula is based on the use of the Bézier-Bernstein representation of the splines. Let p be a polynomial, and let σ be a triangle from Δ composed of the three vertices q_1, q_2, q_3. The Bézier-Bernstein representation of the polynomial p is given by $p(s) = \sum_{i+j+k=d} c_{i,j,k} d! \frac{\alpha^i \beta^j \gamma^k}{i!j!k!}$ where α, β, γ are the barycentric coordinates of the point s with respect to the triangle σ. The coefficients $c_{i,j,k}$ are called the Bézier coordinates of the polynomial p and with the domain points $m_{i,j,k} := (iq_1 + jq_2 + kq_3)/d$ they form the Bézier net given by the points $n_{i,j,k} = (m_{i,j,k}, c_{i,j,k}) \in \mathbb{R}^3$. So any function $f \in \mathcal{S}_d^r(\Delta)$ will be represented by its Bézier net $\mathcal{B}_d(\Delta) := (n_{i,j,k}^\sigma)_{\sigma\in\Delta_2, i+j+k=d}$.

A determining set of a space of splines $\mathcal{S}_d^r(\Delta)$ is a set $D \in \mathcal{B}(\Delta)$ with the property that any function f having its Bézier net verifying $m_{i,j,k}^\sigma = 0$ for each $m_{i,j,k}^\sigma \in D$ then $f = 0$. A determining set is said to be minimal if there is no determining set with fewer elements. Its clear that the dimension of the space of splines is always smaller than the cardinal of a minimal determining set.

The disk of radius l about a vertex $v \in \Delta_0$ is the set of domain points $m_{i,j,k}^\sigma$ that need a number of steps over the grid of domain points, less than l to get to v.

For each vertex v_i we denote by e_i the number of interior edges of distinct slopes determined by the edges around v_i, and E_i is the number of interior edges around the vertex v_i.

Theorem 6.1 ([5]). *Let $\mathcal{S}_d^r(\Delta)$ be a space of splines with $d \leqslant 4r + 1$, and Δ be a trian-*

gulation of a polygonal region of the plane. Then :

$$Dim(\mathcal{S}_d^r(\Delta)) = \frac{(d+1)(d+2)}{2} + \frac{(d-r)(d-r+1)}{2}|\overset{\circ}{\Delta}_1| - \frac{d^2+3d-r^2-3r}{2}|\overset{\circ}{\Delta}_0| + s \tag{2.21}$$

where $s = \sum_{i=1\ldots V_I} \sigma_i$ *and* $s_i = \sum_{j=1\ldots,d-r}(r+j+1-je_i)_+$.

It was shown in [39] that the above mentioned formula is a lower bound of the dimension, while in [5] the proof is completed by showing that there exists a minimal determining set of the space of splines who's number of elements is equal to the above mentioned formula. The minimal determining set that is chosen in this proof is described by:

- $\frac{(2r+1)(2r+2)}{2} + E_i\frac{r(r+1)}{2}$ domain point from the disk of radius $2r$ about each boundary vertex.
- $\frac{(r+1)(r+2)}{2} + E_i\frac{r(r+1)}{2} + \sigma_i$ domain point chosen from the disk of radius $2r$ about each interior vertex.
- For each triangle we take the domain points $\{c_{i,j,k} : i > r, j > r, k > r\}$
- For each edge $e \leqslant i \leqslant r, j < d-2r, k \leqslant d-2r\}$;

The formula of Theorem. 6.1 can be deduced from the one in Theorem. 5.4 applied on the simplicial case. This can be shown by using the formulas:

$$|\overset{\circ}{\Delta}_0| = |\overset{\circ}{\Delta}_1| - |\Delta_2| + 1 \tag{2.22}$$

7 Upper and lower bound for the dimension of $\mathcal{S}_d^r(\Delta)$

In [40], an upper and lower bound for the dimension of $\mathcal{S}_d^r(\Delta)$ have been established using 2.12. This Bound are useful since they can be used fro any value of d.

For each vertex v_i we denote by $\Omega_i := \left\lfloor \frac{E_i r}{E_i - r} \right\rfloor$, $A_i := E_i(r+1) + (1-E_i)\Omega_i$, and $B_i := E_i - 1 - A_i$. We denote also by $\omega_i := \left\lfloor \frac{e_i r}{e_i - r} \right\rfloor$, $a_i := e_i(r+1) + (1-e_i)\omega_i$, and $b_i := e_i - 1 - a_i$.

Theorem 7.1 ([8]). *We have the two following bounds for the dimension of* $\mathcal{S}_k^r(\delta)$

$$\binom{k+2}{2} + |\mathring{\Delta}_0| \binom{k+2-(r+1)}{2}$$
$$- \sum_{i=1}^{|\mathring{\Delta}_0|} \left[t_i \binom{k+2-(r+1)}{2} - b_i \binom{k+2-\Omega_i}{2} + a_i \binom{k+2-(\Omega_i+1)}{2} \right]$$
$$\leqslant Dim(\mathcal{S}(\hat{\Delta})_k^r) \leqslant$$
$$\binom{k+2}{2} + |\mathring{\Delta}_0| \binom{k+2-(r+1)}{2}$$
$$- \sum_{i=1}^{|\mathring{\Delta}_0|} \left[\tilde{t}_i \binom{k+2-(r+1)}{2} - \tilde{b}_i \binom{k+2-\tilde{\Omega}_i}{2} + \tilde{a}_i \binom{k+2-(\tilde{\Omega}_i+1)}{2} \right]$$

The first inequality can be proved by using (2.12) and the fact that $dim\, H^1(\hat{\mathcal{C}})_m \geqslant 0$, we use also the sequence (2.20) to compute $Dim\, J_\tau^{r+1}$ and the Euler formula (2.22). The second inequality is proved in [8] by using an ordering of the vertices. It is shown in the same paper that for a space of splines over a planar simplicial complex that admits a special vertex ordering, the upper bound of Theorem. 7.1 becomes sharper.

Theorem 7.2 ([8]). *Suppose that the vertices of a planar simplicial complex Δ are numbered in such a way that each pair of consecutive vertices are corners of the same triangle. For each γ_i define $\tilde{t}_i$ as the number of edges with different slopes joining the vertex γ_i to a vertex in the boundary of Δ or to one of the first $i-1$ vertices. Then:*

$$Dim(\mathcal{S}(\hat{\Delta})_k^r) \leqslant \binom{k+2}{2} + |\mathring{\Delta}_1| \binom{k+r+1}{2} -$$
$$|\mathring{\Delta}_1| \left[\binom{k+2}{2} - \binom{r+2}{2} \right] + \sum_{i=1}^{|\mathring{\Delta}_0|} \sum_{j=1}^{k-r} (r+j+1-j\tilde{t}_i)_+$$

8 Conclusion

The objective of this chapter was to give an overview of the algebraic geometry and commutative algebra tools used in spline theory, to compute the dimension of the space $\mathcal{S}(\Delta)_m^r$. It turns out that the tools are very efficient in analysing the dimension of the space of splines.

The bivariate case on simplicial complexes is well understood through the existing works, indeed, the formula (2.12) expresses the dimension of the space of splines over a two dimensional simplicial complex using four terms: two of them are straightforward to compute using the formulas (2.16), one way to compute the term $Dim\,(J(\gamma)_m)$ is by using simultaneously an exact sequence such as (2.18) and (2.20), the resulting formula depend only on m and r. Since the homology

space $H^1(\hat{\mathcal{C}})$ has Krull dimension equal to zero 2.2, $dim\, H^1(\hat{\mathcal{C}})_m$ vanish for m sufficiently high, we know that $H^1(\hat{\mathcal{C}}) = 0$ if and only if the module $\mathcal{S}(\hat{\Delta})_r$ is free, and $H^1(\hat{\mathcal{C}})$ can vanish only if Δ is simply connected; we have in the simply connected case $\mathcal{S}(\hat{\Delta})^r$ is free implies $\mathcal{S}(\hat{\Delta})^{r-1}$ is free as well. The freeness of $\mathcal{S}(\hat{\Delta})^r$ can be characterised using the geometry of Δ, for instance if each edge $e \in \Delta$ belongs to a line segment L_Δ that is a union of interior edge from Δ, such that $\partial\Delta \cup L_e \neq \emptyset$, then the space $\mathcal{S}(\Delta)^r$ is free for any r. If the previous geometric property of Δ is not true, then there is an r_0 such that $\mathcal{S}(\Delta)^r$ is free if and only if $r \leqslant r_0$, we have $r_0 \geqslant 0$, and an upper bound r_0(see Theorem 4.2 and in [32] it is shown that $\mathcal{S}^0$ is free), both of them are not sharp according to the existing examples.

In higher dimensional complexes it is less obvious how to find the dimension. We know that the homology of the complex $\hat{\mathcal{C}}$ vanish if $\mathcal{S}(\hat{\Delta})^r$ is free. In that case the dimension can be written by means of the the quotients $\bigoplus_{\gamma\in\overset{\circ}{\Delta}_i} \mathbb{R}[\mathbf{x}]/J(\gamma)$ for $i < d$. By the discussion preceding Theorem 5.4 we know how to compute a resolution of $\mathbb{R}[\mathbf{x}]/J(\gamma)$ if the codimension of γ in $\mathbb{R}^{d+1}$ is equal to two, however, it is less clear how to compute the dimension of such a module of greater codimensions.

The Hilbert polynomial $p_{\mathcal{S}(\Delta)^r}$ is a way to approximate the dimension of $\mathcal{S}(\Delta)_r$. In this chapter we have explained how to compute the three coefficients of highest degree in that polynomial, and thus, in the bivariate case we have the exact formula of $p_{\mathcal{S}(\Delta)^r}$.

An important extension that haven't been detailed in this manuscript is the mixed smoothness splines. In [41] the notion of inverse system is used to generalise the exact sequence (2.20), and give the Hilbert polynomial of a mixed smoothness spline space.

Chapter 3

Basis Computation

To describe and analyse shapes with complex topologies, one often starts with a coarse representation $\mathcal{M}$ that captures the topology and the principal geometric features of the shape. This representation can then be refined and tuned to describe more accurately the actual shape. If the coarse model is a mesh, a classical strategy to obtain a better approximation of the shape is to refine the mesh, by splitting some of its faces. This approach yields piecewise linear representations of the shape, which may require several level of subdivisions in regions with high curvatures, in order to obtain a good approximation of the shape.

In this chapter, we investigate a different strategy to compute accurate shape representations. Instead of splitting the coarse piecewise linear model, we increase the degree of the representation on each face of $\mathcal{M}$ with the aim to obtain better approximation performances with higher order of convergence.

In application, different kind of shapes are approximated, including closed surfaces, like spheres, that cannot be parametrised simply by using one planar domain. This is why we use a mathematical object similar to manifolds and that we call topological surfaces, defined in our context by using parametrisations or transition maps (Definitions 1.1 and 8.1). This topological surfaces are going to be used to parametrise the smooth shapes, and to define differentiable functions on them.

For functions defined over a planar mesh, the usual C^k continuity is sufficient to produce smooth functions, and good quality shapes, while in topological surfaces cuspidal singularities may arise in vertices with valence different from 4 if we use C^k continuity. This is due to the fact that we cannot embed, for instance, 5 squares in the plane and form a fan around one shared vertex between them without changing the angles of the quads, this kind of phenomenons are called vertex enclosure problems, and will be explained in more details in this chapter.

We will use mostly quadrangular faces in $\mathcal{M}$, and tensor product b-spline functions of the same degree and the same knot distributions are used on each face of $\mathcal{M}$. The regularity that we impose across the edges shared by two faces is the continuity of the tangent planes of the parameterizations. This corresponds to geometrically smooth spline functions (as opposed to parametrically smooth spline functions), also called G^1 spline functions. Our aim is to analyse in details the space of G^1 splines on an arbitrary quad mesh and to compute efficiently bases which are suitable for fitting and numerical simulation problems.

The content of this chapter are mainly coming from [42] and [43].

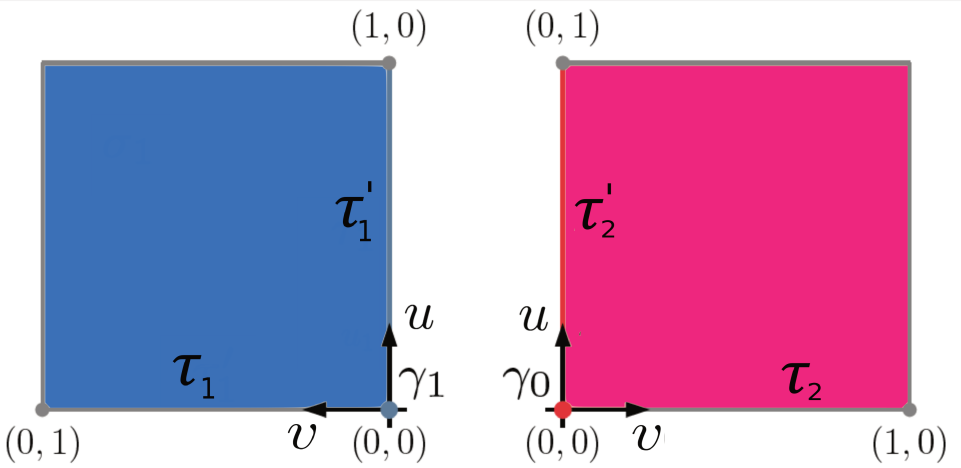

Figure 3.1: Given an edge τ of a topological surface $\mathcal{M}$ that is shared by two polygons $\sigma_1, \sigma_2 \in \mathcal{M}$, we associated a different coordinate system to each of these two faces and consider τ as the pair of edges τ_1 and τ_2 in σ_1 and σ_2, respectively.

1 Definition and notations

We start by describing the gluing conditions that we use for this chapter.

Definition 1.1. *Let σ_1(σ_2 resp.) a polygonal domain in $\mathbb{R}^2$ and τ_1 (τ_2 resp.) be an edge in σ_1 (σ_2 resp.). Two C^k maps $f : \sigma_1 \to \mathbb{R}$, $g : \sigma_2 \to \mathbb{R}$ admits a G^k-**junction** along the two edges τ_1, τ_2 if and only if there exists a C^k-diffeomorphism $\phi : U_1 \to U_2$ between two neighbourhoods U_1, U_2 of the two edges τ_1, τ_2 such that:*

- *ϕ maps τ_1 to τ_2.*
- *ϕ maps the interior points of σ_1 to the exterior points of σ_2.*
- *f, $g \circ \phi$ have the same Taylor expansion of order 1 at each point $(u, 0)$.*

Notice that this is a special case of the aforementioned definition of G^k-junction that uses reparametrisations instead of transition maps.

Let τ be an edge shared by two polygons $\sigma_1, \sigma_2 \in \mathcal{M}_2$, $\tau = \tau_1$ in σ_1, $\tau = \tau_2$ in σ_2 respectively and let $\gamma = (\gamma_1, \gamma_2)$ be a vertex of τ corresponding to γ_2 in σ_2 and to γ_1 in σ_1. We denote by τ_1' (resp. τ_2') the second edge of σ_1 (resp. σ_2) through γ_1 (resp. γ_2). We associate to σ_1 and σ_2 the coordinate system (u, v) such that $\gamma_1 = (0,0)$, $\tau_1 = \{(u,0), u \in [0,1]\}$, $\tau_1' = \{(0,v), v \in [0,1]\}$ in σ_1 and $\gamma_2 = (0,0)$, $\tau_2 = \{(u,0), v \in [0,1]\}$, $\tau_2' = \{(0,v), v \in [0,1]\}$ in σ_2, see Figure 3.1. Using the Taylor expansion at $(0,0)$, a transition map from U_{τ,σ_1} to U_{τ,σ_2} is then of the form

$$\phi\colon (u,v) \longrightarrow (u,v) = \begin{pmatrix} u + v\,\mathfrak{a}_{\tau,\gamma}(u) + v^2\rho_2(u,v) \\ v\,\mathfrak{b}_{\tau,\gamma}(u) + v^2\rho_1(u,v) \end{pmatrix} \tag{3.1}$$

where $\mathfrak{a}_{\tau,\gamma}(u), \mathfrak{b}_{\tau,\gamma}(u), \rho_1(u,v), \rho_2(u,v)$ are C^1 functions. We will refer to it as the canonical form of the transition map ϕ at γ along τ. The functions $[\mathfrak{a}_{\tau,\gamma}, \mathfrak{b}_{\tau,\gamma}]$ are called the *gluing data* at γ along τ on σ_1.

With this transition map form, the G^1 continuity is equivalent to:

$$\begin{aligned} f(u,0) &= g(u,0) && (3.2)\\ \frac{\partial f}{\partial u}(u,0) &= \frac{\partial g}{\partial u}(u,0) && (3.3)\\ \frac{\partial f}{\partial v}(u,0) &= \mathfrak{b}_{\tau,\gamma}(u)\frac{\partial g}{\partial v}(u,0) + \mathfrak{a}_{\tau,\gamma}(u)\frac{\partial g}{\partial u}(u,0) && (3.4)\\ & && (3.5) \end{aligned}$$

for $u \in [0,1]$. We can write the two formulas (3.3) and (3.4) in the matrix form as follows:

$$\begin{pmatrix} \frac{\partial f}{\partial u}(u,0) \\ \frac{\partial f}{\partial v}(u,0) \end{pmatrix} = \begin{pmatrix} 1 & 0 \\ \mathfrak{a}_{\tau,\gamma}(u) & \mathfrak{b}_{\tau,\gamma}(u) \end{pmatrix} \begin{pmatrix} \frac{\partial g}{\partial u}(u,0) \\ \frac{\partial g}{\partial v}(u,0) \end{pmatrix} \tag{3.6}$$

In general the geometric continuity is used to glue several patches together according to a given mesh structure. The geometrically continuous functions are defined over spaces that are quite similar to manifolds and that we call topological surfaces.

Definition 1.2. *A **topological surface** $\mathcal{M}$ is given by:*

- *a collection $\mathcal{M}_2$ of polygons (also called faces of $\mathcal{M}$) in the plane.*
- *a collection of G^k-junctions given by $\phi_{i,j} : \tau_i \mapsto \tau_j$ between polygonal edges from different polygons σ_i and σ_j of $\mathcal{M}_2$,*

where a polygonal edge can be glued with at most one other polygonal edge, and it cannot be glued with itself. The shared edges (resp. the points of the shared edges) are identified with their image by the corresponding homeomorphism. The collection of edges (resp. vertices) is denoted $\mathcal{M}_1$ (resp. $\mathcal{M}_0$).

Over topological surfaces, we will define functions that respect differentiability constraints in the following way.

Definition 1.3. *Let $\mathcal{M}$ be a topological surface defined using the set of polygons $(\sigma_i)_{i\in\mathcal{M}_2}$ and the set of transitions $(\phi_i)_{j\in\mathcal{M}_1}$. A G^k-function on $\mathcal{M}$ is a collection $f = (f_\sigma)_{\sigma\in\mathcal{M}_2}$ of C^k-functions such that for each two faces σ_0 and σ_1 sharing an edge τ with ϕ as transition map, the two functions f_{σ_1} and $f_{\sigma_0} \circ \phi_{0,1}$ have the same Taylor expansion of order 1 (it means that they have a G^k-junction). The function f_σ is called the restriction of f on the face σ.*

In the following sections we will put some restrictions on the type of functions we use on each face, and study the resulting space. The study will focus mainly on determining the degrees of freedom that a space can afford, we will see in particular that we have a special behavior of the degrees of freedom when the gluing function $\mathfrak{a}_{\tau,\gamma}$ vanish.

Definition 1.4. *An edge $\tau \in \mathcal{M}$ which contains the vertex $\gamma \in \mathcal{M}$ is called a* crossing edge at γ *if $\mathfrak{a}_{\tau,\gamma}(0) = 0$ where $[\mathfrak{a}_{\tau,\gamma}, \mathfrak{b}_{\tau,\gamma}]$ is the gluing data at γ along τ. We define $\mathfrak{c}_\tau(\gamma) = 1$ if τ is a crossing edge at γ and $\mathfrak{c}_\tau(\gamma) = 0$ otherwise. By convention, $\mathfrak{c}_\tau(\gamma) = 0$ for a boundary edge. If $\gamma \in \mathcal{M}_0$ is an interior vertex where all adjacent edges are crossing edges at γ, then it is called a* crossing vertex. *Similarly, we define $\mathfrak{c}_+(\gamma) = 1$ if γ is a crossing vertex and $\mathfrak{c}_+(\gamma) = 0$ otherwise.*

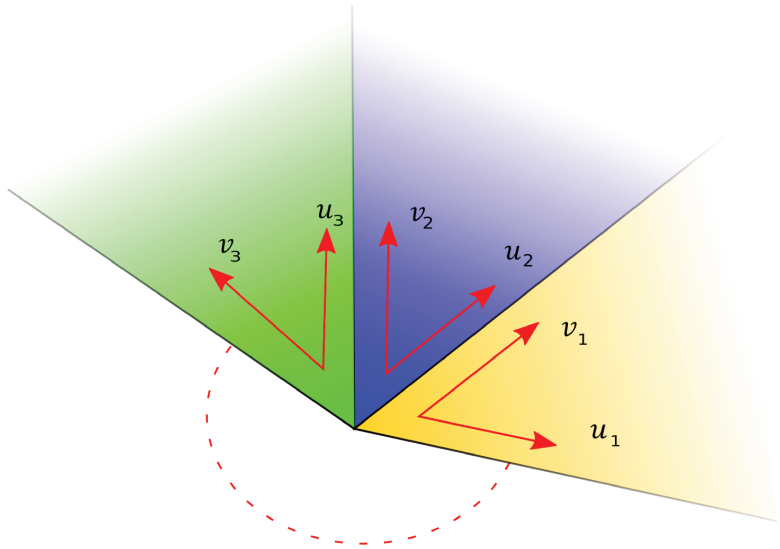

Figure 3.2: Coordinates system used to glue around a vertex

2 Compatibility around a vertex

The G^1-junction condition that we impose along an edge will guaranty that the two glued functions have the same tangent space along the edge as we will explain in the following lines (3.7). However, the interaction between the gluing data of edges close to each other may put over restrictive condition on the resulting space of G-splines. In particular, if the gluing data of the edges around a fixed vertex are adapted, all the G^k- functions over the corresponding topological surface will have vanishing tangent space at that point.

For any G^1 map $f : \mathcal{M} \to \mathbb{R}^n$ with $n \in \mathbb{N}^*$, the tangent space at a point $\gamma \in \mathcal{M}$ is the space $T_\gamma f \subset \mathbb{R}^n$ spanned by the two vectors: $\partial_x f_{|\sigma}(\gamma), \partial_y f_{|\sigma}(\gamma)$ for any face $\sigma \subset \mathcal{M}$ containing γ:

$$T_\gamma f = \{(\partial_x f_{|\sigma}(\gamma), \partial_y f_{|\sigma}(\gamma))(h,s)^t : \ (h,s) \in \mathbb{R}^2\}$$

Because of the G^1 condition this definition of the tangent space doesn't depends on the choice of the representer of γ. Indeed, for a vertex belonging to an internal edge τ shared by two faces σ_1 and σ_2 the tangent space can be written as the space spanned by $\partial_x f_{|\sigma_1}(\gamma), \partial_y f_{|\sigma_1}(\gamma)$ or by $\partial_x f_{|\sigma_2}(\gamma), \partial_y f_{|\sigma_2}(\gamma)$. One consequence of the definition 1.1 of the G^1-junction is the equality of Jacobians expressed in following formula:

$$D_\gamma f_1 = D_\gamma f_2 \circ D_\gamma \phi \tag{3.7}$$

since ϕ is invertible, then $D_\gamma f_1$ and $D_\gamma f_2$ span the same space.

Let $\sigma_1, \ldots, \sigma_l$ be a sequence of faces from the topological surface $\mathcal{M}$ such that σ_i, σ_{i+1} share an edge τ_i with the transition map $\phi_i : \sigma_i \to \sigma_{i+1}$ for $i = 1, \ldots, l-1$, and σ_l,σ_1 share a common edge τ_l with the transition map $\phi_l : \sigma_l \to \sigma_1$. By using the formula (3.7) and a coordinate system as in Fig. 3.2 we deduce that any G^1 map over the topological space $\mathcal{M}$:

$$\begin{pmatrix} \partial_{u_1} f_1 \\ \partial_{v_1} f_1 \end{pmatrix} = \left[\prod_{i=1..l} D_\gamma \phi_i\right] \begin{pmatrix} \partial_{u_1} f_1 \\ \partial_{v_1} f_1 \end{pmatrix} \tag{3.8}$$

In order to get a tangent space $T_\gamma f$ of full dimension (ie. dimension 2) we require that $\prod_{i=1..l} D_\gamma \phi_i = Id$. By using transition maps of the form mentioned in (3.1) we get the following condition:

Condition 2.1 ([44]). *If $\gamma \in \mathcal{M}_0$ is an interior vertex and belongs to the faces $\sigma_1, \ldots, \sigma_l$ that are glued cyclically around γ, then the gluing data $[\mathfrak{a}_i, \mathfrak{b}_i]$ at γ on the edges τ_i between σ_{i-1} and σ_i satisfies*

$$\prod_{i=1}^{l} \begin{pmatrix} 0 & 1 \\ \mathfrak{b}_i(0) & \mathfrak{a}_i(0) \end{pmatrix} = \begin{pmatrix} 1 & 0 \\ 0 & 1 \end{pmatrix}. \tag{3.9}$$

This gives algebraic restrictions on the values $\mathfrak{a}_i(0)$, $\mathfrak{b}_i(0)$. In addition to Condition 2.1, we also consider the following condition around a crossing vertex:

Condition 2.2. *If the vertex γ is a crossing vertex with 4 edges $\tau_1, \ldots, \tau_4$, the gluing data $[\mathfrak{a}_i, \mathfrak{b}_i]$ $i = 1 \ldots 4$ on these edges at γ satisfy*

$$\mathfrak{a}_1'(0) + \frac{\mathfrak{b}_4'(0)}{\mathfrak{b}_4(0)} = -\mathfrak{b}_1(0)\left(\mathfrak{a}_3'(0) + \frac{\mathfrak{b}_2'(0)}{\mathfrak{b}_2(0)}\right), \tag{3.10}$$

$$\mathfrak{a}_2'(0) + \frac{\mathfrak{b}_1'(0)}{\mathfrak{b}_1(0)} = -\mathfrak{b}_2(0)\left(\mathfrak{a}_4'(0) + \frac{\mathfrak{b}_3'(0)}{\mathfrak{b}_3(0)}\right). \tag{3.11}$$

Let us notice that we can write the previous conditions on the gluing data (which in our setting is given by spline functions) as in [21] since they depend on the value of the functions defining the gluing data and are independent of the type of functions. The conditions (3.10) and (3.11) were introduced in [21] in the context of gluing data defined from polynomial functions. They generalize the conditions of [45], where $\mathfrak{b}_i(0) = -1$. The conditions come from the relations between the derivatives and the cross-derivatives of the face functions across the edges at a crossing vertex.

2.1 Example of transition maps

One way to define transition maps which satisfy these conditions, is to compute the values of the transition functions $\mathfrak{a}_\tau, \mathfrak{b}_\tau$ of an edge τ at its end points and then interpolate the values:

1. For all the vertices $\gamma \in \mathcal{M}_0$ and for all the edges $\tau_1, \ldots, \tau_l$ of $\mathcal{M}_1$ that contain γ, choose vectors $\mathbf{u}_1, \ldots, \mathbf{u}_F \in \mathbb{R}^2$ such that the cones in $\mathbb{R}^2$ generated by $\mathbf{u}_i, \mathbf{u}_{i+1}$ form a fan in $\mathbb{R}^2$ and such that the union of these cones is $\mathbb{R}^2$ when γ is an interior vertex. The vector $\mathbf{u}_i$ is associated to the edge τ_i, so that the sectors $\mathbf{u}_{i-1}, \mathbf{u}_i$ and $\mathbf{u}_i, \mathbf{u}_{i+1}$ define the gluing across the edge τ_i at γ.

   The transition map $\phi_{i-1,i}$ at $\gamma = (0,0)$ on the edge τ_i is constructed as:

$$J_{(0,0)}(\phi_{i-1,i})^t = S \circ [\mathbf{u}_i, \mathbf{u}_{i+1}]^{-1} \circ [\mathbf{u}_{i-1}, \mathbf{u}_i] \circ S = \begin{bmatrix} 0 & \mathfrak{b}_i(0) \\ 1 & \mathfrak{a}_i(0) \end{bmatrix}$$

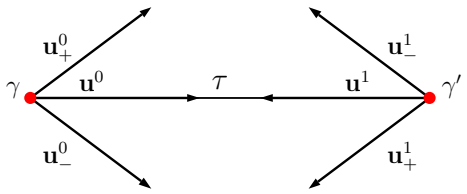

Figure 3.3: The edge $\tau = (\gamma, \gamma')$ is associated to the vectors $\mathbf{u}^0$ and $\mathbf{u}^1$ at the points γ and γ', respectively.

where $S = \begin{bmatrix} 0 & 1 \\ 1 & 0 \end{bmatrix}$, $[\mathbf{u}_i, \mathbf{u}_j]$ is the matrix which columns are the vectors $\mathbf{u}_i$ and $\mathbf{u}_j$, and $|\mathbf{u}_i, \mathbf{u}_j|$ is the determinant of the vectors $\mathbf{u}_i, \mathbf{u}_j$. Thus,

$$\mathfrak{a}_i(0) = \frac{|\mathbf{u}_{i+1}, \mathbf{u}_{i-1}|}{|\mathbf{u}_{i+1}, \mathbf{u}_i|}, \ \mathfrak{b}_i(0) = -\frac{|\mathbf{u}_i, \mathbf{u}_{i-1}|}{|\mathbf{u}_{i+1}, \mathbf{u}_i|}, \tag{3.12}$$

so that $\mathbf{u}_{i-1} = \mathfrak{a}_i(0)\mathbf{u}_i + \mathfrak{b}_i(0)\mathbf{u}_{i+1}$. This implies that Condition 2.1 is satisfied.

2. For all the shared edges $\tau \in \mathcal{M}_1$, we define the functions $\mathfrak{a}_\tau = \frac{a_\tau}{c_\tau}, \mathfrak{b}_\tau = \frac{b_\tau}{c_\tau}$ on the edges τ by interpolation as follows. Assume that the edge τ is associated to the vectors $\mathbf{u}^0$ and $\mathbf{u}^1$, respectively at the end point γ and γ' corresponding to the parameters $u = 0$ and $u = 1$. Let $\mathbf{u}^s_-, \mathbf{u}^s_+ \in \mathbb{R}^2$, $s = 0, 1$ be the vectors which define respectively the previous and next sectors adjacent to u^s_i at the point γ and γ', see Figure 3.3. We define the gluing data so that it interpolates the corresponding value (3.12) at $u = 0$ and $u = 1$ as:

$$\begin{aligned} a_\tau(u) &= \ |\mathbf{u}^0_+, \mathbf{u}^0_-|\mathfrak{d}_0(u) + |\mathbf{u}^1_+, \mathbf{u}^1_-|\mathfrak{d}_1(u) \\ b_\tau(u) &= -|\mathbf{u}^0, \mathbf{u}^0_-|\mathfrak{d}_0(u) - |\mathbf{u}^1, \mathbf{u}^1_-|\mathfrak{d}_1(u) \\ c_\tau(u) &= \ |\mathbf{u}^0_+, \mathbf{u}^0|\mathfrak{d}_0(u) + |\mathbf{u}^1_+, \mathbf{u}^1|\mathfrak{d}_1(u) \end{aligned} \tag{3.13}$$

where $\mathfrak{d}_0(u), \mathfrak{d}_1(u)$ are two Hermite interpolation functions at $u = 0$ and $u = 1$.

Since the derivatives of a_τ, b_τ, c_τ vanish at $u = 0$ and $u = 1$, the conditions (3.10) and (3.11) are automatically satisfied at an end point if it is a crossing vertex.

Another possible construction, with a constant denominator $c_\tau(u) = 1$ is:

$$\begin{aligned} a_\tau(u) &= \ \frac{|\mathbf{u}^0_+, \mathbf{u}^0_-|}{|\mathbf{u}^0_+, \mathbf{u}^0|}\mathfrak{d}_0(u) - \frac{|\mathbf{u}^1_+, \mathbf{u}^1_-|}{|\mathbf{u}^1_+, \mathbf{u}^1|}\mathfrak{d}_1(u) \\ b_\tau(u) &= -\frac{|\mathbf{u}^0, \mathbf{u}^0_-|}{|\mathbf{u}^0_+, \mathbf{u}^0|}\mathfrak{d}_0(u) + \frac{|\mathbf{u}^1, \mathbf{u}^1_-|}{|\mathbf{u}^1_+, \mathbf{u}^1|}\mathfrak{d}_1(u) \\ c_\tau(u) &= 1 \end{aligned} \tag{3.14}$$

The construction (3.14) specializes to the symmetric gluing used for instance in [44, §8.2], [46], [10]:

$$\begin{aligned} a_\tau &= \mathfrak{d}_0(u)\, 2\cos\frac{2\pi}{n_0} - \mathfrak{d}_1(u)\, 2\cos\frac{2\pi}{n_1} \\ b_\tau &= -1 \\ c_\tau &= 1 \end{aligned} \tag{3.15}$$

where n_0 (resp. n_1) is the number of edges at the vertex γ_0 (resp. γ_1). It corresponds to a symmetric gluing, where the angle of two consecutive edges at γ_i is $\frac{2\pi}{n_i}$, and the norms of all the vector $\mathbf{u}_i$ are equal. It is shown in [47] that under the form of the transition maps that we have chosen, the condition 2.1 hold if and only if $a_\tau(0) = 2\cos\frac{2\pi}{n_0}$.

3 Construction of G^1-spline basis

The basis that we want to produce for our space is locally supported. We show in this section how we can split the G^1-splines vector space into three components, and provide a basis for each one of them:

- One component is vertex supported. It means that each basis element of this component has a support around a xgiven vertex.
- The second component is edges supported, ie. each basis element has support along a given edge, and vanish at each vertex.
- One component is faces supported, ie. each basis elements of this component is supported over one given face, and vanish along all the edges.

The approach of splitting the space into the three components have been subject to several works before in geometric continuity [21, 23, 48, 49] as well as in parametric continuity [5, 6]. One strategy for building such a basis is to determine first, the G-spline space that corresponds to gluing two patches together along an edge. This basis is chosen in such a way that it can be pieced together with other basis elements corresponding to another edge sharing a vertex with the first edges. Thus we can form a basis element defined over all the surface, see for instance [22]. In this section we will describe two examples of standard algorithms that can be used to generate basis for the space of G-splines, with different kind of gluing data (See sections 3.1 and 4).

The second strategy is to find a minimal determining set, then set the other bspline coefficients according to the G^1 constraints chosen before.

3.1 Basis construction by piecing patches

To define the space of G^1-splines on $\mathcal{M}$, we will choose each face restriction f_σ to be an element of the space $\mathcal{R}_{d,\mathbf{t}}(\mathcal{M})$ of tensor product b-spline with knots $\mathbf{t} = [t_1, \ldots, t_s] \subset \mathbb{R}$ and of degree d in each variables u and v. An element $f_\sigma \in \mathcal{R}_{d,\mathbf{t}}$ is of the form

$$f_\sigma := \sum_{1 \leqslant i,j \leqslant m} c^\sigma_{i,j}(f_\sigma) b_i(u_\sigma) b_j(v_\sigma),$$

where $c^{\sigma}_{i,j}(f_\sigma) \in \mathbb{R}$ and $b_1, \ldots, b_m$ are the b-spline basis functions of the space $\mathcal{U}_{d,\mathbf{t}}$ of splines of degree d and knots $\mathbf{t}$ in one variable u. We denote by $(b^{\sigma}_{i,j})_{0\leqslant i,j\leqslant m-1}$ the b-spline basis functions on the face σ. With the previous notation, $b^{\sigma}_{i,j} = b_i(u_\sigma)b_j(v_\sigma)$. The functions are represented by a vector $\mathbb{R}^{m^2\times|\mathcal{M}_2|}$ with 1 at the position corresponding to the coefficient $c^{\sigma}_{i,j}$ and 0 elsewhere.

We will consider hereafter gluing data $[\mathfrak{a}_\tau, \mathfrak{b}_\tau]$, which are spline functions $\in \mathcal{U}_{d',\mathbf{t}'}$ of degree d' and knots $\mathbf{t}' = [t'_1, \ldots, t'_{s'}] \subset \mathbb{R}$, such that $t'_1 = \ldots = t'_{d'}$ and $t'_{s'-d'} = \ldots = t'_{s'}$.

Definition 3.1. *We denote by $\mathcal{S}_{d,\mathbf{t}}(\mathcal{M}, \mathfrak{g})$ (or $\mathcal{S}_{d,\mathbf{t}}(\mathcal{M})$ for simplicity) the vector space of G^1-functions on $\mathcal{M}$ for the gluing data $\mathfrak{g}$, with face restrictions f_σ in $\mathcal{R}_{d,\mathbf{t}}$.*

An element in $\mathcal{S}_{d,\mathbf{t}}(\mathcal{M}, \mathfrak{g})$ is in the space $\mathcal{R}_{d,\mathbf{t}}(\mathcal{M})$ of b-spline functions on each face. It will be represented by its b-spline coefficients on each face, that is, by a vector in $\mathbb{R}^{m^2\times|\mathcal{M}_2|}$.

For two vectors $f, f' \in \mathcal{R}_{d,\mathbf{t}}(\mathcal{M}) \equiv \mathbb{R}^{m^2\times|\mathcal{M}_2|}$, we denote by $\langle f, f' \rangle$ the usual scalar product of their b-spline coefficients.

For a vertex γ of a face σ, we denote by T^{σ}_{γ} the map $T^{\sigma}_{\gamma} : \mathcal{S}_{d,\mathbf{t}}(\mathcal{M}, \mathfrak{g}) \to \mathbb{R}^4$ that associates to each differentiable function $f \in \mathcal{S}_{d,\mathbf{t}}(\mathcal{M}, \mathfrak{g})$ the following vector:

$$T^{\sigma}_{\gamma}(f) = \left[\, c^{\sigma}_{0,0}(f),\, c^{\sigma}_{1,0}(f),\, c^{\sigma}_{0,1}(f),\, c^{\sigma}_{1,1}(f) \,\right]$$

where $c_{0,0}, c_{1,0}, c_{0,1}, c_{1,1}$ are the corner b-spline coefficients of $f \in \mathcal{R}_{d,\mathbf{t}}$ corresponding to γ. We call these coefficients, the (first) Taylor coefficients of f around γ. For $\gamma \in \mathcal{M}_0$ an end point of an edge τ shared by the faces σ_0, σ_1, let $T^{\tau}_{\gamma} : (f_0, f_1) \mapsto T^{\sigma_0}_{\gamma}(f_0) \oplus T^{\sigma_1}_{\gamma}(f_1)$.

A desired property for the space of G^1-splines is the possibility to arbitrarily fix the Taylor coefficients at a vertex on a face. This means that at each vertex, we should be able to fix the values, derivatives and cross derivatives and construct a G^1-spline function that interpolates these values and derivatives. This leads to the following definition:

Definition 3.2. *The space $\mathcal{S}_{d,\mathbf{t}}(\mathcal{M}, \mathfrak{g})$ of G^1-spline space is* ample *if for every vertex $\gamma \in \mathcal{M}_0$ and every face $\sigma \in \mathcal{M}_2$ adjacent to γ, the map T^{σ}_{γ} is surjective.*

3.2 Taylor maps

An important tool that we are going to use intensively is the Taylor map associated to a vertex or to an edge of $\mathcal{M}$. For each face σ the space of spline functions over a subdivision into 4 parts as in the figure above will be denoted $\mathcal{R}^r(\sigma)$. Let $\gamma \in \mathcal{M}_0$ be a vertex on a face $\sigma \in \mathcal{M}_2$ belonging to two edges $\tau, \tau' \in \mathcal{M}_1$ of σ. We define the *ring of γ on σ* by $\mathcal{R}^{\sigma}(\gamma) = \mathcal{R}(\sigma)/(\ell^2_\tau, \ell^2_{\tau'})$ where $(\ell^2_\tau, \ell^2_{\tau'})$ is the ideal generated by the squares of ℓ_τ and $\ell_{\tau'}$. The equations $\ell_\tau(u, v) = 0$ and $\ell_{\tau'}(u, v) = 0$ are respectively the equations of τ and τ' in $\mathcal{R}^r(\sigma) = \mathcal{S}^r$.

The *Taylor expansion at γ on σ* is the map

$$T^{\sigma}_{\gamma} : f \in \mathcal{R}^r(\sigma) \mapsto f \mod (\ell^2_\tau, \ell^2_{\tau'}) \text{ in } \mathcal{R}^{\sigma}(\gamma).$$

Choosing an adapted basis of $\mathcal{R}^\sigma(\gamma)$, one can define T^σ_γ by

$$T^\sigma_\gamma(f) = \big[\, f(\gamma),\, \partial_u f(\gamma),\, \partial_v f(\gamma),\, \partial_u\partial_v f(\gamma) \,\big].$$

The map T^σ_γ can also be defined in another basis of $\mathcal{R}^\sigma(\gamma)$ in terms of the b-spline coefficients by

$$T^\sigma_\gamma(f) = \big[\, c^\sigma_{0,0}(f),\, c^\sigma_{1,0}(f),\, c^\sigma_{0,1}(f),\, c^\sigma_{1,1}(f) \,\big]$$

where $c_{0,0}, c_{1,0}, c_{0,1}, c_{1,1}$ are the first b-spline coefficients associated to f on σ at $\gamma = (0,0)$.

We define the Taylor map T_γ on all the faces σ that contain γ,

$$T_\gamma : f = (f_\sigma) \in \oplus_\sigma \mathcal{R}^r(\sigma) \to (T^\sigma_\gamma(f_\sigma)) \in \oplus_{\sigma\supset\gamma}\mathcal{R}^\sigma(\gamma).$$

Similarly, we define T as the Taylor map at all the vertices on all the faces of $\mathcal{M}$.

If $\tau \in \mathcal{M}_1$ is the edge of the face $\sigma(u_\sigma, v_\sigma) \in \mathcal{M}_2$ associated to $v_\sigma = 0$, we define the *restriction along τ on σ* as

$$\begin{array}{rcl} D^\sigma_\tau : \mathcal{R}_{k,r}(\sigma) & \to & \mathcal{R}_{k,r}(\sigma) \\ f = \displaystyle\sum_{0\leqslant i,j\leqslant m} c^\sigma_{i,j}(f) b_i(u_\sigma) b_j(v_\sigma) & \mapsto & \displaystyle\sum_{0\leqslant i\leqslant m, 0\leqslant j\leqslant 1} c^\sigma_{i,j}(f) b_i(u_\sigma) b_j(v_\sigma). \end{array}$$

The restrictions along the edges $v_\sigma = 1$, $u_\sigma = 0$, $u_\sigma = 1$ are defined similarly by symmetry. By convention if τ is not an edge of σ, $D^\sigma_\tau = 0$.

For a face $\sigma \in \mathcal{M}_2$, we define the *restriction along the edges of σ* as

$$\begin{array}{rcl} D^\sigma : \mathcal{R}_{k,r}(\sigma) & \to & \mathcal{R}_{k,r}(\sigma) \\ f = \displaystyle\sum_{0\leqslant i,j\leqslant m} c^\sigma_{i,j}(f) b_i(u_\sigma) b_j(v_\sigma) & \mapsto & \displaystyle\sum_{\substack{i>1, \text{ or} \\ i<m-1, j>1, \\ \text{or } j<m-1}} c^\sigma_{i,j}(f) b_i(u_\sigma) b_j(v_\sigma). \end{array}$$

The edge restriction map along all edges of $\mathcal{M}$ is given by

$$D : f = (f_\sigma) \in \oplus_\sigma \mathcal{R}_{k,r}(\sigma) \to (D^\sigma(f_\sigma)) \in \oplus_\sigma \mathcal{R}_{k,r}(\sigma).$$

3.3 G^1-splines along an edge

We consider first a topological mesh $\mathcal{M}_\tau$ with two faces σ_0, σ_1 sharing an edge τ, with the gluing data $\mathfrak{g}_\tau = (\mathfrak{a}, \mathfrak{b})$.

The G^1-spline functions of $\mathcal{S}_{d,\mathbf{t}}(\mathcal{M}_\tau, \mathfrak{g}_\tau)$ are the pairs $f = (f_0, f_1)$ of b-spline functions $f_0, f_1 \in \mathcal{R}_{d,\mathbf{t}}$, which satisfies the relations (3.2) and (3.5). If τ is defined by $v_1 = 0$ on σ_1 and $u_0 = 0$ on σ_0, these relations involve only the b-spline coefficients $c^{\sigma_1}_{i,j}(f)$, $c^{\sigma_0}_{j,i}(f)$ for $0 \leqslant i \leqslant m-1$ and $0 \leqslant j \leqslant 1$. The other coefficients can be chosen arbitrarily. Let us denote by $\mathcal{S}_\tau$ the space of b-spline functions (f_0, f_1) in $\mathcal{S}_{d,\mathbf{t}}(\mathcal{M}_\tau, \mathfrak{g}_\tau)$ with all these other coefficients equal to 0. The elements of $\mathcal{S}_\tau$ are the G^1-spline functions *supported* along the edge τ.

Let $\gamma, \gamma' \in \mathcal{M}_0$ be the end vertices of τ. We denote $\mathcal{E}_\tau = \mathcal{S}_\tau \cap \ker T_\gamma \cap \ker T_{\gamma'}$. It is the vector space of G^1-spline in $\mathcal{S}_\tau$ supported along τ, with zero b-spline coefficients at γ and γ'.

Let $\mathcal{E}_\tau^\perp$ be the b-splines in $\mathcal{S}_{d,\mathbf{t}}(\mathcal{M}_\tau)$ which are orthogonal to all the elements in $\mathcal{E}_\tau$ for the scalar product on the b-spline coefficients. We denote $\mathcal{S}_{\gamma,\tau} = \mathcal{S}_\tau \cap \mathcal{E}_\tau^\perp \cap \ker T_{\gamma'}^\tau$ and similarly $\mathcal{S}_{\gamma',\tau} = \mathcal{S}_\tau \cap \mathcal{E}_\tau^\perp \cap \ker T_\gamma^\tau$. By construction, we have

$$\mathcal{S}_\tau \supset \mathcal{S}_{\gamma,\tau} \oplus \mathcal{E}_\tau \oplus \mathcal{S}_{\gamma',\tau}.$$

Definition 3.3. *The space $\mathcal{S}_\tau$ is* separable *if $\mathcal{S}_\tau = \mathcal{S}_{\gamma,\tau} \oplus \mathcal{E}_\tau \oplus \mathcal{S}_{\gamma',\tau}$.*

If $\mathcal{S}_\tau$ is separable, then any G^1-spline function $\in \mathcal{S}_\tau$ can be uniquely decomposed as a sum of a G^1-spline function f with $T_\gamma^{\sigma_0}(f) = T_\gamma^{\sigma_1}(f) = T_{\gamma'}^{\sigma_0}(f) = T_{\gamma'}^{\sigma_1}(f) = 0$, a function g determined by its coefficients $T_\gamma^{\sigma_0}(g), T_\gamma^{\sigma_1}(g)$, and a function h determined by its coefficients $T_{\gamma'}^{\sigma_0}(h), T_{\gamma'}^{\sigma_1}(h)$. This implies that the Bézier coefficients of a G^1-spline at a vertex are linearly independent of the Bézier coefficients at the other vertex.

If $\mathcal{S}_\tau$ is not separable, there exists an element in $\mathcal{S}_\tau$ with non-zero Bézier coefficients at the two vertices, linearly independent of the G^1-spline functions with zero coefficients at one of the vertices. If the mesh has more that one edge, this will induce the existence of G^1-spline basis functions attached to vertices, whose support is not included in the neighborhood of cells adjacent to the vertex. Since we are interested in G^1-spline spaces that admit a basis of functions with a local support, hereafter we only consider and construct separable G^1-spline spaces.

We construct now explicit spaces of G^1-spline functions along an edge. We consider b-spline spaces $\mathcal{R}_{d,\mathbf{t}}$ with a small degree d ($d = 2, \dots, 7$) and a small number m^2 of control points per face ($m \leqslant 8$). The knots $\mathbf{t}$ of the b-spline functions are between 0 and 1. The set of distinct knots is a uniform subdivision of the interval $[0, 1]$, so that the b-spline functions share the same knots on the common edges. The gluing data on the edge are of the form $\mathfrak{a}(u) = a\,\Theta_0(u) - b\,\Theta_1(u)$, $\mathfrak{b}(u) = -1$ with a, b two parameters and $\Theta_0(u)$, $\Theta_1(u)$ two functions interpolating 1 at 0 and 1.

Translating the equations (3.2) and (3.5) into linear equations in the $4\,m$ coefficients $c_{i,j}^{\sigma_1}(f)$, $c_{j,i}^{\sigma_0}(f)$ for $0 \leqslant i \leqslant m-1$ and $0 \leqslant j \leqslant 1$, we compute bases of the spaces $\mathcal{S}_\tau, \mathcal{S}_{\gamma,\tau}, \mathcal{E}_\tau, \mathcal{S}_{\gamma',\tau}$ depending on the values of a, b for a given edge τ. This can be precomputed for given degree and knot distribution of b-spline patches and for given type of gluing data (e.g. using a computer algebra system such as Maple).

Basis of $\mathcal{E}_\tau$

We compute a basis $e_1^\tau, \dots, e_l^\tau$ of $\mathcal{E}_\tau$ defined by the equations (3.2), (3.5), $T_\gamma^\tau(f) = 0$ and $T_{\gamma'}^\tau(f) = 0$. Notice that the functions e_i^τ are G^1 splines on the whole topological space $\mathcal{M}$, since they are G^1 along the edge τ and $T_\gamma^\tau(e_i^\tau) = T_{\gamma'}^\tau(e_i^\tau) = 0$. These will be called the *edge basis functions* of the edge τ.

We denote by $\mathcal{B}_\tau^1 = \{b_{i_1,j_1}^{\sigma_{k_1}}, \dots, b_{i_l,j_l}^{\sigma_{k_l}}\}$ a set of free coefficients in the linear system of equations (3.2), (3.5), $T_\gamma^\tau(f) = 0$, $T_{\gamma'}^\tau(f) = 0$. This is a Minimal Determining Set of coefficients for $\mathcal{E}_\tau$.

Basis of $\mathcal{S}_{\gamma,\tau}$

By definition of the space $\mathcal{S}_{\gamma,\tau}$, when the G^1-spline space $\mathcal{S}_\tau$ is separable and ample, the map T^σ_γ is injective on $\mathcal{S}_{\gamma,\tau}$ and its image is at least of dimension 4. This implies that the dimension of $\mathcal{S}_{\gamma,\tau}$ is at least 4. Since there are 3 independent relations between the 8 Taylor coefficients at a vertex γ on the two faces σ, σ' (the coefficients on the common edge are equal and the derivatives along the edges adjacent to γ are dependent), the dimension of $\mathcal{S}_{\gamma,\tau}$ is at most $8-3=5$.

We define $\delta(\gamma,\tau)=0$ if $\dim(\mathcal{S}_{\gamma,\tau})=5$ and $\delta(\gamma,\tau)=1$ otherwise. If τ is a boundary edge, we let $\delta(\gamma,\tau)=0$. By definition $\dim S_{\gamma,\tau}=5-\delta(\gamma,\tau)$ We says that τ is a crossing edge at γ if $\delta(\gamma,\tau)=1$ and a non-crossing edge otherwise. We define $\delta(\gamma)=\min\{\delta(\gamma,\tau)\mid \tau\ni\gamma\}$.

- If $\delta(\gamma,\tau)=1$ (crossing edge), $\dim(\mathcal{S}_{\gamma,\tau})=4$ and a Minimal Determining Set of coefficients is associated to the b-spline functions $\mathcal{B}^0_{\gamma,\tau}=\{b^{\sigma_0}_{0,0},b^{\sigma_0}_{1,0},b^{\sigma_0}_{0,1},b^{\sigma_0}_{1,1}\}$.
- If $\delta(\gamma,\tau)=0$ (non-crossing edge), $\dim(\mathcal{S}_{\gamma,\tau})=5$ and a minimal determining set of $\mathcal{S}_{\gamma,\tau}$ is associated to the b-spline functions $\mathcal{B}_{\gamma,\tau}=\{b^{\sigma_0}_{0,0},b^{\sigma_0}_{1,0},b^{\sigma_0}_{0,1},b^{\sigma_0}_{1,1},b^{\sigma_1}_{1,1}\}$.

These sets are maximal sets of free coefficients in the linear system defining $\mathcal{S}_{\gamma,\tau}$. They are Minimal Determining Sets for $\mathcal{S}_{\gamma,\tau}$.

The space $\mathcal{S}_{\gamma,\tau}=\mathcal{S}_\tau\cap\mathcal{E}^\perp_\tau\cap\ker T^\tau_{\gamma'}$ is defined by the equations (3.2), (3.5), $\langle f,e^\tau_i\rangle=0, i=1,\dots,l$, and $T^\tau_{\gamma'}(f)=0$.

As $\mathcal{B}_{\gamma,\tau}$ is a maximal set of free coefficients in this system, it can be transformed by linear combinations of these equations, into a system of the form

$$\left[\ A_{\gamma,\tau}\ \middle|\ \mathrm{Id}\ \right]\cdot c(f)=0 \tag{3.16}$$

where the columns of $A_{\gamma,\tau}$ are indexed by the coefficients $\mathcal{B}_{\gamma,\tau}$ and the last identity block indexed by the set $\mathcal{C}_{\gamma,\tau}$ of remaining coefficients among all coefficients of b-splines functions supported along τ. The vector $c(f)$ is the vector of all the coefficients of functions supported along τ.

Notice that this matrix $A_{\gamma,\tau}$ can be precomputed for each edge τ, independently of the structure of the mesh. It depends only on the gluing data on τ.

Examples of ample separable spaces

Hereafter, we describe cases of ample separable spaces of G^1-splines for low d and m. In these tables, we give the degree d, the knots $\mathbf{t}$, the number m of control points along the edge, the gluing function $\mathfrak{a}(u)$ and the dimensions of $\mathcal{S}_\tau,\mathcal{S}_{\gamma,\tau},\mathcal{E}_\tau,\mathcal{S}_{\gamma',\tau}$ for different values of a and b.

- $d=2$, $\mathbf{t}=[0^3,\frac14,\frac12,\frac34,1^3]$, $m=6$, $\mathfrak{a}(u)=a\,(1-4u)\mathbf{1}_{[0,\frac14]}-b\,(4u-3)\mathbf{1}_{[\frac34,1]}$

a	b	$\mathcal{S}_\tau$	$S_{\gamma,\tau}$	$\mathcal{E}_\tau$	$\mathcal{S}_{\gamma',\tau}$
$\neq 0$	$\neq 0$	10	4	2	4
$=0$	$\neq 0$	11	4	3	4
$=0$	$=0$	12	4	4	4

This construction is closely related to the construction described in [50] with C^1 biquadratic polynomials on each patch and the extraordinary vertices separated by 4 biquadratic patches.

A construction of G^1-splines which are C^1 bicubic b-splines on each patch with linear gluing data has been proposed in [46]. It applies under some genericity conditions on $\mathcal{M}$. Each face has $6 \times 6 = 36$ b-spline coefficients ($m = 6$). An explicit computation shows that the dimensions of $\mathcal{S}_\tau$, $S_{\gamma,\tau}$, $\mathcal{E}_\tau$, $\mathcal{S}_{\gamma',\tau}$ are respectively 11, 4, 2, 4 for $a \neq 0$, $b \neq 0$. Thus the space is not separable.

- $d = 3$, $\mathbf{t} = [0^4, \frac{1}{3}, \frac{2}{3}, 1^4]$, $m = 6$, $\mathfrak{a}(u) = a\,(1-3u)\mathbf{1}_{[0,\frac{1}{3}]} - b\,(3u-2)\mathbf{1}_{[\frac{2}{3},1]}$.

a	b	$\mathcal{S}_\tau$	$S_{\gamma,\tau}$	$\mathcal{E}_\tau$	$\mathcal{S}_{\gamma',\tau}$
$\neq 0$	$= 0$	10	4	2	4
$= 0$	$= 0$	12	4	4	4

An explicit computation shows that when $a \neq 0, b \neq 0$, i.e. when none of the end points of the edge is a crossing vertex, the space $\mathcal{S}_\tau$ is not separable.

- $d = 3$, $\mathbf{t} = [0^4, \frac{1}{3}, \frac{1}{3}, \frac{2}{3}, \frac{2}{3}, 1^4]$, $m = 8$, $\mathfrak{a}(u) = a\,(1-3u)\mathbf{1}_{[0,\frac{1}{3}]} - b\,(3u-2)\mathbf{1}_{[\frac{2}{3},1]}$ or $\mathfrak{a}(u) = a\,(3u-1)^2\mathbf{1}_{[0,\frac{1}{3}]} - b\,(3u-2)^2\mathbf{1}_{[\frac{2}{3},1]}$.

a	b	$\mathcal{S}_\tau$	$S_{\gamma,\tau}$	$\mathcal{E}_\tau$	$\mathcal{S}_{\gamma',\tau}$
$\neq 0$	$\neq 0$	14	5	4	5
$\neq 0$	$= 0$	15	5	6	4
$= 0$	$= 0$	16	4	8	4

The case where $\mathfrak{a}$ is of degree 1 corresponds to the construction in [51] and [45], where the linear function $\mathfrak{a}$ is replaced by a piecewise linear function. In this case, the transition map is not necessarily C^1.

The second case where $\mathfrak{a}$ is of degree 2 is a new construction. The gluing data $\mathfrak{a}$ is C^1 for any value of a and b.

- $d = 3$, $\mathbf{t} = [0^4, \frac{1}{5}, \frac{2}{5}, \frac{3}{5}, \frac{4}{5}, 1^4]$, $m = 8$, $\mathfrak{a}(u) = a\,(1-5u)\mathbf{1}_{[0,\frac{1}{5}]} - b\,(5u-4)\mathbf{1}_{[\frac{4}{5},1]}$ or $\mathfrak{a}(u) = a\,(1-5u)^2\mathbf{1}_{[0,\frac{1}{5}]} - b\,(5u-4)^2\mathbf{1}_{[\frac{4}{5},1]}$

a	b	$\mathcal{S}_\tau$	$S_{\gamma,\tau}$	$\mathcal{E}_\tau$	$\mathcal{S}_{\gamma',\tau}$
$\neq 0$	$\neq 0$	12	4	4	4
$\neq 0$	$= 0$	14	4	6	4
$= 0$	$= 0$	16	4	8	4

These two cases are also new constructions of G^1-splines. The functions are C^2 on each faces and the gluing data is C^1 for any value of a and b when $\mathfrak{a}$ is of degree 2.

- $d = 4$, $\mathbf{t} = [0^5, \frac{1}{2}, \frac{1}{2}, \frac{1}{2}, 1^5]$, $m = 8$, $\mathfrak{a}(u) = a\,(1-2u)^2\mathbf{1}_{[0,\frac{1}{2}]} - b\,(2u-1)^2\mathbf{1}_{[\frac{1}{2},1]}$

a	b	$\mathcal{S}_\tau$	$S_{\gamma,\tau}$	$\mathcal{E}_\tau$	$\mathcal{S}_{\gamma',\tau}$
$\neq 0$	$\neq 0$	14	5	4	5
$\neq 0$	$= 0$	15	5	6	4
$= 0$	$= 0$	16	4	8	4

This corresponds to the construction described in [10] with C^1 biquartic b-splines on each patch. It is also related to the construction in [52] where biquartic patches with quadratic transition maps are involved.

- $d = 5, \mathbf{t} = [0^6, 1^6], m = 6,$

  For this degree, we consider gluing data of degree 1 when the vertices are not crossing vertices (i.e. $a \neq 0, b \neq 0$): $\mathfrak{a}(u) = a\,(1-u) - b\,u$.

a	b	$\mathcal{S}_\tau$	$S_{\gamma,\tau}$	$\mathcal{E}_\tau$	$\mathcal{S}_{\gamma',\tau}$
$\neq 0$	$\neq 0$	12	5	2	5

  When one of the vertices is a crossing vertex (i.e. $a = 0$ or $b = 0$, we use gluing data of degree 2: $\mathfrak{a}(u) = a\,(1-u)^2$.

a	b	$\mathcal{S}_\tau$	$S_{\gamma,\tau}$	$\mathcal{E}_\tau$	$\mathcal{S}_{\gamma',\tau}$
$\neq 0$	$= 0$	11	5	2	4
$= 0$	$= 0$	12	4	4	4

  This corresponds to the G^1-space used for the IsoGeometric Analysis application in Section 2.

- $d = 7, \mathbf{t} = [0^8, 1^8], m = 8, \mathfrak{a}(u) = a\,(1-u)^2 - b\,u^2$

a	b	$\mathcal{S}_\tau$	$S_{\gamma,\tau}$	$\mathcal{E}_\tau$	$\mathcal{S}_{\gamma',\tau}$
$\neq 0$	$\neq 0$	15	5	5	5
$\neq 0$	$= 0$	15	5	6	4
$= 0$	$= 0$	16	4	8	4

  This is a new construction, which falls in the separable cases studied in [21]. The gluing data is C^1 for any value of a and b.

3.4 G^1-splines around a vertex

We present now a new method to construct G^1-spline basis functions around a vertex $\gamma \in \mathcal{M}_0$ from the analysis of $\mathcal{S}_{\gamma,\tau}$ for $\tau \ni \gamma$, assuming $\mathcal{S}_\tau$ is ample and separable. Let $\sigma_1, \ldots, \sigma_v$ be the faces of $\mathcal{M}$ adjacent to the vertex γ, where v is the valence of γ. We denote by $\mathcal{M}_\gamma$ the sub-topological surface induced by these faces and by $\mathfrak{g}_\gamma$ the corresponding gluing data. We assume that γ is an interior point (the treatment of a boundary point will be similar). The edge between the faces σ_i and σ_{i+1} is $\tau_i = (\gamma, \gamma_i)$ for $i = 1, \ldots, v$ (with the convention that $\sigma_{v+1} = \sigma_1$). The gluing data along the edge τ_i are denoted $\mathfrak{a}_i, \mathfrak{b}_i$. Let $\mathcal{S}_\gamma \subset \mathcal{S}(\mathcal{M}_\gamma, \mathfrak{g}_\gamma)$ be the space of G^1-splines around the vertex γ, with support along the edges τ_i and with zero Taylor coefficients at the exterior vertices γ_i. Since the elements of $\mathcal{S}_\gamma$ have a support along the edges τ_i and zero Taylor coefficients at the exterior vertices γ_i, they define G^1-splines on the global mesh: $S_\gamma \subset \mathcal{S}(\mathcal{M}, \mathfrak{g})$.

The space $\mathcal{E}_\gamma \subset \mathcal{S}_\gamma$ of G^1-splines in $\mathcal{S}_\gamma$ supported along the edges τ_i with zero Taylor coefficients at γ and at the exterior vertices γ_i decomposes as $\mathcal{E}_\gamma = \oplus_{i=1}^f \mathcal{E}_{\tau_i}$ where $\mathcal{E}_{\tau_i}$ is the space of G^1-splines defined in Section 3.3. Any element in $\mathcal{E}_\gamma$ is a

sum of elements with support along the edges τ_i and zero Taylor coefficients at γ and γ_i, that is an element of $\mathcal{E}_{\tau_i}$. A basis of $\mathcal{E}_{\tau_i}$ has been computed in Section 3.3.

The space $\mathcal{S}_\gamma$ decomposes as $\mathcal{S}_\gamma = \mathcal{E}_\gamma \oplus \mathcal{V}_\gamma$ where $\mathcal{V}_\gamma = \mathcal{E}_\gamma^\perp \cap \mathcal{S}_\gamma$ is the space orthogonal (and thus supplementary) to $\mathcal{E}_\gamma$ in $\mathcal{S}_\gamma$ (for the classical inner-product on their b-spline coefficients). We are going to construct a basis of $\mathcal{V}_\gamma$, that we will call the *vertex basis functions* of the vertex γ.

We assume for simplicity that either $v = 4$ and $\delta(\gamma, \tau_i) = 1$ for $i = 1, \dots, 4$ (crossing vertex) or $\delta(\gamma, \tau_i) = 0$ for $i = 1, \dots, v$ (non-crossing vertex).

Vertex basis algorithm Let $\gamma \in \mathcal{M}_0$ be a vertex with adjacent edges $\tau_1, \dots, \tau_v$ and adjacent faces $\sigma_1, \dots, \sigma_v$.

- If $\delta(\gamma, \tau_i) = 1$ (crossing vertex), then let

$$G_\gamma = [b^{\sigma_1}_{0,0}, b^{\sigma_1}_{1,0}, b^{\sigma_1}_{0,1}, b^{\sigma_1}_{1,1}]$$

  be the coefficient matrix of the canonical basis elements $b^{\sigma_1}_{0,0}, b^{\sigma_1}_{1,0}, b^{\sigma_1}_{0,1}, b^{\sigma_1}_{1,1}$.

- If $\delta(\gamma, \tau_i) = 0$, let

$$G_\gamma = [b^{\sigma_1}_{0,0}, b^{\sigma_1}_{1,0}, b^{\sigma_1}_{0,1}, b^{\sigma_1}_{1,1}, , \dots, b^{\sigma_v}_{1,1}]$$

  be the coefficient matrix of the corresponding canonical basis elements.

For $i = 1, \dots, v$, we define the coefficients along the edge τ_i as follows

$$G_\gamma[\mathcal{C}_{\tau_i}, :] := -A_{\gamma,\tau_i} G_\gamma[\mathcal{B}_{\tau_i}, :]$$

where $\mathcal{B}_{\tau_i}$ are the b-spline basis functions indexing the columns of A_{τ_i} and $\mathcal{C}_{\tau_i}$ are indexing the identity block in (3.16).

Proposition 3.4. *The spline functions G_γ constructed by this algorithm form a basis of $\mathcal{V}_\gamma$.*

Proof. For each edge τ_i, the restriction of the elements of G_γ to $\mathcal{M}_{\tau_i}$ are in $\mathcal{S}_{\gamma,\tau_i}$ since, by construction, we have

$$\left[\begin{array}{c|c} A_{\gamma,\tau_i} & \mathrm{Id} \end{array}\right] \left[\begin{array}{c} G_\gamma[\mathcal{B}_{\tau_i}, :] \\ G_\gamma[\mathcal{C}_{\tau_i}, :] \end{array}\right] = \left[\begin{array}{c|c} A_{\gamma,\tau_i} & \mathrm{Id} \end{array}\right] \left[\begin{array}{c} G_\gamma[\mathcal{B}_{\tau_i}, :] \\ -A_{\gamma,\tau_i} G_\gamma[\mathcal{B}_{\tau_i}, :] \end{array}\right] = 0.$$

so that they satisfy the linear relations defining $\mathcal{S}_{\gamma,\tau_i}$. As this is true for all the edges τ_i containing γ, they are in $\mathcal{V}_\gamma$.

If $\delta(\gamma, \tau_i) = 0$ (non-crossing vertex), the coefficients $c^{\sigma_i}_{0,0}, c^{\sigma_i}_{1,0}, c^{\sigma_i}_{0,1}, i = 1, \dots, v$ are linked by the relations $c^{\sigma_i}_{0,0} = c^{\sigma_{i+1}}_{0,0}$, $c^{\sigma_i}_{0,1} = c^{\sigma_{i+1}}_{1,0}$ and $c^{\sigma_{i+1}}_{0,1} - c^{\sigma_{i+1}}_{0,0} = \mathfrak{b}_i(0)(c^{\sigma_i}_{1,0} - c^{\sigma_i}_{0,0}) + \mathfrak{a}_i(0)(c^{\sigma_i}_{0,1} - c^{\sigma_i}_{0,0})$. As the gluing data satisfies the cocyle condition 2.2, this system defines a linear space of dimension 3. The coefficients $c^{\sigma_1}_{1,1}, \dots, c^{\sigma_v}_{1,1}$ are free and the coefficients in $\mathcal{C}_{\tau_i}$ are determined by the relations (3.16). Thus the space $\mathcal{V}_\gamma$ defined by all these equations is of dimension $3 + v$, which is also the number of elements in G_γ.

Let us show that the elements in G_γ are linearly independent. By the linear transformation of the algorithm and the cocyle condition, the matrix $G_\gamma[\mathcal{B}_\gamma, :]$ is not changed and is the identity. Thus the elements G_γ are independent and, therefore, form a basis of $\mathcal{V}_\gamma$.

If $\delta(\gamma, \tau_i) = 1$ (crossing vertex), a similar argument on the coefficients $c_{0,0}^{\sigma_i}, c_{1,0}^{\sigma_i}$, $c_{0,1}^{\sigma_i}, c_{1,1}^{\sigma_i}, i = 1, \ldots, v$ and the cocyle condition 2.2 show that $\mathcal{V}_\gamma$ is of dimension 4. Similarly, $G_\gamma[\mathcal{B}_\gamma, :]$ is the identity matrix and G_γ is a basis of $\mathcal{V}_\gamma$. □

3.5 Dimension formula for $\mathcal{S}_{d,\mathbf{t}}(\mathcal{M}, \mathfrak{g})$

We consider here a degree d, a knot distribution $\mathbf{t}$ which gives a separable and ample space of G^1-splines $\mathcal{S}_{d,\mathbf{t}}(\mathcal{M}, \mathfrak{g})$.

Theorem 3.5. *Assume that $\mathcal{S}_{d,\mathbf{t}}(\mathcal{M}, \mathfrak{g})$ is separable and ample then*

$$\dim \mathcal{S}_{d,\mathbf{t}}(\mathcal{M}, \mathfrak{g}) = ((m-4)^2 + 4) f_2 + \sum_{\tau \in \mathcal{M}_1} \epsilon(\tau) - \sum_{(\gamma,\tau)|\gamma \in \tau} \delta(\gamma, \tau) + 3 f_0 + f_{0,\delta} \tag{3.17}$$

where

- $f_2 = |\mathcal{M}_2|$ *is the number of faces of* $\mathcal{M}$,
- $f_0 = |\mathcal{M}_0|$ *is the number of vertices of* $\mathcal{M}$,
- $f_{0,\delta}$ *is the number of vertices* $\gamma \in \mathcal{M}$ *such that* $\delta(\gamma) = 1$,
- $\epsilon(\tau) = \dim(\mathcal{E}_\tau)$,
- $\delta(\gamma, \tau) = 5 - \dim(\mathcal{S}_{\gamma,\tau})$ *for an interior edge,* $\delta(\gamma, \tau) = 0$ *for a boundary edge.*

Proof. The dimension is obtained by counting the number of basis functions attached to faces, edges, and vertices using the construction of the previous section.

For each face σ, the b-spline basis function with interior control points are basis elements. There are $(m-4)^2$ such elements per face.

For each edge τ, a basis of the space $\mathcal{E}_\tau$ are also basis elements of $\mathcal{S}_{\gamma,\tau}$.

For each vertex γ, the number of basis functions attached to it is $3 + f_\gamma - \sum_{\tau \ni \gamma} \delta(\gamma, \tau) + \delta(\gamma)$, where f_γ is the number of faces adjacent to γ. Since each face has 4 vertices, $\sum_{\gamma \in \mathcal{M}_0} f_\gamma = 4 f_2$.

Summing up all these terms gives formula (3.17). □

3.6 Example

We consider the knot sequence $\mathbf{t} = [0^4, \frac{1}{2}, \frac{1}{2}, 1^4]$ defining bicubic C^1 splines with $m = 6$ control points per edge. We take gluing data of the form $\mathfrak{a}(u) = a\,(1 - 3u)\mathbf{1}_{[0,\frac{1}{3}]} - b\,(3u - 2)\mathbf{1}_{[\frac{2}{3},1]}$. Let τ be an interior edge of $\mathcal{M}$ and let σ_0, σ_1 be the adjacent faces to τ. We have the separability property for $b = 0$:

a	b	$\mathcal{S}_\tau$	$S_{\gamma,\tau}$	$\mathcal{E}_\tau$	$\mathcal{S}_{\gamma',\tau}$
$\neq 0$	$= 0$	11	5	2	4
$= 0$	$= 0$	12	4	4	4

The computation of a basis of $\mathcal{E}_\tau$ for $a \neq 0, b = 0$ yields

$$\mathcal{B}_\tau = [-b^{\sigma_0}_{1,2} + b^{\sigma_1}_{2,1}, -b^{\sigma_0}_{1,3} + b^{\sigma_1}_{3,1}]$$

The relations defining $\mathcal{S}_{\gamma,\tau}$ are of the form

$$\begin{bmatrix} c^{\sigma_1}_{0,0} \\ c^{\sigma_1}_{1,0} \\ c^{\sigma_1}_{0,1} \\ c^{\sigma_0}_{0,2} \\ c^{\sigma_0}_{0,3} \\ c^{\sigma_0}_{1,2} \\ c^{\sigma_0}_{1,3} \\ c^{\sigma_1}_{2,0} \\ c^{\sigma_1}_{2,1} \\ c^{\sigma_1}_{3,0} \\ c^{\sigma_1}_{3,1} \end{bmatrix} = \begin{bmatrix} 1 & 0 & 0 & 0 & 0 \\ 0 & 1 & 0 & 0 & 0 \\ 2-a & a & -1 & 0 & 0 \\ 0 & \frac{a-3}{a} & 0 & \frac{3}{2a} & \frac{3}{2a} \\ 0 & \frac{a-3}{a} & 0 & \frac{3}{2a} & \frac{3}{2a} \\ 0 & \frac{a-3}{a} & 0 & \frac{3}{2a} & \frac{3}{2a} \\ 0 & \frac{a-3}{a} & 0 & \frac{3}{2a} & \frac{3}{2a} \\ 0 & \frac{a-3}{a} & 0 & \frac{3}{2a} & \frac{3}{2a} \\ 0 & \frac{a-3}{a} & 0 & \frac{3}{2a} & \frac{3}{2a} \\ 0 & \frac{a-3}{a} & 0 & \frac{3}{2a} & \frac{3}{2a} \\ 0 & \frac{a-3}{a} & 0 & \frac{3}{2a} & \frac{3}{2a} \end{bmatrix} \begin{bmatrix} c^{\sigma_0}_{0,0} \\ c^{\sigma_0}_{0,1} \\ c^{\sigma_0}_{1,0} \\ c^{\sigma_0}_{1,1} \\ c^{\sigma_1}_{1,1} \end{bmatrix}$$

where $-A_{\gamma,\tau}$ is the matrix appearing in this system.

For a vertex γ of valence 3 (with $a = 2\cos(\frac{2\pi}{3}) = -1$) adjacent to the faces $\sigma_0, \sigma_1, \sigma_2$, the 6 spline basis functions of $\mathcal{S}_\gamma$ are:

$$\begin{aligned}
& b^{\sigma_0}_{0,0} + b^{\sigma_2}_{0,0} + 3\,b^{\sigma_2}_{1,0} + 24\,b^{\sigma_2}_{2,1} + 12\,b^{\sigma_2}_{2,0} + 12\,b^{\sigma_2}_{3,0} + b^{\sigma_1}_{0,0} + 3\,b^{\sigma_1}_{0,1} + 12\,b^{\sigma_1}_{0,2} + 12\,b^{\sigma_1}_{0,3} + 24\,b^{\sigma_1}_{1,3}, \\
& b^{\sigma_0}_{0,1} + 4\,b^{\sigma_0}_{0,2} + 4\,b^{\sigma_0}_{0,3} + 8\,b^{\sigma_0}_{1,3} - b^{\sigma_2}_{1,0} - 8\,b^{\sigma_2}_{2,1} - 4\,b^{\sigma_2}_{2,0} - 4\,b^{\sigma_2}_{3,0} + b^{\sigma_1}_{1,0} + 4\,b^{\sigma_1}_{2,0} + 4\,b^{\sigma_1}_{3,0} - b^{\sigma_1}_{0,1} + 8\,b^{\sigma_1}_{2,1} \\
& \qquad -4\,b^{\sigma_1}_{0,2} - 4\,b^{\sigma_1}_{0,3} - 8\,b^{\sigma_1}_{1,3}, \\
& b^{\sigma_0}_{1,0} + 4\,b^{\sigma_0}_{2,0} + 4\,b^{\sigma_0}_{3,0} + 8\,b^{\sigma_0}_{2,1} + 4\,b^{\sigma_2}_{0,3} + 4\,b^{\sigma_2}_{0,2} + b^{\sigma_2}_{0,1} + 8\,b^{\sigma_2}_{1,3} - b^{\sigma_2}_{1,0} - 8\,b^{\sigma_2}_{2,1} - 4\,b^{\sigma_2}_{2,0} - 4\,b^{\sigma_2}_{3,0} - b^{\sigma_1}_{0,1} \\
& \qquad -4\,b^{\sigma_1}_{0,2} - 4\,b^{\sigma_1}_{0,3} - 8\,b^{\sigma_1}_{1,3}, \\
& -2\,b^{\sigma_0}_{2,0} - 2\,b^{\sigma_0}_{3,0} + b^{\sigma_0}_{1,1} - 3\,b^{\sigma_0}_{2,1} - 2\,b^{\sigma_0}_{0,2} - 2\,b^{\sigma_0}_{0,3} - 3\,b^{\sigma_0}_{1,3} - 2\,b^{\sigma_2}_{0,3} - 2\,b^{\sigma_2}_{0,2} - 3\,b^{\sigma_2}_{1,3} - 2\,b^{\sigma_1}_{2,0} - 2\,b^{\sigma_1}_{3,0} - 3\,b^{\sigma_1}_{2,1}, \\
& -2\,b^{\sigma_0}_{0,2} - 2\,b^{\sigma_0}_{0,3} - 3\,b^{\sigma_0}_{1,3} - 3\,b^{\sigma_2}_{2,1} - 2\,b^{\sigma_2}_{2,0} - 2\,b^{\sigma_2}_{3,0} - 2\,b^{\sigma_1}_{2,0} - 2\,b^{\sigma_1}_{3,0} + b^{\sigma_1}_{1,1} - 3\,b^{\sigma_1}_{2,1} - 2\,b^{\sigma_1}_{0,2} - 2\,b^{\sigma_1}_{0,3} - 3\,b^{\sigma_1}_{1,3}, \\
& -2\,b^{\sigma_0}_{2,0} - 2\,b^{\sigma_0}_{3,0} - 3\,b^{\sigma_0}_{2,1} - 2\,b^{\sigma_2}_{0,3} - 2\,b^{\sigma_2}_{0,2} - 3\,b^{\sigma_2}_{1,3} + b^{\sigma_2}_{1,1} - 3\,b^{\sigma_2}_{2,1} - 2\,b^{\sigma_2}_{2,0} - 2\,b^{\sigma_2}_{3,0} - 2\,b^{\sigma_1}_{0,2} - 2\,b^{\sigma_1}_{0,3} - 3\,b^{\sigma_1}_{1,3}.
\end{aligned}$$

4 Dimension computations using syzygies

The basis construction in the section above is based on the representation of the G^1-splines by using bspline coefficients. This approach is the most used on the literature due to the simplicity of representation, and the adaptivity with CAD systems representation. However considering the bspline functions as piecewise polynomials may give some advantages. Indeed, we will explain in this section that the equation (3.4) makes the partial derivatives of the element functions, coordinates of a well understood object from commutative algebra, that is called a module of syzygies. The syzygies module is the space of solutions of a linear equation who's coefficients and unknowns are polynomials. In this section we

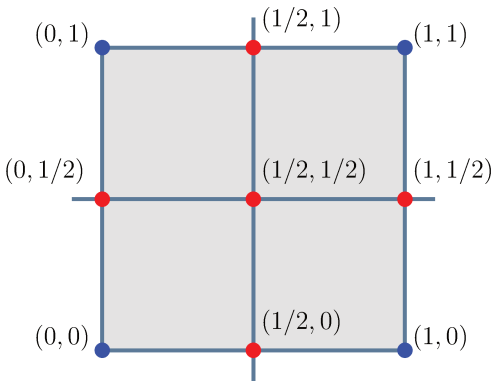

Figure 3.4: The element patches used in this construction are piecewise polynomial functions over a 4-split rectangular domain

will see how this object can be exploited to count the dimension of the space of G^1-Splines. This method has been used the first time in [21]. The study in that paper lead to the computation of the dimension of G^1-splines space over polynomial element patches. We explain in this section how this method can be generalized to the case of quadrangular element patches that are piecewise polynomials over a 4-split subdivision of the quadrangular domain (see Fig. 3.4). The challenge is that the syzygy module is well understood over the ring of polynomials, while we want to compute syzygies over the ring of piecewise polynomials functions with minimal regularity. The solution we propose in this section is to put this module in an exact sequence of modules that are all known, and then apply the Euler characteristic formula to describe the dimension of piecewise polynomial syzygies space. This construction leads to a basis for the module of syzygies over the ring of piecewise polynomials. This space is equivalent to the space of G^1 splines supported on a single edge, over a two patches topology. These basis elements are going to be pieced together with other elements so that they form a basis for the space of G^1-splines over any topology.

4.1 Notation

The method we are presenting in this section is quite similar to the previous one presented in Section 3.1. So we will keep most of the notation with a small difference in the definition.

For instance, the Taylor maps T^{σ}_{γ} will change, we will define them using partial derivatives instead of the bspline coefficients.

4.2 Transition maps

The spline space on the mesh $\mathcal{M}$ is constructed using the transition maps associated to the edges shared by a pair of polygons in $\mathcal{M}$. In the following, the transition maps will be defined from spline functions in $\mathcal{U}_{l,\mathbf{t}}$, of class C^r and degree l, with nodes $0, \frac{1}{2}, 1$ for the gluing data, it means that the knot distribution is given by $\mathbf{t} = [0, \ldots, 0, \frac{1}{2}, \ldots, \frac{1}{2}, 1, \ldots, 1]$ with 0 and 1 of multiplicity $l+1$, $\frac{1}{2}$ of multiplicity $l-r$, to avoid complicated notations we will use $\mathcal{U}_{l,r}$ to denote that

space of splines, and $\mathcal{U}_r$ to denote the union of all the spaces $\mathcal{U}_{l,r}$ for $l \in \mathbb{N}$. We assume that the dimension of $\mathcal{U}_{l,\mathbf{t}}$ is bigger than 4, that is, $2l+1-r \geqslant 4$ and $r \geqslant 0$ so that $l \geqslant \frac{1}{2}(3+r)$, which implies that $l \geqslant 2$.

We choose the two Hermite interpolation functions $\mathfrak{d}_0(u), \mathfrak{d}_1(u) \in \mathcal{U}_{l,\mathbf{t}}$ such that $\mathfrak{d}_0(0) = 1$, $\mathfrak{d}_0(1) = 0$, $\mathfrak{d}_1(0) = 0$, $\mathfrak{d}_1(1) = 1$ and $\mathfrak{d}_0'(0) = \mathfrak{d}_0'(1) = \mathfrak{d}_1'(0) = \mathfrak{d}_1'(1) = 0$. These functions are going to be used to produce the gluing data as we explained in Section 2.1. We can take, for instance,

$$\begin{aligned} \mathfrak{d}_0(u) &= b_0(u) + b_1(u) \\ \mathfrak{d}_1(u) &= b_{m-1}(u) + b_m(u) \end{aligned} \tag{3.18}$$

where $m = 2l - r$. For $l = 2$, $r = 1$, these functions are

$$\mathfrak{d}_0(u) = \begin{cases} 1 - 2u^2 & 0 \leqslant u \leqslant \frac{1}{2} \\ 2(1-u)^2 & \frac{1}{2} \leqslant u \leqslant 1 \end{cases}$$

$$\mathfrak{d}_1(u) = \begin{cases} 2u^2 & 0 \leqslant u \leqslant \frac{1}{2} \\ 1 - 2\,(1-u)^2 & \frac{1}{2} \leqslant u \leqslant 1. \end{cases}$$

For $l = 2$, $r = 0$, these functions are

$$\mathfrak{d}_0(u) = \begin{cases} 1 - 4u^2 & 0 \leqslant u \leqslant \frac{1}{2} \\ 0 & \frac{1}{2} \leqslant u \leqslant 1 \end{cases}$$

$$\mathfrak{d}_1(u) = \begin{cases} 0 & 0 \leqslant u \leqslant \frac{1}{2} \\ 1 - 4\,(1-u)^2 & \frac{1}{2} \leqslant u \leqslant 1. \end{cases}$$

4.3 Splines along an edge

The space $\mathcal{S}_{k,\mathbf{t}}(\mathcal{M})$ of splines over the mesh $\mathcal{M}$ can be splitted into three linearly independent components: $\mathcal{E}_k$, $\mathcal{H}_k$, $\mathcal{F}_k$ (see Section 7) attached respectively to vertices, edges and faces. The objective of this section is to give an alternative way for analysing the component $\mathcal{E}(\tau)$ that corresponds to splines supported along the interior edge τ, shared by two faces $\sigma_1, \sigma_2 \in \mathcal{M}_2$. We will produce a basis for it and provide a dimension formula. We denote by $\mathcal{M}_\tau$ the sub-mesh of $\mathcal{M}$ composed of the two faces σ_1, σ_2 that share the edge τ.

An important step is to analyse the space $\mathrm{Syz}_k^{r,r,r}(a,b,c)$ of syzygies over the base ring $\mathcal{U}_{d,\mathbf{t}}$. The relation of this space with $\mathcal{E}(\tau)_k$ and a basis of $\mathrm{Syz}_k^{r,r,r}(a,b,c)$ are presented in Sections 4.4 and 4.5.

Next in Section 4.6, we study the effect, on $\mathcal{E}(\tau)_k$, of the Taylor map at the two end points of τ and we determine when they can be separated by the Taylor map.

The Section 4.7 shows how to decompose the space $\mathcal{S}_{k,t}(\mathcal{M})$ for the simple mesh $\mathcal{M}_\tau$, using this Taylor maps at the end points of τ. The same technique will be used to decompose the space $\mathcal{S}_{k,r}(\mathcal{M})$, for a general mesh $\mathcal{M}$.

4.4 Relation with syzygies

Suppose we want to glue two functions f_1 and f_2 defined over domains with the coordinates (u_1, v_1) and (u_2, v_2) respectively (see the figure 3.2). If we choose the

gluing data to be $\mathfrak{a} = \frac{a}{c}$ and $\mathfrak{b} = \frac{b}{c}$, with $a, b, c \in \mathcal{U}_{s,l}$ defining the gluing data across the edge $\tau \in \mathcal{M}$, and $(f_1, f_2) \in \mathcal{S}_{k,\mathfrak{t}}(\mathcal{M}_\tau)$, from (3.5) we have that:

$$A(u_1)a(u_1) + B(u_1)b(u_1) + C(u_1)c(u_1) = 0$$

where

$$\begin{aligned} A(u_1) &= \frac{\partial f_2}{\partial v_2}(0, u_1) \in \mathcal{U}_{k-1,0}, \\ B(u_1) &= \frac{\partial f_2}{\partial u_2}(0, u_1) \in \mathcal{U}_{k,1}, \\ C(u_1) &= -\frac{\partial f_1}{\partial v_1}(u_1, 0) \in \mathcal{U}_{k,1}. \end{aligned}$$

These are the conditions imposed by the transition map across τ. According to such data, and if the topological surface $\mathcal{M}_\tau$ contains two faces with one transition map along the shared edge τ, then any differentiable spline functions $f = (f_1, f_2)$ over $\mathcal{M}_\tau$ of bi-degree $\leqslant (k, k)$ is given by the formula:

$$\begin{aligned} f_1(u_1, v_1) = \big(b_1(v_1) + b_0(v_1)\big) \left(a_0 + \int_0^{u_1} A(t)dt\right) \\ - \frac{1}{2k}\, b_1(v_1)C(u_1) + E_1(u_1, v_1) \end{aligned} \tag{3.19}$$

$$\begin{aligned} f_2(u_2, v_2) = \big(b_1(u_2) + b_0(u_2)\big) \left(a_0 + \int_0^{v_2} A(t)dt\right) \\ + \frac{1}{2k}\, b_1(u_2)B(v_2) + E_2(u_2, v_2), \end{aligned} \tag{3.20}$$

since $b_0(0) = 1$, $b_1(0) = 0$, $b_0'(0) = -2k$, and $b_1'(0) = 2k$.

Here $a_0 \in \mathbb{R}$, the functions $E_i \in \ker D_\tau^{\sigma_i}$ for $i = 0, 1$, and A, B, C are spline functions of degree at most $k-1, k, k$ and class C^0, C^1, C^1, respectively.

For $r_1, r_2, r_3, k \in \mathbb{N}$ and $a, b, c \in \mathcal{U}_l^s$, we denote

$$\mathrm{Syz}_k^{r_1,r_2,r_3}(a, b, c) = \big\{(A, B, C) \in \mathcal{U}_{k-1,r_1} \times \mathcal{U}_{k,r_2} \times \mathcal{U}_{k,r_3} \mid A\,a + B\,b + C\,c = 0\big\}.$$

We denote this vector space simply by $\mathrm{Syz}_k^{r_1,r_2,r_3}$ when a, b, c are implicitly given.

By (3.19) and (3.20), the splines in $\mathcal{S}_{l,r}(\mathcal{M}_\tau)$ with a support along the edge τ are in the image of the map:

$$\begin{aligned} \Theta_\tau : \mathbb{R} \times \mathrm{Syz}_k^{0,1,1} &\to \mathcal{S}_{k,r}(\mathcal{M}_\tau) \\ (a_0, (A, B, C)) &\mapsto \left(\left(a_0 + \int_0^{u_1} A(t)dt\right) b_0(v_1)\right. \\ &\quad + \left(a_0 + \int_0^{u_1} A(t)dt - \frac{1}{2k}\, C(u_1)\right) b_1(u_1), \\ &\quad b_0(u_2) \left(a_0 + \int_0^{v_2} A(t)dt\right) \\ &\quad \left. + b_1(u_2) \left(a_0 + \int_0^{v_2} A(t)dt + \frac{1}{2k}\, B(v_2)\right)\right). \end{aligned} \tag{3.21}$$

The classical results on the module of syzygies on polynomial rings described in [21] (see Proposition 4.3 in the reference), will be used in order to prove the corresponding statements in the context of syzygies on spline functions. First, we recall the notation and results concerning the polynomial case. Let a, b, c be polynomials in $R = \mathbb{R}[u]$, such that $\gcd(a,c) = \gcd(b,c) = 1$, then $Z = \mathrm{Syz}(a,b,c)$ is the R-module defined by $\mathrm{Syz}(a,b,c) = \{(A,B,C) \in \mathbb{R}[u]^3 \colon Aa + Bb + Cc = 0\}$. The degree of an element in $\mathrm{Syz}(a,b,c)$ is defined as $\deg(A,B,C) = \max\{\deg(A), \deg(B), \deg(C)\}$, and we are interested in studying the subspace $Z_k \subset \mathrm{Syz}(a,b,c)$ of elements of degree less than or equal to $k-1$. Let us denote $n = \max\{\deg(a), \deg(b), \deg(c)\}$, and

$$e = \begin{cases} 0\,, & \text{if } \min\big(n+1-\deg(a), n-\deg(b), n-\deg(c)\big) = 0 \text{ and} \\ 1\,, & \text{otherwise.} \end{cases}$$

Lemma 4.1. *Using the notation above we have:*

1. *Z is a free $\mathbb{R}[u]$-module of rank 2.*
2. *If μ and ν are the degree of the two free generators of $\mathrm{Syz}(a,b,c)$ with μ minimal, then $\mu + \nu = n$.*
3. *$\dim Z_k = (k-\mu+1)_+ + (k-n+\mu+e)_+$ where $t_+ = \max(0,t)$ for any $t \in \mathbb{Z}$.*
4. *The generators (A_1,B_1,C_1), (A_2,B_2,C_2) of Z can be chosen so that*

$$(a,b,c) = (B_1C_2 - B_2C_1, C_1A_2 - C_2A_1, A_1B_2 - A_2B_1).$$

A basis with minimal degree corresponds to what is called a μ-basis in the literature.

Proof. We study the syzygy module $Z = \mathrm{Syz}(a,b,c)$ using results on graded resolutions. For this purpose, we homogenize a, b and c in degree $d_a = n+1$, $d_b = d_c = n$. Let u_0, u_1 be the homogeneous coordinates, and $\bar{a}, \bar{b}, \bar{c}$ the corresponding homogenizations of a, b, and c. We consider the module of homogeneous syzygies $\mathrm{Syz}(\bar{a},\bar{b},\bar{c})$ over the polynomial ring $S = \mathbb{R}[u_0,u_1]$.

Claim 4.2. *For any $k \geqslant 0$, the elements in Z_k are exactly the syzygies of degree $n+k$ in $\mathrm{Syz}(\bar{a},\bar{b},\bar{c})$ after dehomogenization by setting $u_0 = 1$.*

Proof. It is clear that if $\bar{A}\bar{a} + \bar{B}\bar{b} + \bar{C}\bar{c} = 0$, then by dehomogenization taking $u_0 = 1$, we get a syzygy (A,B,C) of (a,b,c). Moreover, if $\deg(\bar{A}\bar{a}) = \deg(\bar{B}\bar{b}) = \deg(\bar{C}\bar{c}) = n+k$, then $\deg(\bar{A}) = k-1$, $\deg(\bar{B}) = k$ and $\deg(\bar{C}) = k$. It follows that $(A,B,C) \in Z_k$.

On the other hand, any syzygy $(A,B,C) \in Z_k$ is given by polynomials of degree at most $\max\{\deg A, \deg B, \deg C\} \leqslant k$, and since $n = \max\{\deg a, \deg b, \deg c\}$ then we may consider the homogenization of the polynomial $Aa + Bb + Cc$ in degree $n+k$. These polynomials satisfy

$$\begin{aligned} 0 &= u_0^{k+n}(Aa + Bb + Cc)(u_1/u_0) \\ &= u_0^{k-1} \cdot u_0^{n+1} Aa\big(u_1/u_0\big) + u_0^{k} \cdot u_0^{n+} Bb\big(u_1/u_0\big) \\ &\qquad + u_0^{k} \cdot u_0^{n} Cc\big(u_1/u_0\big). \end{aligned}$$

It is easy to check that

$$\bar{A} = u_0^{k-1} A(u_1/u_0), \quad \bar{B} = u_0^k B(u_1/u_0), \quad \bar{C} = u_0^k C(u_1/u_0)$$

are all polynomials in $\mathbb{R}[u_1, u_0]$, and define a syzygy of $\bar{a}, \bar{b}, \bar{c}$ of degree $n + k$. Let us also notice that the polynomials

$$\bar{a} = u_0^{n+1} a(u_1/u_0),\ \bar{b} = u_0^n b(u_1/u_0),\ \text{and } \bar{c} = u_0^n c(u_1/u_0)$$

are precisely the homogenization of a, b, c in degree d_a, d_b, d_c, respectively.

□

As $gcd(a, b, c) = 1$, we have $gcd(\bar{a}, \bar{b}, \bar{c}) = u_0$ if $e = 1$, and $gcd(\bar{a}, \bar{b}, \bar{c}) = 1$ otherwise.

Let $I = (\bar{a}, \bar{b}, \bar{c})$ be the ideal generated by $\bar{a}, \bar{b}, \bar{c}$ in S. If $gcd(\bar{a}, \bar{b}, \bar{c}) = 1$ then there exists $t_0 \in \mathbb{N}$ such that $\forall t \geqslant t_0$, $I_t = (u_0, u_1)^t$ and in that case, $\dim_{\mathbb{R}}(S/I)_t = 0$ for t sufficiently large. It follows that the Hilbert polynomial $HP_{S/I}$ of S/I is the zero polynomial.

For the second case, namely if $gcd(\bar{a}, \bar{b}, \bar{c}) = u_0$, since $\gcd(a, b, c) = 1$ then the polynomials $\bar{a}/u_0$, $\bar{b}/u_0$ and $\bar{c}/u_0$ have gcd equal to 1. Hence there exists $t_0 \in \mathbb{N}$ such that $\forall t \geqslant t_0$, $I_t = u_0\,(u_0, u_1)^{t-1}$. In this case $\dim_{\mathbb{R}}(S/I)_t = 1$ for t sufficiently large, and it follows that the Hilbert polynomial $HP_{S/I}$ is the constant polynomial equal to 1.

Then the exact sequence

$$0 \to I \to S \to S/I \to 0$$

implies that

$$HP_I(t) = HP_S(t) - HP_{S/I}(t) = \binom{t+1}{1} - e, \tag{3.22}$$

where HP_M is the Hilbert polynomial of the module M.

By the Graded Hilbert Syzygy Theorem, we get a resolution of the form

$$0 \longrightarrow S(-d_1) \oplus \cdots \oplus S(-d_L) \xrightarrow{\lambda} S(-d_a) \oplus S(-d_b) \oplus S(-d_c) \longrightarrow I \longrightarrow 0.$$

Notice that this resolution is not necessarily minimal. Since this is an exact sequence, then the Hilbert polynomial of the middle term is the sum of the other two Hilbert polynomials, and applying (3.22) we get

$$3t - (d_a + d_b + d_c) + 3 = (t - d_1 + 1) + \cdots + (t - d_L + 1) + (t + 1) - e.$$

It follows that $L = 2$ which proves *(i)*. Furthermore, we have that the degrees d_1 and d_2 of the syzygies satisfy $d_1 + d_2 = d_a + d_b + d_c - e$.

The matrix Λ representing λ is a 3×2 matrix

$$\begin{pmatrix} \bar{A}_1 & \bar{A}_2 \\ \bar{B}_1 & \bar{B}_2 \\ \bar{C}_1 & \bar{C}_2 \end{pmatrix}$$

the first column corresponding to the generator of degree d_1 and the second of degree d_2. These two syzygies correspond to vectors of polynomial coefficients

of degree $\mu = d_1 - \min(d_a, d_b, d_c)$ and $\nu = d_2 - \min(d_a, d_b, d_c)$. By Definition, $\min(d_a, d_b, d_c) = n$, and also $d_a + d_b + d_c = 3n + 1$. Let us assume that $d_1 \leqslant d_2$, then μ is the smallest degree of the coefficient vector of a syzygy of $(\bar{a}, \bar{b}, \bar{c})$, and $\nu = n - \mu + 1 - e$.

By exactness, the two columns of Λ generate $\mathrm{Syz}(\bar{a}, \bar{b}, \bar{c})$. The dehomogenization (by setting $u_0 = 1$) of the syzygies in $\mathrm{Syz}(\bar{a}, \bar{b}, \bar{c})$ leads to syzygies of (a, b, c) over $\mathbb{R}[u_1]$. In particular, it is straightforward to show that the dehomogenization (A_i, B_i, C_i) of $(\bar{A}_i, \bar{B}_i, \bar{C}_i)$ for $i = 1, 2$ generate $Z = \mathrm{Syz}(a, b, c)$ as a module over $\mathbb{R}[u_1]$. This proves *(2)*.

By Claim 4.2, the space Z_k is in correspondence with the space of homogeneous syzygies of degree $n + k$, which is spanned by the multiples of degree $n + k$ of $(\bar{A}_1, \bar{B}_1, \bar{C}_1)$ and $(\bar{A}_2, \bar{B}_2, \bar{C}_2)$. Therefore,

$$\begin{aligned} \dim Z_k &= (n + k - d_1 + 1)_+ + (n + k - d_2 + 1)_+ \\ &= (k - \mu + 1)_+ + (k - \nu + 1)_+ \end{aligned}$$

with $\nu = n - \mu + 1 - e$. This proves *(3)*.

The point *(4)* is a consequence of Hilbert-Burch theorem. More details on this proof can be found in [53, Chapter 6, § 4.17]. □

In the following we state the analogous to Lemma 4.1 in the context of syzygies on spline functions. We consider $\mathrm{Syz}_k^{r,r,r}$ as defined above. It is the set of spline functions $(A, B, C) \in \mathcal{U}_{k-1,r} \times \mathcal{U}_{k,r} \times \mathcal{U}_{r,k}$ such that $A\,a + B\,b + C\,c = 0$. An element of $\mathrm{Syz}_k^{r,r,r}$ is a triple of pairs of polynomials $((A_1, A_2), (B_1, B_2), (C_1, C_2))$. Let $R = \mathbb{R}[u]$, $R_k = \{p \in R \mid \deg(p) \leqslant k\}$, $\mathcal{Q}^r = R/((2u-1)^{r+1})$ and $\mathcal{Q}_k^r = R_k/((2u-1)^{r+1})$.

The elements $f = (f_1, f_2)$ of $\mathcal{U}_{k,r+1}$ are pairs of polynomials $f_1, f_2 \in R_k$ such that $f_1 - f_2 \equiv 0 \pmod{(2u-1)^{r+1}}$. Let $a = (a_1, a_2), b = (b_1, b_2), c = (c_1, c_2) \in \mathcal{U}_r$ with $\gcd(a_1, c_1) = \gcd(a_2, c_2) = \gcd(b_1, c_1) = \gcd(b_2, c_2) = 1$. We consider the following sequence:

$$0 \longrightarrow \mathrm{Syz}_k^{r,r,r} \longrightarrow \mathrm{Syz}_{1,k} \times \mathrm{Syz}_{2,k} \xrightarrow{\phi} \mathcal{Q}_{k-1}^r \times \mathcal{Q}_k^r \times \mathcal{Q}_k^r \xrightarrow{\psi} \mathcal{Q}_{n_1+k}^r \longrightarrow 0 \quad (3.23)$$

where $\mathrm{Syz}_{1,k} = \mathrm{Syz}_k(a_1, b_1, c_1)$, $\mathrm{Syz}_{2,k} = \mathrm{Syz}_k(a_2, b_2, c_2)$, and

- $\psi(f, g, h) = a_1 f + b_1 g + c_1 h$,
- $\phi(A, B, C) = (A_1 - A_2, B_1 - B_2, C_1 - C_2) \pmod{(2u-1)^{r+1}}$.

Lemma 4.3. *The sequence* (3.23) *is exact for* $k \geqslant n_1 + r$ *where* $n_1 = \max\{\deg(a_1), \deg(b_1), \deg(c_1)\}$.

Proof. Since b_1, c_1 are coprime, the map $\psi : (f, g, h) \in R_{k-1} \times R_k \times R_k \mapsto a_1 f + b_1 g + c_1 h \in R_{n_1+k}$ is surjective for $k \geqslant n_1 - 1$. The map ϕ, obtained by working modulo $(2u-1)^{r+1}$, remains surjective.

We have to prove that $\ker(\psi) = \mathrm{Im}(\phi)$. If $(A, B, C) \in \mathrm{Syz}_1 \times \mathrm{Syz}_2$ then $\psi \circ \phi(A, B, C) = (A_1 a_1 + B_1 b_1 + C_1 c_1) - (A_2 a_1 + B_2 b_1 + C_2 c_1) = -(A_2 a_1 + B_2 b_1 + C_2 c_1)$. Because $a, b, c \in \mathcal{U}_r$, we have $a_1 \equiv a_2 \pmod{(2u-1)^{r+1}}$, $b_1 \equiv b_2 \pmod{(2u-1)^{r+1}}$ and $c_1 \equiv c_2 \pmod{(2u-1)^{r+1}}$, so that

$$\psi \circ \phi(A, B, C) \equiv -(A_2 a_2 + B_2 b_2 + C_2 c_2) \equiv 0 \pmod{(2u-1)^{r+1}}.$$

This implies that $\mathrm{Im}(\phi) \subset \ker(\psi)$.

Conversely, if $\psi(f,g,h) = 0$ with $\deg(f) \leqslant r$, $\deg(g) \leqslant r$, $\deg(h) \leqslant r$ then $fa_1 + gb_1 + hc_1 = d\,(2u-1)^{r+1}$ for some polynomial $d \in R$ of degree $\leqslant n_1 - 1$. Since $\gcd(b_1, c_1) = 1$, there exists $p, q \in R_{n_1-1}$ such that $d = p\,b_1 + q\,c_1$, we deduce that:

$$(2u-1)^{r+1}d = (2u-1)^{r+1}\,(p\,b_1 + q\,c_1) = f\,a_1 + g\,b_1 + h\,c_1,$$

with $\deg((2u-1)^{r+1}p) \leqslant n_1 + r$. This yields

$$f\,a_1 + (g - p(2u-1)^{r+1})\,b_1 + (h - (2u-1)^{r+1}q)\,c_1 = 0. \tag{3.24}$$

Since $k \geqslant n_1 + r$, this implies that $((f,0),(g-(2u-1)^{r+1}p,0),(h-(2u-1)^{r+1}q,0)) \in \mathrm{Syz}_{1,k} \times \mathrm{Syz}_{2,k}$ and its image by ϕ is (f,g,h). This shows that $\ker(\psi) \subset \mathrm{Im}(\phi)$ and implies the equality of the two vector spaces.
By construction, the kernel of ϕ is the pair of triples $((A_1,B_1,C_1),(A_2,B_2,C_2))$ in $\mathrm{Syz}_{1,k} \times \mathrm{Syz}_{2,k}$ such that $A_1 - A_2 \equiv B_1 - B_2 \equiv C_1 - C_2 \equiv 0 \pmod{(2u-1)^{r+1}}$, that is, the set $\mathrm{Syz}_k^{r,r,r}$ of triples $(A,B,C) \in \mathcal{U}_{k-1}^r \times \mathcal{U}_k^r \times \mathcal{U}_k^r$ such that $A\,a + B\,b + C\,c = 0$.

This show that the sequence (3.23) is exact. □

We deduce the dimension formula:

Proposition 4.4. *Let (p_1,q_1) (resp. (p_2,q_2)) be a basis of Syz_1 (resp. Syz_2) of minimal degree (μ_1,ν_1) (resp. (μ_2,ν_2)) and e_1, e_2 defined as above for (a_1,b_1,c_1) and (a_2,b_2,c_2). For $k \geqslant \min(n_1,n_2) + r$,*

$$\begin{aligned}\dim(\mathrm{Syz}_k^{r,r,r}) = (k-\mu_1+1)_+ + (k-n_1+\mu_1+e_1)_+ + (k-\mu_2+1)_+ \\ + (k-n_2+\mu_2+e_2)_+ - \min(r+1,k) - (r+1).\end{aligned}$$

This dimension is denoted $d_\tau(k,r)$.

Proof. By symmetry, we may assume that $n_1 = \min(n_1,n_2)$. For $k \geqslant n_1 + r$, the sequence (3.23) is exact and we have

$$\dim \mathrm{Syz}_k^{r,r,r} = \dim \mathrm{Syz}_{1,k} + \dim \mathrm{Syz}_{2,k} - \dim \mathcal{Q}_{k-1}^r - 2\dim \mathcal{Q}_k^r + \dim \mathcal{Q}_{n_1+k}^r.$$

We have $\dim \mathcal{Q}_{k-1}^r = \min(r+1,k)$ and $\dim \mathcal{Q}_k^r = \dim \mathcal{Q}_{n_1+k}^r = r+1$, since $k \geqslant n_1 + r$. This leads to the formula, using Lemma 4.1. □

4.5 Basis of the syzygy module

The diagram (3.23) allows us to construct a basis for the space of syzygies $\mathrm{Syz}_k^{r,r,r}$ associated to the gluing data $a,b,c \in \mathcal{U}_r$. In the rest of this section we will show how to construct such a basis.

Lemma 4.5. *Assume that $k \geqslant n_1 + r$. Using the notation of Proposition 4.4, we have the following assertions:*

- *For any $\mathfrak{p}_2 \in \mathrm{Syz}_{2,k}$, there exists $\mathfrak{p}_1 \in \mathrm{Syz}_{1,k}$ such that $(\mathfrak{p}_1,\mathfrak{p}_2) \in \ker(\phi)$.*

- *There exist* $t,\ s \in \mathbb{N}$ *such that if* $\mathcal{G} = \{(p_1(2u-1)^i, 0) : 0 \leqslant i \leqslant t\} \bigcup \{(q_1(2u-1)^j, 0) : 0 \leqslant j \leqslant l\}$ *then* $\phi(\mathcal{G})$ *is a basis of the vector space* $\ker(\psi)$.
- $\ker(\phi) \bigoplus \langle \mathcal{G} \rangle = \mathrm{Syz}_{1,k} \times \mathrm{Syz}_{2,k}$.

Proof. Let $\mathfrak{p}_2 = (A_2, B_2, C_2) \in \mathrm{Syz}_{2,k}$. As $\phi((0, \mathfrak{p}_2)) = (f, g, h)$ is in $\ker(\psi)$ (since $\psi \circ \phi = 0$), we can construct $\mathfrak{p}_1 \in \mathrm{Syz}_{1,k}$ such that $\phi((\mathfrak{p}_1, 0)) = \phi((0, \mathfrak{p}_2))$ as we did in the proof of Lemma 4.3 for $(f, g, h) \in \ker(\psi)$ using relation (3.24). This gives an element of the form $(\mathfrak{p}_1, 0) \in \mathrm{Syz}_{1,k} \times \{0\}$, and finally $(\mathfrak{p}_1, \mathfrak{p}_2) \in \ker(\phi)$, this proves the first point.

The second point follows from the fact that $\phi(\mathrm{Syz}_{1,k} \times \{0\}) = \ker(\psi)$ (since by Lemma 4.3, the sequence (3.23) is exact) and that $\{(p_1(2u-1)^i, 0) : \ i \leqslant k - \mu_1\} \bigcup \{(q_1(2u-1)^j, 0) : j \leqslant k - \nu_1\}$ is a basis of $\mathrm{Syz}_{1,k} \times \{0\}$ as a vector space, thus the image of this basis is a generating set for $\ker(\psi)$. Since it is a R-module, it has a basis as described in the second point of this lemma.

The third point is a direct consequence of the second one. □

Considering the map in (3.22), the first point of the lemma has an intuitive meaning: any function defined on a part of $\mathcal{M}_\tau$ and that satisfies the gluing conditions imposed by a_1, b_1, c_1 can be extended to a function over $\mathcal{M}_\tau$ that satisfies the gluing conditions a, b, c. The third point allows us to define the projection π_1^r of an element on $\ker(\phi)$ along $\langle \mathcal{G} \rangle$.

Let $(\tilde{p_2}, p_2)$, $(\tilde{q_2}, q_2)$ be the two projections of $(0, p_2)$ and $(0, q_2)$ by π_1^r respectively. We denote:

- $\mathcal{Z}_1^r = \{(0, (2u-1)^i p_2) : r+1 \leqslant i \leqslant k - \mu_2\}$
- $\mathcal{Z}_2^r = \{(0, (2u-1)^i q_2) : r+1 \leqslant i \leqslant k - \nu_2\}$
- $\mathcal{Z}_3^r = \{((2u-1)^i q_1, 0) : r+1 \leqslant i \leqslant k - \mu_1\}$
- $\mathcal{Z}_4^r = \{((2u-1)^i p_1, 0) : r+1 \leqslant i \leqslant k - \nu_2\}$
- $\mathcal{Z}_5^r = \{(2u-1)^i (\tilde{p_2}, p_2) : 0 \leqslant i \leqslant r\}$
- $\mathcal{Z}_6^r = \{(2u-1)^i (\tilde{q_2}, q_2) : 0 \leqslant i \leqslant r\}$
- $\mathcal{Z}^r = \mathcal{Z}_1^r \bigcup \mathcal{Z}_2^r \bigcup \mathcal{Z}_3^r \bigcup \mathcal{Z}_4^r \bigcup \mathcal{Z}_5^r \bigcup \mathcal{Z}_6^r$

Proposition 4.6. *Using the notation above we have the following:*

- *The set* $\mathcal{Z}^r$ *is a basis of the vector space* $\mathrm{Syz}_k^{r,r,r}$.
- *The set* $\mathcal{Y} = \{(0, (2u-1)^{r+1} p_2), (0, (2u-1)^{r+1} q_2), (\tilde{p_2}, p_2), (\tilde{q_2}, q_2), ((2u-1)^{r+1} q_1, 0), ((2u-1)^{r+1} p_1, 0)\}$ *is a generating set of the* R*-module* $\mathrm{Syz}^{r,r,r}$.

Proof. The cardinal of $\mathcal{Z}^r$ is equal to the dimension of $\mathrm{Syz}_k^{r,r,r}$, we have to prove that it is a free set. Let $\mathfrak{a} = (\mathfrak{a}_i)$, $\mathfrak{b} = (\mathfrak{b}_i)$, $\mathfrak{c} = (\mathfrak{c}_i)$, $\mathfrak{d} = (\mathfrak{d}_i)$, $\mathfrak{e} = (\mathfrak{e}_i)$, $\mathfrak{f} = (\mathfrak{f}_i)$ for $i \in \{0, \ldots, k\}$ a set of coefficients. Suppose that:

$$
\begin{aligned}
0 = &\sum_{i=0}^{r} \mathfrak{a}_i (2u-1)^i (\tilde{p_2}, p_2) + \sum_{i=0}^{r} \mathfrak{b}_i (2u-1)^i (\tilde{q_2}, q_2) \\
&+ \sum_{i=0}^{k-r-\nu_1} \mathfrak{c}_i ((2u-1)^{i+r+1} q_1, 0) + \sum_{i=0}^{k-r-\mu_1} \mathfrak{e}_i ((2u-1)^{i+r+1} p_1, 0) \\
&+ \sum_{i=0}^{k-r-\mu_2} \mathfrak{d}_i (0, (2u-1)^{r+i+1} p_2) + \sum_{i=0}^{k-r-\nu_2} \mathfrak{f}_i (0, (2u-1)^{i+r+1} q_2).
\end{aligned}
$$

Then we have the following equations,

$$
\begin{aligned}
0 = &\sum_{i=0}^{r} \mathfrak{a}_i (2u-1)^i \tilde{p_2} + \sum_{i=0}^{r} \mathfrak{b}_i (2u-1)^i \tilde{q_2} + \sum_{i=0}^{k-r-\nu_1} \mathfrak{c}_i (2u-1)^{r+1+i} q_1 \\
&+ \sum_{i=0}^{k-r-\mu_1} \mathfrak{e}_i (2u-1)^{r+1+i} p_1 \qquad (3.25) \\
0 = &\sum_{i=0}^{r} \mathfrak{a}_i (2u-1)^i p_2 + \sum_{i=0}^{r} \mathfrak{b}_i (2u-1)^i q_2 + \sum_{i=0}^{k-r-\mu_2} \mathfrak{d}_i (2u-1)^{r+1+i} p_2 \\
&+ \sum_{i=0}^{k-r-\nu_2} \mathfrak{f}_i (2u-1)^{r+1+i} q_2 \qquad (3.26)
\end{aligned}
$$

We know that p_2 and q_2 are free generators of Syz_2, by (3.26) this means that all the coefficients $\mathfrak{a}_i$, $\mathfrak{b}_i$, $\mathfrak{d}_i$, $\mathfrak{f}_i$ that are used in the equation are zero. Replacing in the equation(3.25) we get in the same way that the other coefficients $\mathfrak{c}_i, \mathfrak{e}_i$ are zero, so the set is free. Finally since the set $\mathcal{Y}$ does not change when k changes, then $\mathcal{Y}$ generates $\mathrm{Syz}^{r,r,r}$. □

We have similar results if we proceed in a symmetric way exchanging the role of the first and second polynomial components of the spline functions. The corresponding basis of $\mathrm{Syz}_k^{r,r,r}$ is denoted $\mathcal{Z}'^r$ and the generating set of the R-module is

$$
\begin{aligned}
\mathcal{Y}' = \big\{ &\big(0, (2u-1)^{r+1} p_2\big), \big(0, (2u-1)^{r+1} q_2\big), \big(p_1, \tilde{p_1}\big), \\
&\big(q_1, \tilde{q_1}\big), \big((2u-1)^r q_1, 0\big), \big((2u-1)^r p_1, 0\big) \big\}.
\end{aligned}
$$

It remains to compute the dimension and a basis for $\mathrm{Syz}_k^{r-1,r,r}$. We deduce them from those of $\mathrm{Syz}_k^{r-1,r-1,r-1}$ and $\mathrm{Syz}_k^{r,r,r}$. They depend on the gluing data as we explain hereafter.

Proposition 4.7.

- *If* $a(1/2) \neq 0$ *then* $\mathrm{Syz}_k^{r,r,r} = \mathrm{Syz}_k^{r-1,r,r}$, *otherwise we have that* $\dim(\mathrm{Syz}_k^{r-1,r,r}) = \dim(\mathrm{Syz}_k^{r,r,r}) + 1$.
- *For the second case, an element in* $\mathrm{Syz}_k^{r-1,r,r} \setminus \mathrm{Syz}_k^{r,r,r}$ *is of the form:* $\alpha(2u-1)^r(0, p_2) + \beta(2u-1)^r(0, q_2)$, *with* $\alpha, \beta \in \mathbb{R}$.

For the proof of this proposition we need the following lemma that can be proved exactly in the same way as Proposition 4.6 above.

Lemma 4.8. *The set* $\tilde{\mathcal{Z}}^{r-1} = \mathcal{Z}'^{r} \bigcup \{(2u-1)^r(0,p_2), (2u-1)^r(0,q_2)\}$ *is a basis of* $\mathrm{Syz}_k^{r-1,r-1,r-1}$.

Proof of Proposition 4.7. We denote $p_1 = (p_1^1, p_1^2, p_1^3)$, and $q_1 = (q_1^1, q_1^2, q_1^3)$, where p_i^j and q_i^j are polynomials. Suppose that there exists $(A,B,C) \in \mathrm{Syz}_k^{r-1,r,r} \setminus \mathrm{Syz}_k^{r,r,r}$, then by the previous lemma we can choose $(A,B,C) = \alpha(2u-1)^r(0,p_2) + \beta(2u-1)^r(0,q_2)$ with $\alpha, \beta \in \mathbb{R}$, that is:

$$\begin{cases} A = \alpha(0,(2u-1)^r p_2^1) + \beta(0,(2u-1)^r q_2^1) \\ B = \alpha(0,(2u-1)^r p_2^2) + \beta(0,(2u-1)^r q_2^2) \\ C = \alpha(0,(2u-1)^r p_2^3) + \beta(0,(2u-1)^r q_2^3) \end{cases}$$

But since $B, C \in \mathcal{U}_r$, we deduce:

$$\begin{cases} (2u-1)^{r+1} \text{ divides } B_2 - B_1 = (2u-1)^r(\alpha p_2^2 + \beta q_2^2) \\ (2u-1)^{r+1} \text{ divides } C_2 - C_1 = (2u-1)^r(\alpha p_2^3 + \beta q_2^3) \end{cases}$$

This means that

$$\begin{cases} \alpha p_2^2(\frac{1}{2}) + \beta q_2^2(\frac{1}{2}) = 0 \\ \alpha p_2^3(\frac{1}{2}) + \beta q_2^3(\frac{1}{2}) = 0 \end{cases}$$

As the determinant of this system is exactly $p_2^2(\frac{1}{2})q_2^3(\frac{1}{2}) - p_2^3(\frac{1}{2})q_2^2(\frac{1}{2}) = a(\frac{1}{2})$, we deduce the two points of the proposition. □

Lemma 4.8 implies the following proposition:

Proposition 4.9. *The dimension of* $\mathrm{Syz}_k^{r-1,r,r}$ *is* $\tilde{d}_\tau(k,r) = d_\tau(k,r) + \delta_\tau$ *with* $\delta_\tau = 1$ *if* $a(\frac{1}{2}) = 0$ *and* 0 *otherwise.*

4.6 Separation of vertices

We analyze now the separability of the spline functions on an edge, that is when the Taylor map at the vertices separate the spline functions.

Let $f = (f_1, f_2) \in \mathcal{R}(\sigma_1) \oplus \mathcal{R}(\sigma_2)$ of the form $f_i(u_i, v_i) = p_i + q_i\,u_i + \tilde{q}_i\,v_i + s_i\,u_i v_i + r_i\,u_i^2 + \tilde{r}_i\,v_i^2 + \cdots$. Then

$$T_\gamma(f) = [p_1, q_1, \tilde{q}_1, s_1, p_2, q_2, \tilde{q}_2, s_2].$$

If $f = (f_1, f_2) \in \mathcal{S}_{k,r}(\mathcal{M}_\tau)$, then taking the Taylor expansion of the gluing condition (3.5) centered at $u_1 = 0$ yields

$$\begin{aligned} q_2 + s_1\,u_1 &= (\mathfrak{a}(0) + \mathfrak{a}'(0)u_1 + \cdots)\,(\tilde{q}_2 + 2\,\tilde{r}_2\,u_1 + \cdots) \\ &\quad + (\mathfrak{b}(0) + \mathfrak{b}'(0)u_1 + \cdots)\,(q_2 + s_2\,u_1 + \cdots) \end{aligned} \tag{3.27}$$

Combining (3.27) with (3.2) yields

$$\begin{aligned} p_1 &= p_2 \\ q_1 &= \tilde{q}_2 \\ r_1 &= \tilde{r}_2 \\ \tilde{q}_1 &= \mathfrak{a}(0)\,\tilde{q}_2 + \mathfrak{b}(0)\,q_2 \\ s_1 &= 2\,\mathfrak{a}(0)\,\tilde{r}_2 + \mathfrak{b}(0)\,s_2 + \mathfrak{a}'(0)\,\tilde{q}_2 + \mathfrak{b}'(0)\,q_2. \end{aligned}$$

Let $\mathcal{H}(\gamma)$ be the linear space spanned by the vectors $[p_1, q_1, \tilde{q}_1, s_1, p_2, q_2, \tilde{q}_2, s_2]$, which are solution of these equations.

If $\mathfrak{a}(0) \neq 0$, it is a space of dimension 5 otherwise its dimension is 4. Thus $\dim \mathcal{H}(\gamma) = 5 - \mathfrak{c}_\tau(\gamma)$.

In the next proposition we use the notation of the previous section.

Proposition 4.10. *For $k \geqslant \nu_1 + 1$ we have $T_\gamma(\mathcal{S}_{k,r}(\mathcal{M}_\tau)) = \mathcal{H}(\gamma)$. In particular* $\dim(T_\gamma(\mathcal{S}_{k,r}(\mathcal{M}_\tau))) = 5 - c_\tau(\gamma)$.

Proof. By construction we have $T_\gamma(\mathcal{S}_{k,r}(\mathcal{M}_\tau)) \subset \mathcal{H}(\gamma)$. Let us prove that they have the same dimension. If $(A, B, C) \in \mathrm{Syz}_k^{r,r,r}$ with $A = (A_1, A_2)$,$B = (B_1, B_2)$,$C = (C_1, C_2)$, then (A_1, B_1, C_1) is an element of the R-module spanned by $p_1 = (p_1^1, p_1^2, p_1^3)$, $q_1 = (q_1^1, q_1^2, q_1^3)$, ie $(A, B, C) = a_1((1-2u)^{r+1}p_1, 0) + P(p_1, \tilde{p_1}) + Q(q_1, \tilde{q_1})$. Let $f = (f_1, f_2) = \Theta_\tau(a_0, (A, B, C))$ (see (3.21)), then it is easy to see that:

$$T_\gamma(f) = \begin{bmatrix} f_1(\gamma) \\ \partial_{u_1} f_1(\gamma) \\ \partial_{u_2} f_2(\gamma) \\ -\partial_{v_1} f_1(\gamma) \\ \partial_{u_2}\partial_{v_2} f_2(\gamma) \\ -\partial_{u_1}\partial_{v_1} f_1(\gamma) \end{bmatrix} \tag{3.28}$$

$$= \begin{bmatrix} 1 & 0 & 0 & 0 & 0 & 0 \\ 0 & p_1^1(0) & p_1^1(0) & q_1^1(0) & 0 & 0 \\ 0 & p_1^2(0) & p_1^2(0) & q_1^2(0) & 0 & 0 \\ 0 & p_1^3(0) & p_1^3(0) & q_1^3(0) & 0 & 0 \\ 0 & p_1^{2\prime}(0) - 2(r+1)p_1^2(0) & p_1^{2\prime}(0) & q_1^{2\prime}(0) & p_1^2(0) & q_1^2(0) \\ 0 & p_1^{3\prime}(0) - 2(r+1)p_1^3(0) & p_1^{3\prime}(0) & q_1^{3\prime}(0) & p_1^3(0) & q_1^3(0) \end{bmatrix} \begin{bmatrix} a_0 \\ a_1 \\ P(0) \\ Q(0) \\ P'(0) \\ Q'(0) \end{bmatrix}$$

The second column of the matrix is linearly dependent on the third and fifth columns. Using the same argument as in the proof of [21, Proposition 4.7] on the first and 4 last columns of this matrix, we prove that its rank is $5 - c_\tau^\gamma$. By taking $P, Q \in R_1$ of degree $\leqslant 1$, which implies that $k \geqslant \max(\deg(P\,p_1), \deg(Q\,q_1)) = \nu_1 + 1$, the vector $[a_0, P(0), Q(0), P'(0), Q'(0)]$ can take all the values of $\mathbb{R}^5$ and we have $T_\gamma(\mathcal{S}_{k,r}(\mathcal{M}_\tau)) = \mathcal{H}(\gamma)$. This ends the proof. □

We consider now the separability of the Taylor map at the two end points γ, γ'.

Proposition 4.11. *Assume that $k \geqslant \max(\nu_1 + 2, \nu_2 + 2, \mu_1 + r + 1, \mu_2 + r + 1)$. Then $T_{\gamma,\gamma'}(\mathcal{S}_{k,r}(\mathcal{M}_\tau)) = (\mathcal{H}(\gamma), \mathcal{H}(\gamma'))$ and* $\dim T_{\gamma,\gamma'}(\mathcal{S}_{k,r}(\mathcal{M}_\tau)) = 10 - \mathfrak{c}_\tau(\gamma) - \mathfrak{c}_\tau(\gamma')$.

Proof. The inclusion $T_{\gamma,\gamma'}(\mathcal{S}_{k,r}(\mathcal{M}_\tau)) \subseteq (\mathcal{H}(\gamma), \mathcal{H}(\gamma'))$ is clear by construction. For the converse, we show that the image of $T_{\gamma,\gamma'} \circ \Theta_\tau$ contains $(\mathcal{H}(\gamma), 0)$ and then by symmetry we have that $(0, \mathcal{H}(\gamma))$ is in the image of $T_{\gamma,\gamma'} \circ \Theta_\tau$. Let $f = (f_1, f_2) = \Theta_\tau(a_0, (A, B, C)) \in \mathcal{S}_{k,r}(\mathcal{M}_\tau)$ with $(A, B, C) = a_1((1-2u)^{r+1}p_1, 0) + P(p_1, \tilde{p_1}) + Q(q_1, \tilde{q_1})$ and $P, Q \in \mathcal{U}_{2,r}$. The image of f by T_γ is of the form (3.28).

The image of f by $T_{\gamma'}$ is of the form

$$T_{\gamma'}(f) = \begin{bmatrix} f_1(\gamma') \\ \partial_{u_1} f_1(\gamma') \\ \partial_{u_2} f_2(\gamma') \\ -\partial_{v_1} f_1(\gamma') \\ \partial_{u_2}\partial_{v_2} f_2(\gamma') \\ -\partial_{u_1}\partial_{v_1} f_1(\gamma') \end{bmatrix}$$

$$= \begin{bmatrix} 1 & t_1 & 0 & 0 & 0 & 0 \\ 0 & 0 & \tilde{p}_1^1(1) & \tilde{q}_1^1(1) & 0 & 0 \\ 0 & 0 & \tilde{p}_1^2(1) & \tilde{q}_1^2(1) & 0 & 0 \\ 0 & 0 & \tilde{p}_1^3(1) & \tilde{q}_1^3(1) & 0 & 0 \\ 0 & 0 & \tilde{p}_1^{2\prime}(1) & \tilde{q}_1^{2\prime}(1) & \tilde{p}_1^2(1) & \tilde{q}_1^2(1) \\ 0 & 0 & \tilde{p}_1^{3\prime}(1) & \tilde{q}_1^{3\prime}(1) & \tilde{p}_1^3(1) & \tilde{q}_1^3(1) \end{bmatrix} \begin{bmatrix} a_0 \\ a_1 \\ P(1) \\ Q(1) \\ P'(1) \\ Q'(1) \end{bmatrix} + \begin{bmatrix} L_1(P) + L_2(Q) \\ 0 \\ 0 \\ 0 \\ 0 \\ 0 \end{bmatrix}$$

with $t_1 = \int_0^{1/2} (1-2u)^{r+1} p_1^1 du$, $L_1(P) = \int_0^1 P\, \tilde{p}_1^1 du$, $L_2(Q) = \int_0^1 Q\, \tilde{q}_1^1 du$. By choosing $P(1) = P'(1) = Q(1) = Q'(1) = 0$ and $a_0 + t_1 a_1 = 0$, we have an element in the kernel of this matrix. By choosing $a_0, P(0), P'(0), Q(0), Q'(0)$ and a_1 such that $a_0 + t_1 a_1 + L_1(P) + L_2(Q) = 0$, we can find a solution to the system (3.28) for any $f \in \mathcal{S}_k(\mathcal{M}_\tau)$. Therefore, constructing spline coefficients $P, Q \in \mathcal{U}_2^r$ which interpolate prescribed values and derivatives at $0, 1$, we can construct spline functions $f \in \mathcal{S}_k(\mathcal{M}_\tau)$ such that $T_\gamma(f)$ span $\mathcal{H}(\gamma)$ and $T_{\gamma'}(f) = 0$. The degree of the spline is $k \geqslant \max(\nu_1 + 2, \mu_1 + r + 1)$. By symmetry, for $k \geqslant \max(\nu_2 + 2, \mu_2 + r + 1)$, we have $(0, \mathcal{H}(\gamma')) \subset T_{\gamma,\gamma'}(\mathcal{S}_{k,1}(\mathcal{M}_\tau)$, which concludes the proof. □

Definition 4.12. *The separability $\mathfrak{s}(\tau)$ of the edge τ is the minimal k such that*

$$T_{\gamma,\gamma'}(\mathcal{S}_{k,r}(\mathcal{M}_\tau)) = (T_\gamma(\mathcal{S}_{k,r}(\mathcal{M}_\tau)), T_{\gamma'}(\mathcal{S}_{k,r}(\mathcal{M}_\tau)))$$

.

The previous proposition shows that $\mathfrak{s}(\tau) \leqslant \max(\nu_1 + 2, \nu_2 + 2, \mu_1 + r + 1, \mu_2 + r + 1)$.

4.7 Decomposition and dimension

Let $\tau \in \mathcal{M}_1$ be an interior edge τ shared by the cells $\sigma_0, \sigma_1 \in \mathcal{M}_2$. The Taylor map along the edge τ of $\mathcal{M}_\tau$ is

$$\begin{aligned} D_\tau \colon \mathcal{R}_k(\sigma_0) \oplus \mathcal{R}_k(\sigma_1) &\to \mathcal{R}_k(\sigma_0) \oplus \mathcal{R}_k(\sigma_1) \\ (f_0, f_1) &\mapsto (D_\tau^{\sigma_0}(f_0), D_\tau^{\sigma_1}(f_1)). \end{aligned}$$

Its image is the set of splines of $\mathcal{R}_{k,r}(\sigma_1) \oplus \mathcal{R}_{k,r}(\sigma_2)$ with *support along* τ. The kernel is the set of splines of $\mathcal{R}_{k,r}(\sigma_1) \oplus \mathcal{R}_{k,r}(\sigma_2)$ with vanishing b-spline coefficients along the edge τ. The elements of $\ker(D_\tau)$ are smooth splines in $\mathcal{S}_{k,r}(\mathcal{M}_\tau)$. Let $W_k(\tau) = D_\tau(\mathcal{S}_{k,r}(\mathcal{M}_\tau))$. It is the set of splines in $\mathcal{S}_{k,r}(\mathcal{M}_\tau)$ with a support along τ. As D_τ is a projector, we have the decomposition

$$\mathcal{S}_{k,r}(\mathcal{M}_\tau) = \ker(D_\tau) \oplus W_k(\tau). \tag{3.29}$$

From the relations (3.19) and (3.20), we deduce that $W_k(\tau) = \operatorname{Im}\Theta_\tau$. Since Θ_τ is injective, thus $\dim(W_k(\tau)) = \dim \operatorname{Syz}_{k-1}^{r,r,r} + 1 = d_\tau(k,r) + 1$ and $W_k(\tau) \neq \{0\}$ when $k \geqslant \mu_1$ and $k \geqslant \mu_2$ (Lemma (4.1) (iii)).

The map $T_{\gamma,\gamma'}$ defined in Section 3.2 induces the exact sequence

$$0 \to \mathcal{K}_k(\tau) \to \mathcal{S}_{k,r}(\mathcal{M}_\tau) \xrightarrow{T_{\gamma,\gamma'}} \mathcal{H}(\tau) \to 0 \tag{3.30}$$

where $\mathcal{K}_k(\tau) = \ker(T_{\gamma,\gamma'})$ and $\mathcal{H}(\tau) = T_{\gamma,\gamma'}(\mathcal{S}_{k,r}(\mathcal{M}_\tau))$.

Definition 4.13. *For an interior edge $\tau \in \mathcal{M}_1^o$, let $\mathcal{E}_k(\tau) = \ker(T_{\gamma,\gamma'}) \cap W_k(\tau) = \ker(T_{\gamma,\gamma'}) \cap \operatorname{Im} D_\tau$ be the set of splines in $\mathcal{S}_{k,r}(\mathcal{M}_\tau)$ with their support along τ and with vanishing Taylor expansions at γ and γ'. For a boundary edge $\tau' = (\gamma, \gamma')$, which belongs to a face σ, we also define $\mathcal{E}_k(\tau')$ as the set of elements of $\mathcal{R}_{k,r}(\sigma)$ with their support along τ' and with vanishing Taylor expansions at γ and γ'.*

Notice that the elements of $\mathcal{E}_k(\tau)$ have their support along τ and that their Taylor expansion at γ and γ' vanish. Therefore, their Taylor expansion along all (boundary) edges of $\mathcal{M}_\tau$ distinct from τ also vanish.

As $\ker(D_\tau) \subset \mathcal{K}_k(\tau)$, we have the decomposition

$$\mathcal{K}_k(\tau) = \ker(D_\tau) \oplus \mathcal{E}_k(\tau). \tag{3.31}$$

We deduce the following result

Lemma 4.14. *For an interior edge $\tau \in \mathcal{M}_1^o$ and for $k \geqslant \mathfrak{s}(\tau)$, the dimension of $\mathcal{E}_k(\tau)$ is*

$$\dim \mathcal{E}_k(\tau) = \tilde{d}_\tau(k,r) - 9 + \mathfrak{c}_\tau(\gamma) + \mathfrak{c}_\tau(\gamma').$$

Proof. From the relations (3.29), (3.30) and (3.31), we have

$$\begin{aligned} \dim \mathcal{E}_k(\tau) &= \dim \mathcal{K}_k(\tau) - \dim \ker(D_\tau) \\ &= \dim \mathcal{S}_{k,r}(\mathcal{M}_\tau) - \dim \mathcal{H}_k(\tau) - \dim \mathcal{S}_{k,r}(\mathcal{M}_\tau) + \dim W_k(\tau) \\ &= \dim W_k(\tau) - \dim \mathcal{H}_k(\tau), \end{aligned}$$

which gives the formula using Proposition 4.11. □

Remark 4.15. *When τ is a boundary edge, which belongs to the face $\sigma \in \mathcal{M}_2$, we have $\mathcal{S}_{k,r}(\mathcal{M}_\tau) = \mathcal{R}_{k,r}(\sigma)$ and $\dim \mathcal{E}_k(\tau) = 2(m+1) - 8 = 4k - 2r - 6$.*

4.8 Basis functions associated to an edge

Suppose that $\mathcal{B}_k^r = \{\beta_i\}_{i=0\ldots l}$ with $l = \dim \operatorname{Syz}_{k-1}^{r-1,r,r}$ and $\beta_i = (\beta_i^1, \beta_i^2, \beta_i^3)$, is a basis of $\operatorname{Syz}_{k-1}^{r-1,r,r}$. We know also that $\mathcal{E}_k = \{f = \Theta_\tau(a_0, (A,B,C)) : T_{\gamma,\gamma'}(f) = 0, (A,B,C) \in \operatorname{Syz}_{k-1}^{r-1,r,r}\}$, but we have:

$$\begin{aligned} T_{\gamma,\gamma'}(f) &= \begin{pmatrix} T_\gamma \\ T_{\gamma'} \end{pmatrix} \\ &= \begin{pmatrix} c_0, A(0), -C(0), -C'(0), & c_0, B(0), A(0), B'(0) \\ c_0 + \int_0^1 A(u)du, A(1), -C(1), & C'(1), c_0 + \int_0^1 A(u)du, B(1), A(1), B'(1) \end{pmatrix} \end{aligned}$$

Suppose that $(A, B, C) = \left(\sum b_i\beta_i^1, \sum b_i\beta_i^2, \sum b_i\beta_i^3\right)$ with $b_i \in \mathbb{R}$, then $T_{\gamma,\gamma'}(f) = 0$ is equivalent to the system:

$$\begin{cases} a_0 = 0 \\ \sum b_i\beta_i^1(0) = 0 \\ \sum b_i\beta_i^2(0) = 0 \\ \sum b_i\beta_i^3(0) = 0 \\ \sum b_i\beta_i^{2'}(0) = 0 \\ \sum b_i\beta_i^{3'}(0) = 0 \\ \sum b_i \int_0^1 \beta_i(t)dt = -a_0 \end{cases} \quad \begin{cases} \sum b_i\beta_i^1(1) = 0 \\ \sum b_i\beta_i^2(1) = 0 \\ \sum b_i\beta_i^3(1) = 0 \\ \sum b_i\beta_i^{2'}(1) = 0 \\ \sum b_i\beta_i^{3'}(1) = 0 \end{cases} \tag{3.32}$$

The system (3.32) directly depends on the gluing data (3.1) along the edge via equations (3.19) and (3.20), see Section 4.4 above. An explicit solution requires the computation of a basis for the syzygy module, which is constructed in Section 4.5. The image by Θ_τ (defined in (3.21)) of a basis of the solutions of this system yields a basis of $\mathcal{E}_k$.

5 Splines around a vertex

In this section, we analyse the spline functions, attached to a vertex, that is, the spline functions which Taylor expansions along the edges around the vertex vanish. We analyse the image of this space by the Taylor map at the vertex, and construct a set of linearly independent spline functions, which images span the image of the Taylor map. These form the set of basis functions, attached to the vertex.

Let us consider a topological surface $\mathcal{M}_\gamma$ composed by quadrilateral faces $\sigma_1, \ldots, \sigma_{F(\gamma)}$ sharing a single vertex γ, and such that the faces σ_i and σ_{i-1} have a common edge $\tau_i = (\gamma, \delta_i)$, for $i = 2, \ldots, F(\gamma)$. If γ is an interior vertex then we identify the indices modulo $F(\gamma)$ and τ_1 is the common edge of $\sigma_{F(\gamma)}$ and σ_1, see Fig. 3.5.

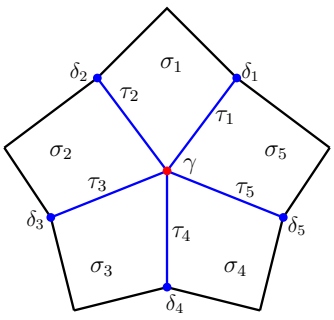

Figure 3.5: Topological surface $\mathcal{M}_\gamma$ composed by $F(\gamma) = 5$ quadrilateral faces glued around the vertex γ.

The gluing data attached to each of the edges τ_i will be denoted by $\mathfrak{a}_i = \frac{a_i}{c_i}$, $\mathfrak{b}_i = \frac{b_i}{c_i}$. By a change of coordinates we may assume that γ is at the origin $(0, 0)$, and the edge τ_i is on the line $v_i = 0$, where (u_{i-1}, v_{i-1}) and (u_i, v_i) are the coordinate

systems associated to σ_{i-1} and σ_i, respectively. Then the transition map at γ across τ_i from σ_i to σ_{i-1} is as given by

$$\phi_{\tau_i}\colon (u_i, v_i) \to \begin{pmatrix} v_i \mathfrak{b}_i(u_i) \\ u_i + v_i \mathfrak{a}_i(u_i) \end{pmatrix};$$

following the notation in (3.1), we have $\phi_{\tau_i} = \phi_{i-1,i}$.

The restriction along the boundary edges of $\mathcal{M}_\gamma$ is defined by

$$D_\gamma\colon \bigoplus_{i=1}^{F(\gamma)} \mathcal{R}(\sigma_i) \to \bigoplus_{\substack{\tau \in \partial\mathcal{M}_\gamma \\ \tau \not\ni \gamma}} \mathcal{R}^{\sigma_i}(\tau)$$
$$(f_i)_{i=1}^{F(\gamma)} \mapsto \left(D_\tau^{\sigma_i}(f_i)\right)_{\tau \not\ni \gamma}$$

where $D_\tau^{\sigma_i}$ is the Taylor expansion along τ on σ_i, see Section 3.2.

Let $\mathcal{V}_k(\gamma)$ be the set of spline functions of degree $\leqslant k$ on $\mathcal{M}_\gamma$ that vanish at the first order derivatives along the boundary edges:

$$\mathcal{V}_k(\gamma) = \ker D_\gamma \cap \mathcal{S}_{k,r}(\mathcal{M}_\gamma). \tag{3.33}$$

The gluing data and the differentiability conditions in (3.5) lead to conditions on the coefficients of the Taylor expansion of f_i, namely

$$f_i(u_i, v_i) = p + q_i u_i + q_{i+1} v_i + s_i u_i v_i + r_i u_i^2 + r_{i+1} v_i^2 + \cdots \tag{3.34}$$

with $p, q_i, s_i, r_i \in \mathbb{R}$, and for $i = 2, \ldots, F$ the following two conditions are satisfied

$$q_{i+1} = \mathfrak{a}_i(0) q_i + \mathfrak{b}_i(0) q_{i-1} \tag{3.35}$$
$$s_i = 2\mathfrak{a}_i(0) r_i + \mathfrak{b}_i(0) s_{i-1} + \mathfrak{a}_i'(0) q_i + \mathfrak{b}_i'(0) q_{i-1}. \tag{3.36}$$

Let $\mathcal{H}(\gamma)$ be the space spanned by the vectors $\mathbf{h} = [p, q_1, \ldots, q_{F(\gamma)}, s_1, \ldots, s_{F(\gamma)}]$ such that p, $q_1, \ldots, q_{F(\gamma)}$, $s_1, \ldots, s_{F(\gamma)}$, $r_1, \ldots, r_{F(\gamma)} \in \mathbb{R}$ give a solution for (3.35) and (3.36). The following result was proved in [21, Proposition 5.1] in the case of polynomial splines.

Proposition 5.1. *For a topological surface $\mathcal{M}_\gamma$ consisting of $F(\gamma)$ quadrangles glued around an interior vertex γ,*

$$\dim \mathcal{H}(\gamma) = 3 + F(\gamma) - \sum_{\tau \ni \gamma} \mathfrak{c}_\tau(\gamma) + \mathfrak{c}_+(\gamma),$$

where $\mathfrak{c}_\tau(\gamma)$, $\mathfrak{c}_+(\gamma)$ are as in Definition 1.4.

Since the vectors in $\mathcal{H}(\gamma)$ only depend on the Taylor expansion of f at γ, and f can be seen as a polynomial spline in a neighborhood of γ, then the proof of Proposition 5.1 follows the same argument as the one in [21].

Proposition 5.2. *For a topological surface $\mathcal{M}_\gamma$ as before, if $\mathfrak{s}(\tau_i)$ denotes the separability of the edge τ_i as in Definition 4.12, then*

$$T_\gamma\big(\mathcal{V}_k(\gamma)\big) = \mathcal{H}(\gamma),$$

for every $k \geqslant \max\{\mathfrak{s}(\tau_i)\colon i = 1, \ldots, F(\gamma)\}$.

Proof. By definition (see (3.33)), the elements of $\mathcal{V}_k(\gamma)$ satisfy the conditions (3.35) and (3.36) on the Taylor expansion of f, then $T_\gamma\big(\mathcal{V}_k(\gamma)\big) \subseteq \mathcal{H}(\gamma)$.

Let us consider a vector $\mathbf{h} = [p, q_1, \dots, q_{F(\gamma)}, s_1, \dots, s_{F(\gamma)}] \in \mathcal{H}(\gamma)$, we need to prove that this vector is in the image $T_\gamma\big(\mathcal{V}_k(\gamma)\big)$. In fact, by Proposition 4.11 applied to $\tau_i = [\gamma, \delta_i]$, there exists $(f_i^{\tau_i}, f_{i-1}^{\tau_i}) \in \mathcal{S}_{k,r}(\mathcal{M}_{\tau_i})$ such that $T_\gamma(f_i^{\tau_i}, f_{i-1}^{\tau_i}) = [p, q_i, q_{i+1}, s_i, p, q_{i-1}, q_i, s_{i-1}]$ and $T_{\delta_i}(f_i^{\tau_i}, f_{i-1}^{\tau_i}) = 0$ for $k \geqslant \mathfrak{s}(\tau_i)$, for $i = 2, \dots, F$. Let us notice that in such case, $T_\gamma^{\sigma_i}(f_i^{\tau_i}) = T_\gamma^{\sigma_i}(f_i^{\tau_{i+1}})$. Thus, it follows that there exists $g_i \in \mathcal{R}_k(\sigma_i)$ such that $T_{\tau_i}^{\sigma_i}(g_i) = f_i^{\tau_i}$ and $T_{\tau_{i+1}}^{\sigma_i}(g_i) = f_i^{\tau_{i+1}}$. The spline g_i is constructed by taking the coefficients of $f_i^{\tau_i}$ and $f_i^{\tau_{i+1}}$ in $\mathcal{R}^{\sigma_i}(\tau_i)$ and $\mathcal{R}^{\sigma_i}(\tau_{i+1})$, respectively (see Section 3.2). Since $T_{\delta_i}^{\sigma_i}(f_i^{\tau_i}) = T_{\delta_i}^{\sigma_i}(g_i) = 0$ and $T_{\delta_{i+1}}^{\sigma_i}(f_i^{\tau_{i+1}}) = T_{\delta_{i+1}}^{\sigma_i}(g_i) = 0$ then $T_\tau^{\sigma_i}(g_i) = 0$ for every edge $\tau \in \sigma_i$ such that $\gamma \notin \tau$. Let $\mathbf{g} = [g_1, g_2, \dots, g_{F(\gamma)}]$ where $g_i \in \mathcal{R}_k(\sigma_i)$ is as previously constructed. Then $\mathbf{g}$ and their first derivatives vanish on the edges in $\partial\mathcal{M}_\gamma$, and $\mathbf{g}$ satisfies the gluing conditions along all the interior edges τ_i of $\mathcal{M}_\gamma$, i.e. $\mathbf{g} \in \mathcal{S}_{k,r}(\mathcal{M}_\gamma) \cap \ker D_\gamma$. Hence $\mathbf{g} \in \mathcal{V}_k(\gamma)$, and by construction $T_\gamma(\mathbf{g}) = \mathbf{h}$. □

Given a topological surface $\mathcal{M}$, let T be the Taylor map at all the vertices of $\mathcal{M}$, as defined in Section 3.2. We have the following exact sequence

$$0 \to \mathcal{K}_k(\mathcal{M}) \to \mathcal{S}_{k,r}(\mathcal{M}) \xrightarrow{T} \mathcal{H}_k(\mathcal{M}) \to 0 \tag{3.37}$$

where $\mathcal{H}_k(\mathcal{M}) = T\big(\mathcal{S}_{k,r}](\mathcal{M})\big)$ and $\mathcal{K}_k(\mathcal{M}) = \ker T \cap \mathcal{S}_{k,r}(\mathcal{M})$. Let us define $\mathfrak{s}^* = \max\{\mathfrak{s}(\tau) \colon \tau \in \mathcal{M}_1\}$. From Proposition 4.11, we know that $\mathfrak{s}^* \leqslant 2 + \max\{v_i^\tau \colon \text{ for } i = 1, 2 \text{ and } \tau \in \mathcal{M}_1\} + \min(3, r)$, where (u_i^τ, v_i^τ) for $i = 1, 2$ are the degrees of the generators of Syz_1 and Syz_2, respectively, with $u_i^\tau \leqslant v_i^\tau$.

Proposition 5.3. *Let $F(\gamma)$ and $\mathcal{H}(\gamma)$ be as defined above for each vertex $\gamma \in \mathcal{M}_0$, then for every $k \geqslant \mathfrak{s}^*$ we have $T(\mathcal{S}_{k,r}(\mathcal{M})) = \prod_\gamma \mathcal{H}(\gamma)$ and*

$$\dim T(\mathcal{S}_{k,r}(\mathcal{M})) = \sum_{\gamma \in \mathcal{M}_0} (F(\gamma) + 3) - \sum_{\gamma \in \mathcal{M}_0} \sum_{\tau \ni \gamma} \mathfrak{c}_\tau(\gamma) + \sum_{\gamma \in \mathcal{M}_0} \mathfrak{c}_+(\gamma).$$

Proof. The statement follows directly applying Propositions 5.2 and 5.1 to each vertex $\gamma \in \mathcal{M}_0$, with M_γ the sub-mesh of $\mathcal{M}$ which consists of the quadrangles in $\mathcal{M}$ containing the vertex γ. □

5.1 Basis functions associated to a vertex

Given a topological surface $\mathcal{M}$, for each vertex $\gamma \in \mathcal{M}_0$, let us consider the sub-mesh $\mathcal{M}_\gamma$ consisting of all the faces $\sigma \in \mathcal{M}$ such that $\gamma \in \sigma$, as before, we denote this number of such faces by $F(\gamma)$. From Proposition 5.3 we know the dimension of $T(\mathcal{S}_{k,r}(\mathcal{M}))$ for $k \geqslant \mathfrak{s}^*$. In the following, we construct a set of linearly independent splines $\mathcal{B}_0 \subseteq \mathcal{S}_{k,r}(\mathcal{M})$ such that $\mathrm{span}\{T(f) \colon f \in \mathcal{B}_0\} = T(\mathcal{S}_{k,r}(\mathcal{M}))$.

Let us take a vertex $\gamma \in \mathcal{M}_0$ and consider the b-spline representation of the elements $f_\sigma \in \mathcal{R}_k(\sigma)$ for $\sigma \in \mathcal{M}_\gamma$. We construct a set $\mathcal{B}_0(\gamma) \subset \mathcal{S}_{k,r}(\mathcal{M}_\gamma)$ of linearly independent spline function as follows:

- First we add one basis function f attached to the value at γ, such that $T^{\sigma}_{\gamma}(f_\sigma)(\gamma) = 1$ for every $\sigma \in \mathcal{M}_\gamma$. Let us notice that if we define $g_\sigma = \sum_{0\leqslant i,j\leqslant 1} N_i(u_\sigma)N_j(v_\sigma)$ for every $\sigma \in \mathcal{M}_\gamma$, and g on $\mathcal{M}_\gamma$ such that $g|_\sigma = g_\sigma$, then $g(\gamma) = 1$. We lift g to a spline f on $\mathcal{M}_\gamma$ such that f is in the image of the map Θ_τ defined in (3.21), for every $\tau \in \mathcal{M}_1$ attached to γ.

- We add two basis functions g, h supported on $\mathcal{M}_\gamma$ and attached to the first derivatives at γ. Namely, let us consider $g_{\sigma_1} = (1/2k)\big(N_0(u_{\sigma_1}) + N_1(u_{\sigma_1})\big)N_1(v_{\sigma_1})$, and $h_{\sigma_1} = (1/2k)N_1(u_{\sigma_1})\big(N_0(v_{\sigma_1}) + N_1(v_{\sigma_1})\big)$. The conditions (3.35) and (3.36) allow us to find g_{σ_i} and h_{σ_i}, for $i = 2, \ldots, F(\gamma)$ from g_{σ_1} and h_{σ_1}, respectively. Thus, we define g and h on $\mathcal{M}_\gamma$ by taking $g|_\sigma = g_\sigma$ and $h|_\sigma = h_\sigma$. Since g and h by construction satisfy the gluing conditions (3.2) and (3.5) along the edges, then they are splines in the image $\mathcal{S}_{k,r}(\mathcal{M}_\gamma)$ of Θ_τ for every interior edge $\tau \in \mathcal{M}_\gamma$.

- For each edge τ_i for $i = 1, \ldots, F(\gamma)$, let us define the function $g_{\sigma_i} = c^{\sigma_i}_{1,1}(g_{\sigma_i})N_1(u_{\sigma_i})N_1(v_{\sigma_i})$, where $c^{\sigma_i}_{1,1}(g_{\sigma_i}) = 1/4k^2$ if τ_i is not a crossing edge, and equal to zero otherwise. Then, for every fix edge $\tau_i \in \mathcal{M}_\gamma$ attached to γ we construct a spline g on $\mathcal{M}_\gamma$ such that $g|_{\sigma_i} = g_{\sigma_i}$, and $g|_{\sigma_j}$ for $j \neq i$ are determined by g_{σ_i} and the gluing data at γ, according to (3.35) and (3.36). The previous construction produces $F(\gamma) - \sum_{\tau\ni\gamma} \mathfrak{c}_\tau(\gamma)$ (non-zero) spline functions. These splines, by construction, are in the image of Θ_τ (3.21) along all the edges $\tau \in \mathcal{M}_1$ attached to γ.

- If γ is a crossing vertex, by definition all the edges attached to γ are crossing edges. In this case, we define $g_{\sigma_1} = (1/4k^2)N_1(u_{\sigma_1})N_1(v_{\sigma_1})$, and determine g_{σ_i} for $i = 2, \ldots, F(\gamma)$ using the gluing data at γ and conditions (3.35) and (3.36). Defining g on $\mathcal{M}_\gamma$ by $g|_{\sigma_i} = g_{\sigma_i}$ we obtain a spline in $\mathcal{S}_{k,r}(\mathcal{M}_\gamma)$.

Let us notice that if τ_i is a crossing edge then, following the notation in the Taylor expansion of $g_i(u_i, v_i)$ in (3.34), the coefficient $s_i = \partial_{u_{\sigma_i}}\partial_{v_{\sigma_i}} g_i(u_i, v_i)|_\gamma$ becomes dependent on s_{i-1}, q_i and q_{i-1} and therefore there is no additional basis function associated to the edge τ_i.

Applying the previous construction to every $\gamma \in \mathcal{M}_0$, we obtain a collection of splines $\mathcal{B}_0(\gamma) \subseteq \mathcal{S}_{k,r}(\mathcal{M}_\gamma)$ for each $\gamma \in \mathcal{M}_0$. We lift the splines $f \in \mathcal{S}_{k,r}(\mathcal{M}_\gamma)$ to functions on $\mathcal{M}$ by defining $f_\sigma = 0$ for every $\sigma \notin \mathcal{M}_\gamma$. To simplify the exposition, we abuse the notation, and will also call f the lifted spline on $\mathcal{M}$, and $\mathcal{B}_0(\gamma)$ the collection of those splines.

Definition 5.4. *For a topological surface $\mathcal{M}$, let $\mathcal{B}_0 \subseteq \mathcal{S}_{k,r}(\mathcal{M})$ be the set of linearly independent functions defined by*

$$\mathcal{B}_0 = \bigcup_{\gamma\in\mathcal{M}_0} \mathcal{B}_0(\gamma), \tag{3.38}$$

where $\mathcal{B}_0(\gamma) \subseteq \mathcal{S}_{k,r}(\mathcal{M}_\gamma)$, for each vertex $\gamma \in \mathcal{M}$.

By construction, the collection of splines in $\mathcal{B}_0(\gamma)$, for each vertex $\gamma \in \mathcal{M}_0$, and $\mathcal{B}_0$, are linearly independent. Moreover, the number of elements in $\mathcal{B}_0$ coincides with the dimension of $\mathcal{H}_k(\mathcal{M})$ and hence they constitute a basis for the spline space $\mathcal{S}_{k,r}(\mathcal{M})$ whose Taylor map T (3.37) is not zero.

6 Splines on a face

Let $\mathcal{F}_k(\mathcal{M})$ be the spline functions in $\mathcal{S}_{k,r}(\mathcal{M})$ with vanishing Taylor expansion along all the edges of $\mathcal{M}$, that is, $\mathcal{F}_k(\mathcal{M}) = \mathcal{S}_{k,r}(\mathcal{M}) \cap \ker D$.

An element f is in $\mathcal{F}_k(\mathcal{M})$ if and only if $c^{\sigma}_{i,j}(f) = 0$ for $i \leqslant 1$ or $i \geqslant m-1$, $j \leqslant 1$ or $j \geqslant m-1$ for all $\sigma \in \mathcal{M}_2$.

Let $\mathcal{F}_k(\sigma)$ be the elements in $\mathcal{F}_k(\mathcal{M})$ with $c^{\sigma'}_{i,j}(f) = 0$ for $0 \leqslant i, j \leqslant m$ and $\sigma' \neq \sigma$.

- The dimension of $\mathcal{F}_k(\sigma)$ is $(2k-r-3)^2_+$.
- A basis of $\mathcal{F}_k(\sigma)$ is $b_i(u_\sigma)b_j(v_\sigma)$ for $1 < i, j < m-1$.

We easily check that $\mathcal{F}_k(\mathcal{M}) = \oplus_\sigma \mathcal{F}_k(\sigma)$, which implies the following result:

Lemma 6.1. *The dimension of $\mathcal{F}_k(\mathcal{M})$ is $(2k-r-3)^2_+ F_2$, where F_2 is the number of (quadrangular) faces of $\mathcal{M}$.*

Basis functions associated to a face. The set $\mathcal{F}_k(\mathcal{M})$ of basis functions associated to faces is obtained by taking the union of the bases of $\mathcal{F}_k(\sigma)$ for all faces $\sigma \in \mathcal{M}_2$, that is,

$$\mathcal{B}_2 := \{b_i(u_\sigma)b_j(v_\sigma), 1 < i, j < m-1, \sigma \in \mathcal{M}_2\}. \tag{3.39}$$

7 Dimension and basis of Splines on $\mathcal{M}$

We have now all the ingredients to determine the dimension of $\mathcal{S}_{k,r}(\mathcal{M})$ and a basis.

Theorem 7.1. *Let $\mathfrak{s}^* = \max\{\mathfrak{s}(\tau) \mid \tau \in \mathcal{M}_1\}$. Then, for $k \geqslant \mathfrak{s}^*$,*

$$\dim \mathcal{S}_{k,r}(\mathcal{M}) \;=\; (2k-r-3)^2 F_2 + \textstyle\sum_{\tau \in \mathcal{M}_1} \tilde{d}_\tau(k,r) + 4F_2 - 9F_1 + 3F_0 + F_+$$

where

- *$\tilde{d}_\tau(k)$ is the dimension of the syzygies of the gluing data along τ in degree $\leqslant k$,*
- *F_2 is the number of rectangular faces,*
- *F_1 is the number of edges,*
- *F_0 (resp. F_+) is the number of (resp. crossing) vertices,*

Proof. By construction, $\mathcal{K}_k(\mathcal{M}) = \mathcal{S}_{k,r}(\mathcal{M}) \cap \ker T$ is the set of splines in $\mathcal{S}_{k,r}(\mathcal{M})$, which Taylor expansion at all the vertices vanish and $\mathcal{H}_k(\mathcal{M})$ is the image of $\mathcal{S}_{k,r}(\mathcal{M})$ by the Taylor map T. Thus we have the following exact sequence:

$$0 \to \mathcal{K}_k(\mathcal{M}) \to \mathcal{S}_{k,r}(\mathcal{M}) \xrightarrow{T} \mathcal{H}_k(\mathcal{M}) \to 0. \tag{3.40}$$

By construction, $\mathcal{E}_k(\mathcal{M})$ is the set of splines in $\mathcal{K}_k(\mathcal{M})$ with a support along the edges of $\mathcal{M}$, so that $D(\mathcal{K}_k(\mathcal{M})) = \mathcal{E}_k(\mathcal{M})$. The kernel of $D : \oplus_\sigma \mathcal{R}_k(\mathcal{M}) \to \oplus_\sigma \mathcal{R}_k(\mathcal{M})$ is $\mathcal{F}_k(\mathcal{M})$. As $\mathcal{F}_k(\mathcal{M}) \subset \mathcal{K}_k(\mathcal{M})$, we have the exact sequence

$$0 \to \mathcal{F}_k(\mathcal{M}) \to \mathcal{K}_k(\mathcal{M}) \xrightarrow{D} \mathcal{E}_k(\mathcal{M}) \to 0. \tag{3.41}$$

From the exact sequences (3.40) and (3.41), we have

$$\begin{aligned} \dim \mathcal{S}_k^{1,r}(\mathcal{M}) &= \dim \mathcal{H}_k(\mathcal{M}) + \dim \mathcal{K}_k(\mathcal{M}) \\ &= \dim \mathcal{H}_k(\mathcal{M}) + \dim \mathcal{E}_k(\mathcal{M}) + \dim \mathcal{F}_k(\mathcal{M}) \end{aligned}$$

We deduce the dimension formula using Lemma 4.14, Proposition 5.1 and Lemma 6.1. □

Basis of $\mathcal{S}_{k,r}(\mathcal{M})$. A basis of $\mathcal{S}_{k,r}(\mathcal{M})$ is obtained by taking

- the basis $\mathcal{B}_0$ of $\mathcal{V}_k(\mathcal{M})$ attached to the vertices of $\mathcal{M}$ and defined in (3.38),
- the basis $\mathcal{B}_1$ of $\mathcal{E}_k(\mathcal{M})$ attached to the edges of $\mathcal{M}$ and defined in (3.32),
- the basis $\mathcal{B}_2$ of $\mathcal{F}_k(\mathcal{M})$ attached to the faces of $\mathcal{M}$ and defined in (3.39).

To illustrate the construction, we detail an example of a simple mesh, where a point of valence 3 is connected to three boundary crossing point. The construction can be extended to points of arbitrary valencies, in a more complex mesh.

We consider the mesh $\mathcal{M}$ composed of 3 rectangles $\sigma_1, \sigma_2, \sigma_3$ glued around an interior vertex γ, along the 3 interior edges τ_1, τ_2, τ_3. There are 6 boundary edges and 6 boundary vertices $\delta_1, \delta_2, \delta_3$, $\epsilon_1, \epsilon_2, \epsilon_3$. We use the symmetric gluing

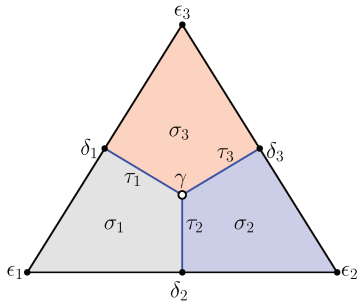

Figure 3.6: Smooth corner.

corresponding to the angle $\frac{2\pi}{3}$ at γ and $\frac{\pi}{2}$ at $\delta_1, \delta_2, \delta_3$.

We choose the gluing data $[a, b, c]$ along an edge τ_i given by Formula (3.14):

$$\begin{aligned} a(u) &= \mathfrak{d}_0(u) \\ b(u) &= -\mathfrak{d}_0(u) - \mathfrak{d}_1(u) \\ c(u) &= \mathfrak{d}_0(u) + \mathfrak{d}_1(u) \end{aligned}$$

where $\mathfrak{d}_0 = \tilde{N}_0(u) + \tilde{N}_1(u)$, $\mathfrak{d}_1 = \tilde{N}_2(u) + \tilde{N}_3(u) + \tilde{N}_4(u)$ for the b-spline basis $\tilde{N}_0, \ldots, \tilde{N}_5$ of $\mathcal{U}_{0,2}$ and where $u = 0$ corresponds to γ. This gives

$$a(u) = \begin{cases} -1 + 4\,u^2 & 0 \leqslant u \leqslant \frac{1}{2} \\ 0 & \frac{1}{2} \leqslant u \leqslant 1 \end{cases}, b(u) = -1, \quad c(u) = 1;$$

The degrees of the μ-bases of the different components are respectively $\mu_1 = 0, \nu_1 = 2, \mu_2 = 0, \nu_2 = 0$. Thus the separability is reached from the degree $k \geqslant 4$.

We are going to analyze the spline space $\mathcal{S}_4^{1,1}(\mathcal{M})$ for specific gluing data. An element $f \in \mathcal{S}_4^{1,1}(\mathcal{M})$ is represented on each cell σ_i $(i = 1, 2, 3)$ by a tensor product b-spline of class C^1 with 8×8 b-spline coefficients:

$$f_k := \sum_{0 \leqslant i,j \leqslant 7} c_{i,j}^k(f) N_{i,j}(u_k, v_k),$$

where $N_{i,j}(u, v) = N_i(u)N_j(v)$ and $\{N_0(u), \ldots, N_7(u)\}$ is the basis of $\mathcal{U}_{k,1}$. We describe an element $f \in \mathcal{S}_4^{1,1}(\mathcal{M})$ as a triple of b-spline functions

$$\left[\sum_{0 \leqslant i,j \leqslant 7} c_{i,j}^1 N_{i,j}\,,\ \sum_{0 \leqslant i,j \leqslant 7} c_{i,j}^2 N_{i,j}\,,\ \sum_{0 \leqslant i,j \leqslant 7} c_{i,j}^3 N_{i,j} \right].$$

The separability is reached at degree 4 and we have the following basis elements, described by a triple of functions which are decomposed in the b-spline bases of each face:

• The number of basis functions attached to γ is $6 = 1 + 2 + 3$.

– The basis function associated to the value at γ is

$$\begin{aligned}\Big[& N_{0,0} + \frac{1}{3} N_{0,2} + N_{0,3} + N_{0,4} + 2\, N_{1,3} + 2\, N_{1,4} + \frac{1}{3} N_{2,0} + N_{3,0} + N_{4,0}, \\ & N_{0,0} + \frac{1}{3} N_{2,0} + N_{3,0} + N_{4,0} + 3\, N_{0,1} + \frac{31}{3} N_{0,2} + 17\, N_{0,3} + 17\, N_{0,4} \\ & \qquad + 14\, N_{1,2} + 34\, N_{1,3} + 34\, N_{1,4}, \\ & N_{0,0} + 3\, N_{1,0} + \frac{31}{3} N_{2,0} + 17\, N_{3,0} + 17\, N_{4,0} + \frac{1}{3} N_{0,2} + N_{0,3} + N_{0,4} \\ & \qquad + 2\, N_{1,3} + 2\, N_{1,4} \Big].\end{aligned}$$

– The two basis functions associated to the derivatives at γ are

$$\begin{aligned}\Big[& N_{0,1} + \frac{10}{3} N_{0,2} + \frac{16}{3} N_{0,3} + \frac{16}{3} N_{0,4} + \frac{14}{3} N_{1,2} + \frac{32}{3} N_{1,3} + \frac{32}{3} N_{1,4}\,, \\ & N_{1,0} + \frac{10}{3} N_{2,0} + \frac{16}{3} N_{3,0} + \frac{16}{3} N_{4,0}\,, \\ & - N_{0,1} - \frac{10}{3} N_{0,2} - \frac{16}{3} N_{0,3} - \frac{16}{3} N_{0,4} - \frac{16}{3} N_{1,2} - \frac{32}{3} N_{1,3} - \frac{32}{3} N_{1,4} \\ & \qquad - N_{1,0} - \frac{10}{3} N_{2,0} - \frac{16}{3} N_{3,0} - \frac{16}{3} N_{4,0} \Big], \\ \Big[& N_{1,0} + \frac{10}{3} N_{2,0} + \frac{16}{3} N_{3,0} + \frac{16}{3} N_{4,0}\,, \\ & - N_{0,1} - \frac{10}{3} N_{0,2} - \frac{16}{3} N_{0,3} - \frac{16}{3} N_{0,4} - \frac{14}{3} N_{1,2} - \frac{32}{3} N_{1,3} - \frac{32}{3} N_{1,4}\,, \\ & - N_{1,0} - \frac{10}{3} N_{2,0} - \frac{16}{3} N_{3,0} - \frac{16}{3} N_{4,0} + N_{0,1} + \frac{10}{3} N_{0,2} + \frac{16}{3} N_{0,3} \\ & \qquad + \frac{16}{3} N_{0,4} + \frac{14}{3} N_{1,2} + \frac{32}{3} N_{1,3} + \frac{32}{3} N_{1,4} \Big].\end{aligned}$$

– The three basis functions associated to the cross derivatives at γ are

$$\Big[-\frac{4}{3} N_{0,2} - \frac{8}{3} N_{0,3} - \frac{8}{3} N_{0,4} + N_{1,1} - \frac{4}{3} N_{1,2} - \frac{16}{3} N_{1,3} - \frac{16}{3} N_{1,4}\,, \\ - \frac{4}{3} N_{2,0} - \frac{8}{3} N_{3,0} - \frac{8}{3} N_{4,0}\,,\ 0 \Big],$$

$$\Big[-\frac{4}{3} N_{2,0} - \frac{8}{3} N_{3,0} - \frac{8}{3} N_{4,0}\,, \\ -\frac{4}{3} N_{0,2} - \frac{8}{3} N_{0,3} - \frac{8}{3} N_{0,4} - \frac{4}{3} N_{1,2} - \frac{16}{3} N_{1,3} - \frac{16}{3} N_{1,4}\,, \\ -\frac{4}{3} N_{2,0} - \frac{8}{3} N_{3,0} - \frac{8}{3} N_{4,0} + N_{1,1} - \frac{4}{3} N_{0,2} - \frac{8}{3} N_{0,3} - \frac{8}{3} N_{0,4} \\ - \frac{4}{3} N_{1,2} - \frac{16}{3} N_{1,3} - \frac{16}{3} N_{1,4} \Big],$$

$$\Big[-\frac{4}{3} N_{2,0} - \frac{8}{3} N_{3,0} - \frac{8}{3} N_{4,0}\,,\ 0\,, \\ - \frac{4}{3} N_{0,2} - \frac{8}{3} N_{0,3} - \frac{8}{3} N_{0,4} - \frac{4}{3} N_{1,2} - \frac{16}{3} N_{1,3} - \frac{16}{3} N_{1,4} \Big].$$

• There are $4 = 1 + 2 + 2 - 1$ basis functions attached to δ_i:

$$\big[N_{0,7}\,,\ N_{7,0} + 2\,N_{7,1}\,,\ 0\big], \big[N_{0,6}\,,\ N_{6,0} + 2\,N_{6,1}\,,\ 0\,\big], \big[N_{1,7}\,,\ -N_{7,1}\,, 0\,\big], \big[N_{1,6}\,, -N_{6,1}\,,\ 0\,\big].$$

The basis functions associated to the other boundary points δ_2, δ_3 are obtained by cyclic permutation.

• There are $5 = 14 - 5 - 4$ basis functions attached to edge τ_1:

$$\big[-N_{1,2}\,,\ N_{2,1}\,,\ 0\,\big], \big[-N_{1,3}\,,\ N_{3,1}\,,\ 0\,\big], \big[-N_{1,4}\,,\ N_{4,1}\,,\ 0\,\big], \\ \big[-N_{1,5}\,,\ N_{5,1}\,,\ 0\,\big], \big[N_{0,5} + 2\,N_{1,5}\,,\ N_{5,0}\,,\ 0\,\big].$$

The basis functions associated to the other edges τ_2, τ_3 are obtained by cyclic permutation.

• For the remaining boundary points, boundary edges and faces, we have the following 36×3 basis functions

$$\big[N_{i,j}\,,\ 0\,,\ 0\,\big], \big[0\,,\ N_{i,j}\,,\ 0\,\big], \big[0\,,\ 0\,,\ N_{i,j}\,\big], \quad \text{for } 2 \leqslant i, j \leqslant 7.$$

The dimension of the space $\mathcal{S}_4^{1,1}(\mathcal{M})$ is $6 + 3 \times (4 + 5 + 36) = 141$.

A similar construction applies for an edge of a general mesh connecting an interior vertex γ of any valency $\neq 4$ to another vertex γ'. If γ' is a crossing vertex, the numbers of basis functions attached to the vertices and the edge do not change. If γ' is not a crossing vertex, the number of basis functions attached to the non-crossing vertex γ' becomes 5 and there are 4 basis functions attached to the edges. In the case, where the edge connects two crossing vertices, there are 4 basis functions attached to each crossing vertex and 8 basis functions attached to the edge.

The gluing data used in this construction require a degree 4 for the separability. For the mesh of Figure 3.6, it is possible to use linear gluing data and bi-cubic

b-spline patches. The dimension of bi-cubic G^1 splines with the linear gluing data is 72. Depending on the topology of the mesh and the choice of the gluing data, it is possible to use low degree b-spline patches for the construction of G^1 splines. In Figure 3.7, examples of G^1 bicubic spline surfaces are shown, for meshes with valencies at most 3, 4 and 6. The G^1 surface is obtained by least-square projection of a G^0 spline onto the space of G^1 splines.

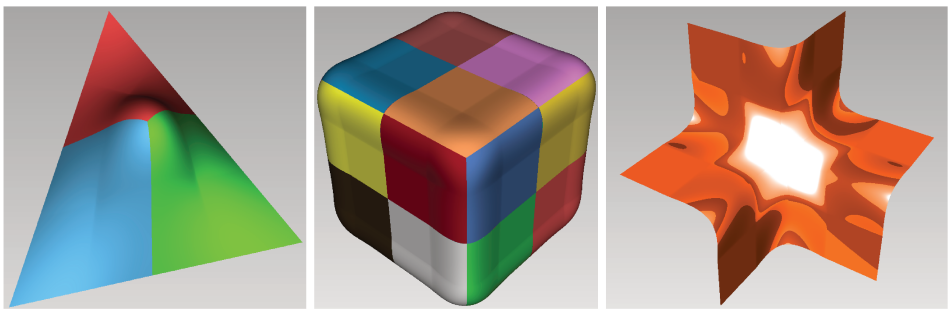

Figure 3.7: Examples of bi-cubic G^1 surfaces

8 Geometric continuity using reparametrisation

In this section we will see how can we generalise the definition of the G^k continuity and adapt it to a new frame of work, that allows the use of homology theory, as in Chapter 2. We start by defining what is a G^k-Junctions:

Definition 8.1 (G^k junction)**.** *Let σ_1, σ_2 be two polygonal domains in the Euclidean two dimensional space E and let $e_1 \in \partial\sigma_1$, $e_2 \in \partial\sigma_2$ be two edges from the boundary of this two polygons. We assume the following:*

- *There exists two open sets $\mathcal{O}_1$, $\mathcal{O}_2$ of E containing respectively the edges e_1, e_2.*
- *There exists two polygonal domains D_1, D_2 in $\mathbb{R}^2$ sharing a boundary edge e.*
- *There exists an open set $\mathcal{O}$ containing e and two C^k diffeomorphisms $\phi : \mathcal{O} \to \mathcal{O}_1$ and $\psi : \mathcal{O} \to \mathcal{O}_2$.*
- *We assume that $\phi(\mathcal{O} \cap D_1) = \sigma_1 \cap \mathcal{O}_1$, $\psi(\mathcal{O} \cap D_2) = \sigma_2 \cap \mathcal{O}_2$, $\phi(e) = e_1$, $\psi(e) = e_2$.*

*Then we say that σ_1, σ_2 admit a G^k-**connection** along the edges e_1, e_2 given by the reparametrisations $(\phi, \psi, \mathcal{O})$.*

*If two C^k maps $f_1 : \sigma_1 \to \mathbb{R}$, $f_2 : \sigma_2 \to \mathbb{R}$ verify $\partial_{i,j}(f_1 \circ \phi)(x) = \partial_{i,j}(f_2 \circ \psi)(x)$ for each i, j such that $i + j \leqslant k$ and at each point $x \in e$ then we will say that f_1 and f_2 admits a G^k-**junction** along the two edges e_1, e_2 given by the triple $(\phi, \psi, \mathcal{O})$.*

The line supporting the segment line $\phi^{-1}(e_1)$ is called **the junction line** of $(\phi, \psi, \mathcal{O})$. We use it to define algebraically the G^k-junction:

Proposition 8.2. *We keep the notations of 8.1, and suppose that ϕ and ψ are polynomials.*

Two C^k maps $f_1 : \sigma_1 \to \mathbb{R}$, $f_2 : \sigma_2 \to \mathbb{R}$ admits a G^k-junction along the two edges e_1, e_2 given by the triple $(\phi, \psi, \mathcal{O})$ if and only if the polynomial $f_1 \circ \phi - f_2 \circ \psi$ is divisible by the $k+1^{th}$ power of the junction line l of $(\phi, \psi, \mathcal{O})$, ie. $f_1 \circ \phi - f_2 \circ \psi \equiv 0 \, mod \, l^{k+1}$.

Proof. direct consequence of the proposition 1.2 in [7] □

In the following we will take the notation $\phi^*(f) := f \circ \phi$ for the pull back of a map f using another map ϕ.

Definition 8.3. *We keep the same notation as in Definition 8.1.*

We say that two reparametrisations $(\phi_1, \psi_1, \mathcal{O}_1)$ $(\phi_2, \psi_2, \mathcal{O}_2)$ are **equivalent** *if the following two sets are the same:*

- *The set of couple (f_1, f_2), $f_1 : \sigma_1 \to \mathbb{R}$, $f_2 : \sigma_2 \to \mathbb{R}$, admitting a G^k junction along the two edges e_1, e_2 given by the triple $(\phi_1, \psi_1, \mathcal{O}_1)$.*
- *The set of couple (f_1, f_2), $f_1 : \sigma_1 \to \mathbb{R}$, $f_2 : \sigma_2 \to \mathbb{R}$, admitting a G^k junction along the two edges e_1, e_2 given by the triple $(\phi_2, \psi_2, \mathcal{O}_2)$.*

Definition 8.4 (Topological Surface)**.** *Let $\mathcal{I} = (\sigma_i)_{i=1,\dots,m}$ be a collection of square domains and $\mathcal{T} = ((\phi_j, \psi_j, \mathcal{O}))_{j=1\dots r}$ be a set of G^k connections between edges of the domains σ_i. We assume that an edge can only be connected to at most one other edge from another domain. We consider the equivalence relation over the disjoint union of all the domains $M = \coprod_i \sigma_i$ that is defined by: $x \sim y$ if and only if there exists $(\phi, \psi, \mathcal{O}) \in \mathcal{T}$ and $z \in \mathcal{O}$ such that $\phi(z) = x$ and $\psi(z) = y$. The quotient $\mathcal{M} = {}^{M}/_{\sim}$ is called the* **topological surface** *of the couple $(\mathcal{I}, \mathcal{T})$.*

Definition 8.5 (The space of G^k-Splines)**.** *We keep the notations of Definition 8.4. We say that a map $f : \mathcal{M} \to \mathbb{R}$ is G^k over the topological surfaces $\mathcal{M}$ if there exists a set of maps $f_1, \dots, f_n$, with $f_i : \sigma_i \to \mathbb{R}$ and $f_{|\sigma_i} = f_i$ for $i \in 1 \dots n$, such that for each G^k connection $(\phi, \psi, \mathcal{O}) \in \mathcal{T}$ between σ_i, σ_j along $e_i \in \sigma_i, e_j \in \sigma_j$ the corresponding maps f_i, f_j admits a G^k-junction between σ_i, σ_j along e_i, e_j given by $(\phi, \psi, \mathcal{O})$. The space of G^k-Splines over $\mathcal{M}$ is denoted by $\mathcal{S}^k(\mathcal{M})$.*

Let $(\mathcal{M}, \mathcal{I}, \mathcal{T})$ be a topological surfaces and γ a vertex from $\mathcal{M}$, **the star topology** $\mathcal{M}_\gamma$ of γ in $\mathcal{M}$ is the topological surface formed by all the faces $\sigma \in \mathcal{I}$ that are neighbors to γ, and all the connections $c \in \mathcal{T}$ along edges containing γ. We will denote by $\mathcal{I}_\gamma$ and $\mathcal{T}_\gamma$ the set of face and connections of $\mathcal{M}_\gamma$ respectively.

Suppose that the domains of $\mathcal{M}_\gamma$ are $\sigma_0, \dots, \sigma_m$, and that σ_i, σ_{i+1} share the edge e_i in $\mathcal{M}_\gamma$ (the index is taken modulo m). Let $\phi = (\phi_i)_{i=0\dots m}$ be the sequence of C^k diffeomorphisms $\phi_i : \mathcal{O}_i \to \tilde{\mathcal{O}}_i$ with $\sigma_i \subset \tilde{\mathcal{O}}_i$, such that for any $i \in 0 \dots m$ the object $(\phi_i, \phi_{i+1}, \mathcal{O}_i \cap \mathcal{O}_{i+1})$ form a connection along the edge e_i that is equivalent to the one given by $\mathcal{M}_\gamma$, we will say then that ϕ is a **vertex based reparametrisation** of $\mathcal{M}_\gamma$.

A topological surface $(\mathcal{M}, \mathcal{I}, \mathcal{C})$ with $\mathcal{I} = (\sigma_i)_{i=0\dots m}$ is said to have a **planar based reparametrisation** if the two following conditions are satisfied (the same notations of Definition 8.1 are used):

- There exists a sequence of maps $\phi_0, \ldots, \phi_n$ with $\phi_i : \mathcal{O}_i \to \sigma_i$ such that for each G^k-connection $(\phi, \psi, \mathcal{O}) \in \mathcal{C}$ along an edge e from $\mathcal{M}$ shared by the two faces σ_i, σ_j, the reparametrisation given by $(\phi_i, \phi_j, \mathcal{O}_i \cap \mathcal{O}_j)$ is equivalent to $(\phi, \psi, \mathcal{O})$.
- The sets $\phi_i^{-1}(\sigma_i^\circ)$ are two by two disjoint.[1]

In this case the union of all the sets $\phi_i^{-1}(\sigma_i)$ will form a polyhedral complex, that we will denote Δ. $\mathcal{M}_2$, $\mathcal{M}_1$ and $\mathcal{M}_0$ will denote the sets of faces, edges and vertices of $\mathcal{M}$ respectively, an interior edge is an edge that belongs to at least two faces, the set of all interior edges is denoted by $\mathcal{M}_1^\circ$, and the set of all the interior vertices is denoted by $\mathcal{M}_0^\circ$.

8.1 Chain complex methods for G^k-continuity

If a topological surface has a planar based reparametrisation then we can construct a chain complex in the following way: let $C_2 = \bigoplus_{\sigma \in \mathcal{M}_2} \mathbb{R}[\mathbf{x}]$, $C_1 = \bigoplus_{\tau \in \mathcal{M}_1^\circ} \mathbb{R}[\mathbf{x}] \Big/ I_\tau^k$, $C_0 = \bigoplus_{\gamma \in \mathcal{M}_0^\circ} \mathbb{R}[\mathbf{x}] \Big/ I_\gamma^k$, where I_τ is the junction line along the edge τ and $I_\gamma = \sum_{\gamma \in_\tau} I_\tau$.

We define the boundary complex by:

$$\mathcal{C} : C_2 \xrightarrow{\partial_2} C_1 \xrightarrow{\partial_1} C_0 \tag{3.42}$$

where

$$\partial_2(\oplus_\sigma f_\sigma) = \bigoplus_{\tau \in \sigma_i \cap \sigma_j} \varepsilon_\tau(\phi_i^*(f_{\sigma_i}) - \phi_j^*(f_{\sigma_j})) \tag{3.43}$$

the sign ε_τ is induced from the first map in the complex of the relative homology of the polyhydral mesh of $\mathcal{M}$ over its boundary $\mathcal{M} / \partial\mathcal{M}$ as in chapter 2. The map ∂_1 is exactly the second map in the complex of the relative homology.

8.2 Homogenisation of the boundary complex

The goal of the study is to find the dimension of the space of G^k-Splines up to a given degree. This is why we will bound the degree in the first term of the boundary complex $\mathcal{C}$. In order to have graded maps in the double complex we will consider the homogeneous version of the complex $\mathcal{C}$ (as done in Section 2). By using the notation of Definition 8.4, we will embed the domains σ_i of the topological surface $\mathcal{M}$ in $\mathbb{R}^3$ using the homogenization map h that maps each point $(x, y) \in \mathbb{R}^2$ to the point $(x, y, 1) \in \mathbb{R}^3$. We get the new 3-dimensional conical domains $\hat{\sigma_i}$ formed of the base $h(\sigma_i)$ and the vertex $(0, 0, 0) \in \mathbb{R}^3$. We embed the complex Δ in the same way so that we form the cone of Δ, that is the polyhedral complex $\hat{\Delta}$ who's faces are the cones formed of the base $h(\phi_i(\sigma_i))$ and the vertex $(0, 0, 0)$. The homogenisation of the reparametrisation maps is done in the following way: for each reparametrisation ϕ_i let s_i be the maximal polynomial degree over the three components of ϕ_i, and let $s = max_{i=1\ldots m}(s_i)$,

[1] We use A° to denote the interior of a set A

the homogenization of ϕ_i is $\hat{\phi}_i(x,y,z) = z^s\phi(\frac{x}{z},\frac{y}{z})$. An element f of $\mathcal{R}$ is going to be homogenized by the formula $\hat{f}(x,y,z) = z^d f(\frac{x}{z},\frac{y}{z})$ where d is the degree at which we want to homogenise.

By considering the set of all domains $\hat{\mathcal{I}} = (\hat{\sigma}_i)_i$ with their reparametrizations $\hat{\phi}_i$, and their induced connection:

$$\hat{\mathcal{T}} = \{(\hat{\phi}_i, \hat{\phi}_j, \mathcal{O}_i \cap \mathcal{O}_j) | \sigma_1, \sigma_2 \in \mathcal{I} \, admiting \, a \, G^k \, connection\}$$

we construct a 3 dimensional G^k-topology that we will denote $(\hat{\mathcal{M}}, \hat{\mathcal{I}}, \hat{\mathcal{T}})$. The boundary complex corresponding to this topology is denoted by:

$$\hat{\mathcal{G}} : \bigoplus_{\sigma\in\mathcal{M}_2} \mathbb{R}[\mathbf{x}] \xrightarrow{\partial_2} \bigoplus_{\tau\in\mathcal{M}_1^\circ} \mathbb{R}[\mathbf{x}]/\hat{I}_\tau^k \xrightarrow{\partial_1} \bigoplus_{\gamma\in\mathcal{M}_0^\circ} \mathbb{R}[\mathbf{x}]/\hat{I}_\gamma^k \tag{3.44}$$

where $\mathbf{x}$ denotes the three variables x_1, x_2, x_3.

Under this setting, all the differential maps of the double complex d_i^j and ∂_i for any i, j are graded for the polynomial grading:

- ∂_2 is of degree $t(s-1)$ over the set $\bigoplus_{\sigma\in\hat{\mathcal{M}}_2} \mathbb{R}[\mathbf{x}]_t$ of elements of degree equal to t.
- ∂_1 is of degree 0.

According to t we will consider the complex $\mathcal{GC}_t$ with the following form:

$$\hat{\mathcal{G}}_t : \bigoplus_{\sigma\in\mathcal{M}_2} \mathbb{R}[\mathbf{x}]_t \xrightarrow{\partial_2} \bigoplus_{\tau\in\mathcal{M}_1^\circ} (\mathbb{R}[\mathbf{x}]/\hat{I}_\tau^k)_{ts} \xrightarrow{\partial_1} \bigoplus_{\gamma\in\mathcal{M}_0^\circ} (\mathbb{R}[\mathbf{x}]/\hat{I}_\gamma^k)_{ts} \tag{3.45}$$

that we use to compute the space of splines of degree t. The homology group in the first term is the space of splines, while in the last term the homology is the same as the last term homology group in the complex (2.3), so it is equal to zero. By comparing the image of the map ∂_2 in the two complexes $\mathcal{G}_t$, and $\mathcal{C}_{ts}$ we see that $Im(\partial_2)$ in $\mathcal{G}_t$, is a subset of $Im(\partial_2)$ in $\mathcal{C}_{ts}$, while the kernel of ∂_1 in the two complexes is the same, we deduce that $dim(H_1(\mathcal{C}_t)) \leqslant dim(H_1(\mathcal{G}_t))$. In Theorem 4.6 it is stated that the codimension of $H_1(\mathcal{C})$ as an $\mathbb{R}[\mathbf{x}]$-module is equal to 0, that means that the Hilbert polynomial of that module has degree zero. In the other hand, the module structure on the graded vector space of G-splines is not well defined, so we cannot define the Krull dimension on this spaces.

9 Multi-uv coordinates complex

Let $\mathcal{M}_\tau$ be a topological surface made of two polygons σ_1, σ_2 that share the edge τ, and suppose that for each one of the two faces we have a local uv-coordinates system (u_1, v_1) and (u_2, v_2). The following is a way to define G^r-junction equivalent to Definition 1.1. This definition will be used only with polynomial patches, so all the maps ϕ, f, g are supposed to be polynomial.

Definition 9.1. *Let σ_1(σ_2 resp.) a polygonal domain in $\mathbb{R}^2$ and τ_1 (τ_2 resp.) an edge in σ_1 (resp.σ_2). Two polynomial maps $f : \sigma_1 \to \mathbb{R}$, $g : \sigma_2 \to \mathbb{R}$ admits a G^r-junction along the two edges τ_1, τ_2 if and only if there exists a polynomial C^r-diffeomorphism $\phi : U_1 \to U_2$ between two neighbourhoods U_1, U_2 of the two edges τ_1, τ_2 such that:*

- *ϕ maps τ_1 to τ_2.*
- *ϕ maps the interior points of σ_1 to the exterior point of σ_2.*
- *$f(u_1, v_1) - g(u_2, v_2) \in I^{r+1}$, where I^r is an ideal of generated by the polynomials: $u_2 - \phi_1(u_1, v_1)$, $v_2 - \phi_2(u_1, v_1)$, and $l^r_{\tau_2}$, here ϕ_1 and ϕ_2 are the two coordinates of ϕ, and the polynomial l_{τ_2} is the linear equation defining the hyperplane that supports the edge τ_2.*

Before defining the complex, point out that Definitions 1.1 and 9.1 are equivalent to the Definition 8.1 when one of the two parametrisations is the identity. Moreover the homogenisation is possible in the definition of the G^r-continuity above exactly as we have done in Section 8.2. So now we will speak about the homogenized version where the ideal I^r in the definition above is replaced by its homogenisation in $\mathbb{R}[u_\sigma, v_\sigma, w_\sigma]$. Let Δ be a d-dimensional complex, $\mathcal{R}_\sigma = \mathbb{R}[u_\sigma, v_\sigma, w_\sigma]$, and for $S \subset \mathcal{M}$ let $\mathcal{R}_S = \otimes_{\sigma \in S} \mathcal{R}_\sigma$ be the ring of polynomials with the variables $(u_\sigma)_{\sigma \in S}, (v_\sigma)_{\sigma \in S}, (w_\sigma)_{\sigma \in S}$. If an edge τ is shared by the two faces σ_1 and σ_2 then we denote $\mathcal{R}_\tau$ the ring of polynomials $\mathcal{R}_{\sigma_1} \otimes \mathcal{R}_{\sigma_2}$, and if a vertex γ is shared by the faces $\sigma_1, \dots, \sigma_F$ then $\mathcal{R}_\gamma = \oplus_{i=1\dots F} \mathcal{R}_i$. We define the complex:

$$\mathcal{C} : \mathcal{C}^2 \xrightarrow{\partial_2} \mathcal{C}^1 \xrightarrow{\partial_1} \mathcal{C}^0$$

with:

$$\mathcal{C}^d = \oplus_{\sigma \in \mathcal{M}_d} \mathcal{R}_\sigma \tag{3.46}$$

$$\mathcal{C}^i = \oplus_{\sigma \in \mathcal{M}_i} \mathcal{R}_\sigma / J(\sigma) \qquad for\, i \in \{1, 0\} \tag{3.47}$$

$$J(\tau) = I^{r+1}_\tau \qquad for\, \tau \in \mathcal{M}_1 \tag{3.48}$$

$$J(\gamma) = \sum_{\gamma \in \tau} I^{r+1}_\tau \qquad for\, \tau \in \mathcal{M}_i,\ \ i < d-1 \tag{3.49}$$

with ∂_i a differential map similar to the one we use in relative homology simplicial complex $\Delta/\partial\Delta$(see Section 2).

Another possible construction is to define the equivalent exact sequence to 2.19, again by using the homogenisation of all the polynomials. We define it in the following way: Let ∂ be the incidence matrix of the dual graph of a given topological surface, with columns indexed by maximal faces. for each vector of polynomials $V = (p_1, \dots, p_n)$ we denote by $Diag(V)$ the diagonal matrix who's diagonal components are the coefficients of V. For each two faces σ_1 and σ_2 in $\mathcal{M}$ sharing the edge τ with a transition ϕ_τ from σ_1 to σ_2, we define by ψ_1, ψ_2 the homogenisation of the two polynomials $u_{\sigma_2} - \phi^1_\tau(u_{\sigma_1}, v_{\sigma_1})$ and $v_{\sigma_2} - \phi^2_\tau(u_{\sigma_1}, v_{\sigma_1})$. Let $L_1 = [\tau_1, \dots, \tau_n]$ be the list of edges ordered in the same way we did for the lines of the incidence matrix, and $V_1 = (l^r_i)_{i \in L_1}$ $V_2 = (\psi_i)_{i \in L_1}$ the two vector of polynomials. We denote also by $L_2 = [\sigma_1, \dots, \sigma_m]$ a list with an ordering of the faces similar to the columns of ∂. Then we define the following map: $P : (\bigoplus_{\sigma \in L_2} \mathcal{R}_\sigma) \oplus (\bigoplus_{\tau \in L_1} \mathcal{R}_\tau) \oplus (\bigoplus_{\tau \in L_1} \mathcal{R}_\tau) \to \bigoplus_{\tau \in L_1} \mathcal{R}_\tau$ that consists on multiplying by the matrix $(\partial | Diag(V_1) | Diag(V_2))$. This map induces the following exact sequence:

$$0 \to \mathcal{S}_{r,l}(\mathcal{M}) \to (\bigoplus_{\sigma \in L_2} \mathcal{R}_\sigma) \oplus (\bigoplus_{\tau \in L_1} \mathcal{R}_\tau) \oplus (\bigoplus_{\tau \in L_1} \mathcal{R}_\tau) \to \bigoplus_{\tau \in L_1} \mathcal{R}_\tau \to coker(P) \to 0 \tag{3.50}$$

The advantage of this construction comparing to the one in section 8.1 is that the maps are graded vector spaces homomorphism.

The complex proposed in the previous sections has an important drawback: the differential maps of the complexes are not module homomorphisms. Thus it is not possible to speak about the Krull dimension of the homology, so it is not possible to deduce the degree of the Hilbert polynomial of that spaces in the way we did in the Chapter 2. However it is still possible to speak about the Hilbert functions of graded vector spaces. This make the constructions above possibly useful for computing the dimension.

10 Conclusion

We have investigated in this chapter how to construct a basis for the space of G^1-splines. We started the chapter by giving some of the constraints that one has to impose on the gluing data so that the space of G-splines is ample (ie has enough degrees of freedom), and we avoid the appearance of singularities at the vertices.

This chapter includes two methods of construction of basis, both of them uses the piecing strategy (see introduction of Section 3). The first one describe the G^1-constraints along the edges using the bspline coefficients of the G^1-functions, constructs a bases for two patches topologies, and peace them to form a global basis.

The second method is different in two main things, one is that the splines along the edges are considered as solution for the syzygy space. Another point is that the basis construction algorithm describes systems to solve, who's variables are the values and derivatives of the G^1-functions, and not the bspline coefficients.

Chapter 4

Shape modelling

1 Shape Smoothing

1.1 Introduction

Subdivision schemes such as Catmull-Clark scheme are powerfull tools to produce smooth surfaces that can be easily controlled from a coarse mesh. They became very popular in graphics and animation for their capacities to control easily shapes. However from a geometric modelling point of view, they have some drawbacks: At extraordinary vertices, they are composed of infinitely many rings of piecewise polynomial surfaces and have no explicit analytic representation. Though the limit subdivision surface is smooth, it may not be curvature continuous around an extraordinary vertex [54].

In this chapter, we describe a new explicit scheme to compute a smooth piecewise polynomial surface from a quadrangular mesh. The constructed surface is geometrically smooth everywhere and C^2 except in the neighbourhood of extraordinary vertices. The polynomial patches associated to the faces of the quadrangular mesh are bi-quintic Bézier parameterisations. The Catmull-Clark subdivision scheme is used to compute the control points of b-spline patches associated to the faces of the quadrangular mesh. The nearest geometrically smooth bi-quintic spline surface is then explicitly computed by projection on the space of G^1 splines after a degree elevation of the patches. Therefore, it is a G^1 approximation of the Catmull-Clark subdivision surface. These constructions are described explicitly by masks and do not required the solution of linear systems or to solve any optimisation problem.

We also present a new scheme to compute a basis of the space of geometrically smooth functions on the quadrangular mesh. G^0 basis elements are first constructed. The G^1 basis is obtained by a smoothing step. We describe explicit masks to compute these elements from the G^0 elements.

The chapter is organized as follows. The next section presents related prior works. Section 2 provides the notation and definitions of geometric continuity. In Section 3, we present the masks for the construction of G^1 surfaces made of bi-quintic faces and the scheme for the construction of basis functions of the space of G^1 bi-quintic b-spline surfaces. In Section 4, experimentation results are presented.

1.2 Prior works

Many methods have been proposed to construct geometrically smooth surfaces from quadrangular meshes. This started with the initial work of Catmull-Clark on subdivision surfaces [15]. The subdivision surface cannot be represented by a finite collection of b-spline patches.

Several works focused on the construction G^1 surfaces, with b-spline faces, using different types of b-spline patches on the faces of the topological surface [55], [56], [45], [57], [58], [21], [59], [60], [42]. These works addressed the solution of the G^1 constraints, but focussed less on their use for the construction of high quality G^1 surfaces from quadrangular control meshes.

Constructions of G^1 surfaces based on quadrangular mesh subdivision schemes have been investigated for instance in [61] using 4 triangular cubic patches on each face, or inserting nodes in b-splines patches in [62]. In [63] an approximately G^1 surface construction based on Catmull-Clark subdivision scheme is presented.

Some recent works propose methods to compute high quality geometrically smooth surfaces over quadrangular meshes. The construction of G^2 surfaces is investigated by solving a constraint minimization problem, using bi-septic patches in [64] or using bi-quintic patches in [65]. In [66], [9], the G^1 surface construction is guided by bi-quintic or rings of bi-quartic b-spline surfaces that minimize some energy. Thus, these constructions involve complex and non-explicit schemes for producing the G^1 surfaces. In our smoothing method, instead of computing smooth guide surfaces, we use the Approximate Catmull-Clark surface as a guide and project it explicitly on the space of G^1 spline surfaces. This direct and simpler approach provides surfaces of good quality as we will see in the experimentation section.

The construction of basis functions of the space of G^1 splines on a quadrangular mesh have been investigated for instance in [21], [42], [60], [23], [49], [67]. These methods involved the solution of linear systems depending on the topology of the mesh or the way patches are glued along edges. They require some pre-computation and some case analysis. Other alternative basis constructions involving singular b-spline functions are studied and exploited, for instance, in [68] for design and analysis on quadrangular planar meshes that satisfy some topological conditions. None of these approaches provide an explicit and systematic scheme to compute regular basis functions.

2 Definitions

2.1 Topological surface

We denote by $\mathcal{M}$ the *topological surface* which supports the spline functions. In this paper, $\mathcal{M}$ will be a quadrangular mesh given by

- a collection $\mathcal{M}_0$ of points in $\mathbb{R}^3$,
- a collection $\mathcal{M}_2$ of quadrangular faces,
- a collection $\mathcal{M}_1$ of edges which are either shared by two faces or on the boundary.

For each quadrangular face $\sigma \in \mathcal{M}_2$, we have a parameter domain $D_\sigma = [0,1]^2$ and parameters u_σ, v_σ. The number of elements of $\mathcal{M}_i$ $(i = 0, 1, 2)$ is denoted M_i. The valence $\mathfrak{v}(\gamma)$ of a vertex $\gamma \in \mathcal{M}_0$ is the number of faces $\sigma \in \mathcal{M}_2$ s.t. $\gamma \in \sigma$. Let $\mathfrak{c}(\gamma) = \cos(\frac{2\pi}{\mathfrak{v}(\gamma)})$. A vertex is called singular if it is an interior vertex with valence $\mathfrak{v} \neq 4$.

2.2 Surface representation

A spline function f on $\mathcal{M}$ will be represented by a collection $f = (f_\sigma)_{\sigma \in \mathcal{M}_2}$ of b-spline functions, one for each face: The function f_σ associated to the face σ is represented by

$$f_\sigma := \sum_{1 \leqslant i,j \leqslant m} b^\sigma_{i,j}(f) N_i(u_\sigma) N_j(v_\sigma),$$

where $b^\sigma_{i,j}(f) \in \mathbb{R}$ and $N_1, \ldots, N_m$ are the b-spline basis functions of the space $\mathcal{U}_{d,\mathbf{t}}$ of splines of degree d and knots $\mathbf{t}$. Hereafter, we will represent a spline function f by its coefficient vector $[f] = (b^\sigma_{i,j}(f)) \in \mathbb{R}^{m^2 M_2}$.

In this paper, we consider $d = 5$ and the knots $\mathbf{t} = \{0^6, 1^6\}$ so that $m = 6$. The basis functions $N_1(u), \ldots, N_6(u)$ are the Bernstein polynomials of degree 5 on the interval $[0,1]$. Each function f_σ is a bi-quintic polynomial in the variables (u_σ, v_σ).

2.3 Geometric continuity

For an edge τ shared by two polygons $\sigma_0, \sigma_1 \in \mathcal{M}_2$, we consider transition maps ϕ_{σ_0,σ_1} between the two faces which are, in suitable frames, of the form:

$$(u_1, v_1) \mapsto (u_0, v_0) \quad = \quad \begin{pmatrix} v_1 \frac{a_1(u_1)}{a_0(u_1)} + v_1^2 \rho_1(u_1, v_1) \\ u_1 + v_1 \frac{a_2(u_1)}{a_0(u_1)} + v_1^2 \rho_2(u_1, v_1) \end{pmatrix}$$

where $a_0(u_1), a_1(u_1), a_2(u_1), \rho_1(u_1, v_1), \rho_2(u_1, v_1)$ are C^1 functions. The shared edge is defined by $v_1 = 0$ on σ_1 and by $u_0 = 0$ on σ_0. The functions $[a_0(u_1), a_1(u_1), a_2(u_1)]$ are called the *gluing data* at γ along τ on σ_1.

The geometrically smooth constraint corresponds to the following relations: $\forall u_1 \in [0,1]$,

$$\begin{array}{rcl} f_1(u_1, 0) & = & f_0(0, u_1) \\ a_0(u_1) \frac{\partial f_1}{\partial v_1}(u_1, 0) & = & a_1(u_1) \frac{\partial f_0}{\partial u_0}(0, u_1) + a_2(u_1) \frac{\partial f_0}{\partial v_0}(0, u_1) \end{array}$$

where $f_1 = f_{\sigma_1}$, $f_0 = f_{\sigma_0}$ are the restrictions of f on the faces σ_0, σ_1.

In the following, we will suppose that each singular vertex is isolated from the other singular vertices by at least one layer of ordinary vertices, and we will use the following gluing data along an edge $\tau = (\gamma_0, \gamma_1)$: $a_0(u) = 1$, $a_1(u) = -1$ and

- if $\mathfrak{v}(\gamma_0) \neq 4$ and $\mathfrak{v}(\gamma_1) = 4$, $a_2(u) = \mathfrak{c}(\gamma_0)(1-u)^2$,
- if $\mathfrak{v}(\gamma_0) = 4$ and $\mathfrak{v}(\gamma_1) = 4$, $a_2(u) = 0$.

They satisfy the compatibility conditions around a vertex, required to define ample spline spaces on $\mathcal{M}$ (see e.g. [45], [21], [42]). The relations between the control points of two faces sharing an edge are given in Fig 4.2.

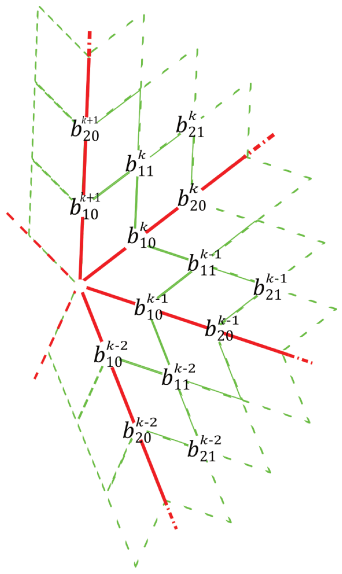

Figure 4.1: Indices of the b-spline coefficients around a vertex with the convention that $b^k_{i,0} \equiv b^{k-1}_{0,i}$ for $i \in 0 \ldots 5$, $k = 1, \ldots, \mathfrak{v}$.

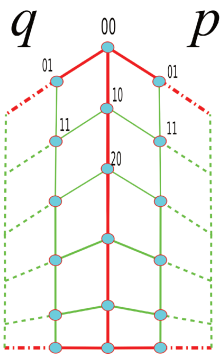

$$q_{0,1} = 2\,(1-\mathfrak{c})\,p_{0,0} + 2\,\mathfrak{c}\,p_{1,0} - p_{0,1} \tag{4.1}$$
$$q_{1,1} + p_{1,1} = 2/5\,\mathfrak{c}\,p_{0,0} + 2\,(1-\mathfrak{c})\,p_{1,0} + 8/5\,\mathfrak{c}\,p_{2,0} \tag{4.2}$$
$$q_{2,1} + p_{2,1} = -1/5\,\mathfrak{c}\,p_{0,0} + \mathfrak{c}\,p_{1,0} + 2\,(1-\mathfrak{c})\,p_{2,0} + 6/5\,\mathfrak{c}\,p_{3,0} \tag{4.3}$$
$$q_{3,1} + p_{3,1} = 2\,p_{3,0} - 1/5\,\mathfrak{c}\,p_{4,0} + 1/5\,\mathfrak{c}\,p_{5,0} \tag{4.4}$$
$$p_{3,0} = -p_{0,0}/10 + p_{1,0}/2 - p_{2,0} - p_{4,0}/2 + p_{5,0}/10 \tag{4.5}$$
$$q_{4,1} + p_{4,1} = 2\,p_{4,0} \tag{4.6}$$
$$q_{5,1} + p_{5,1} = 2\,p_{5,0} \tag{4.7}$$
$$\tag{4.8}$$

Figure 4.2: Relations between the coefficients of two bi-quintic Bézier patches around an edge.

3 Construction

In the construction, explicit formulae for the coefficients of the b-spline patches of the face of $\mathcal{M}$ will be described. We use the notation of Fig. 4.1 for the b-spline coefficients on faces. The faces around a vertex γ are indexed counter-clockwise from $k = 1$ to $k = \mathfrak{v}$. If the vertex γ is a boundary vertex, we assume that the first face for $k = 1$ is a boundary face. We define an equivalence relation on the coefficients by $b^{k+1}_{i,0} \equiv b^k_{0,i}$ for $i = 0, \ldots, 5$.

3.1 Catmull-Clark based construction

In a first step, we construct bi-quintic patches that approximate Catmull-Clark subdivision surfaces. A two-level construction is employed. At the first level, points $e^k_{i,j}$ associated to a half-edge are computed (see Fig. 4.3). The construction

follows the Approximate Catmull-Clark (ACC) construction described in [63]. At

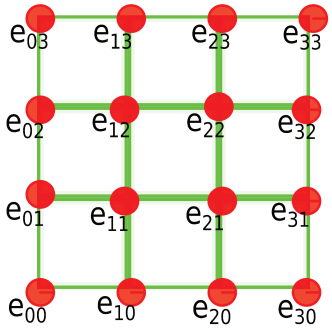

Figure 4.3: Labeling for Bézier bicubic control points.

this level, new vertex points $e^k_{0,0}$ and half-edge points $e^k_{1,1}$ are computed. If the vertex is a boundary vertex and has valence 1 or 2, then the computation of $e^k_{0,0}$ is adapted and new edge points $e^k_{1,0}$ are computed. The masks for these points are given in Fig. 4.5 and Fig. 4.6 for an interior vertex and the masks for the coefficients $e_{i,j}$ associated to boundary points are given in Fig. 4.4.

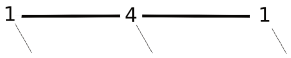

(a) Mask for $e_{0,0}$ at a boundary vertex with $\mathfrak{v} = 2$

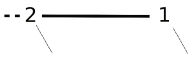

(b) Mask for $e_{1,0}$ at a boundary vertex with $\mathfrak{v} = 2$

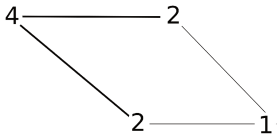

(c) Mask for $e_{1,1}$ at a boundary vertex with $\mathfrak{v} = 1$

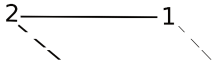

(d) Mask for $e_{1,0}$ at a boundary vertex with $\mathfrak{v} = 1$

Figure 4.4: Masks of $e_{i,j}$ for a boundary vertex

At the second level, the coefficients $h^k_{i,j}$ $(0 \leqslant i, j \leqslant 5)$ are computed using the following relations in terms of the vertex point $e^k_{0,0}$ and the half-edge points $e^i_{1,1}$, $e^i_{2,1}$, $e^i_{1,2}$, $e^i_{2,2}$, $i = k-1, k, k+1$ for an interior vertex:

$$
\begin{aligned}
h^k_{0,0} &= e^k_{0,0} \\
h^k_{1,0} &= \tfrac{3}{10}\, e^k_{1,1} + \tfrac{3}{10}\, e^{k-1}_{1,1} + \tfrac{2}{5}\, e^k_{0,0} \\
h^k_{1,1} &= \tfrac{4\, e^k_{0,0}}{25} + \tfrac{3}{5}\, e^k_{1,1} + \tfrac{3\, e^{k+1}_{1,1}}{25} + \tfrac{3\, e^{k-1}_{1,1}}{25} \\
h^k_{2,0} &= \tfrac{3\, e^k_{2,1}}{20} + \tfrac{3\, e^{k-1}_{1,2}}{20} + \tfrac{3}{10}\, e^k_{1,1} + \tfrac{3}{10}\, e^{k-1}_{1,1} + \tfrac{1}{10}\, e^k_{0,0} \\
h^k_{2,1} &= \tfrac{51\, e^k_{1,1}}{100} + \tfrac{3\, e^{k-1}_{1,1}}{25} + \tfrac{1}{25}\, e^k_{0,0} + \tfrac{6\, e^k_{2,1}}{25} + \tfrac{3\, e^{k-1}_{1,2}}{50} + \tfrac{3\, e^{k+1}_{1,1}}{100} \\
h^k_{2,2} &= \tfrac{e^k_{0,0}}{100} + \tfrac{21\, e^k_{1,1}}{50} + \tfrac{3\, e^{k+1}_{1,1}}{100} + \tfrac{3\, e^{k-1}_{1,1}}{100} + \tfrac{9\, e^k_{2,2}}{100} + \tfrac{39\, e^k_{1,2}}{200} \\
&\quad + \tfrac{39\, e^k_{2,1}}{200} + \tfrac{3\, e^{k+1}_{2,1}}{200} + \tfrac{3\, e^{k-1}_{1,2}}{200}
\end{aligned}
$$

For the boundary vertices we use the following combinations:

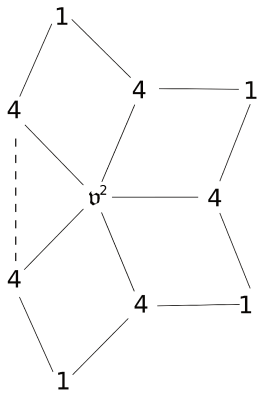

Figure 4.5: Mask for $e_{0,0}$ at an interior vertex.

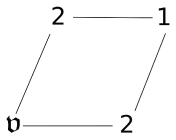

Figure 4.6: Mask for $e_{1,1}$ at an interior vertex.

- Valence 2 boundary vertex, with $k = 1$:

$$
\begin{aligned}
h^k_{0,0} &= e^k_{0,0} \\
h^k_{0,1} &= \tfrac{3}{10}\, e^{k+1}_{1,1} + \tfrac{3}{10}\, e^k_{1,1} + 2/5\, e^k_{0,0} \\
h^k_{0,2} &= \tfrac{3\, e^{k+1}_{2,1}}{20} + \tfrac{3\, e^k_{1,2}}{20} + 3/10\, e^{k+1}_{1,1} + \tfrac{3}{10}\, e^k_{1,1} + \tfrac{1}{10}\, e^k_{0,0} \\
h^k_{1,0} &= 3/5\, e^k_{1,0} + 2/5\, e^k_{0,0} \\
h^k_{1,1} &= \tfrac{4\, e^k_{0,0}}{25} + \tfrac{12\, e^k_{1,1}}{25} + \tfrac{3\, e^{k+1}_{1,1}}{25} + \tfrac{6\, e^k_{1,0}}{25} \\
h^k_{1,2} &= \tfrac{3\, e^{k+1}_{1,1}}{25} + \tfrac{12\, e^k_{1,1}}{25} + \tfrac{1}{25}\, e^k_{0,0} + \tfrac{6\, e^k_{1,2}}{25} + \tfrac{3\, e^{k+1}_{2,1}}{50} + \tfrac{3\, e^k_{1,0}}{50} \\
h^k_{2,0} &= \tfrac{3}{10}\, e^k_{2,0} + 3/5\, e^k_{1,0} + \tfrac{1}{10}\, e^k_{0,0} \\
h^k_{2,1} &= \tfrac{6\, e^k_{1,0}}{25} + \tfrac{1}{25}\, e^k_{0,0} + \tfrac{9\, e^k_{2,1}}{50} + \tfrac{39\, e^k_{1,1}}{100} + \tfrac{3\, e^k_{2,0}}{25} + \tfrac{3\, e^{k+1}_{1,1}}{100} \\
h^k_{2,2} &= \tfrac{e^k_{0,0}}{100} + \tfrac{39\, e^k_{1,1}}{100} + \tfrac{3\, e^{k+1}_{1,1}}{100} + \tfrac{3\, e^k_{1,0}}{50} + \tfrac{9\, e^k_{2,2}}{100} + \tfrac{39\, e^k_{1,2}}{200} \\
&\quad + \tfrac{9\, e^k_{2,1}}{50} + \tfrac{3\, e^{k+1}_{2,1}}{200} + \tfrac{3\, e^k_{2,0}}{100}
\end{aligned}
$$

$$
\begin{aligned}
h^{k+1}_{0,0} &= e^{k+1}_{0,0} \\
h^{k+1}_{0,1} &= 3/5\, e^{k+1}_{0,1} + 2/5\, e^{k+1}_{0,0} \\
h^{k+1}_{0,2} &= \tfrac{3}{10}\, e^{k+1}_{0,2} + 3/5\, e^{k+1}_{0,1} + \tfrac{1}{10}\, e^{k+1}_{0,0} \\
h^{k+1}_{1,0} &= \tfrac{3}{10}\, e^{k+1}_{1,1} + \tfrac{3}{10}\, e^{k}_{1,1} + 2/5\, e^{k+1}_{0,0} \\
h^{k+1}_{1,1} &= \tfrac{4\, e^{k+1}_{0,0}}{25} + \tfrac{12\, e^{k+1}_{1,1}}{25} + \tfrac{6\, e^{k+1}_{0,1}}{25} + \tfrac{3\, e^{k}_{1,1}}{25} \\
h^{k+1}_{1,2} &= \tfrac{6\, e^{k+1}_{0,1}}{25} + \tfrac{1}{25}\, e^{k+1}_{0,0} + \tfrac{9\, e^{k+1}_{1,2}}{50} + \tfrac{3\, e^{k+1}_{0,2}}{25} + \tfrac{39\, e^{k+1}_{1,1}}{100} + \tfrac{3\, e^{k}_{1,1}}{100} \\
h^{k+1}_{2,0} &= \tfrac{3\, e^{k+1}_{2,1}}{20} + \tfrac{3\, e^{k}_{1,2}}{20} + \tfrac{3}{10}\, e^{k+1}_{1,1} + \tfrac{3}{10}\, e^{k}_{1,1} + \tfrac{1}{10}\, e^{k+1}_{0,0} \\
h^{k+1}_{2,1} &= \tfrac{12\, e^{k+1}_{1,1}}{25} + \tfrac{3\, e^{k}_{1,1}}{25} + \tfrac{1}{25}\, e^{k+1}_{0,0} + \tfrac{6\, e^{k+1}_{2,1}}{25} + \tfrac{3\, e^{k}_{1,2}}{50} + \tfrac{3\, e^{k+1}_{0,1}}{50} \\
h^{k+1}_{2,2} &= \tfrac{e^{k+1}_{0,0}}{100} + \tfrac{39\, e^{k+1}_{1,1}}{100} + \tfrac{3\, e^{k+1}_{0,1}}{50} + \tfrac{3\, e^{k}_{1,1}}{100} + \tfrac{9\, e^{k+1}_{2,2}}{100} \\
&\quad + \tfrac{9\, e^{k+1}_{1,2}}{50} + \tfrac{39\, e^{k+1}_{2,1}}{200} + \tfrac{3\, e^{k+1}_{0,2}}{100} + \tfrac{3\, e^{k}_{1,2}}{200}
\end{aligned}
$$

- Valence 1 boundary vertex:

$$
\begin{aligned}
h^{k}_{0,0} &= e^{k}_{0,0} \\
h^{k}_{1,0} &= 3/5\, e^{k}_{1,0} + 2/5\, e^{k}_{0,0} \\
h^{k}_{1,1} &= \tfrac{4\, e^{k}_{0,0}}{25} + \tfrac{9\, e^{k}_{1,1}}{25} + \tfrac{6\, e^{k}_{0,1}}{25} + \tfrac{6\, e^{k}_{1,0}}{25} \\
h^{k}_{2,0} &= \tfrac{3}{10}\, e^{k}_{2,0} + 3/5\, e^{k}_{1,0} + \tfrac{1}{10}\, e^{k}_{0,0} \\
h^{k}_{2,1} &= \tfrac{6\, e^{k}_{1,0}}{25} + \tfrac{1}{25}\, e^{k}_{0,0} + \tfrac{9\, e^{k}_{2,1}}{50} + \tfrac{9\, e^{k}_{1,1}}{25} + \tfrac{3\, e^{k}_{2,0}}{25} + \tfrac{3\, e^{k}_{0,1}}{50} \\
h^{k}_{2,2} &= \tfrac{e^{k}_{0,0}}{100} + \tfrac{9\, e^{k}_{1,1}}{25} + \tfrac{3\, e^{k}_{0,1}}{50} + \tfrac{3\, e^{k}_{1,0}}{50} + \tfrac{9\, e^{k}_{2,2}}{100} + \tfrac{9\, e^{k}_{1,2}}{50} \\
&\quad + \tfrac{9\, e^{k}_{2,1}}{50} + \tfrac{3\, e^{k}_{0,2}}{100} + \tfrac{3\, e^{k}_{2,0}}{100}
\end{aligned}
$$

The remaining coefficients $h^k_{i,j}$ are obtained by symmetry. The relative simple form of these relations is due to the use of the formula $e^k_{1,0} = \frac{e^k_{1,1}+e^{k-1}_{1,1}}{2}$.

These relations correspond to the degree elevation to compute the control coefficients $h^k_{i,j}$ of the bi-5 patches from the bi-3 patches associated to the ACC construction.

3.2 Generation of smooth surfaces

The second step of the construction is to smooth the surface, that is to satisfy the G^1 constraints. We use the coefficients $h^k_{i,j}$ and compute new control points $b^k_{i,j}$ of the b-spline patch surface which has geometrically smooth junctions between the neighbouring patches. The coefficients $b^k_{i,j}$ are computed by orthogonal projection of the coefficients $h^k_{i,j}$ on the solution space of the G^1 equations. The equations (4.1), (4.6) and (4.7) are already satisfied by the output of the ACC algorithm, so we don't change the corresponding coefficients.

The other coefficients are expressed by linear combinations of the previous coefficients. They are described by masks. A (red) circle indicates the coefficient, which is computed and weights attributed to some previous coefficients are the coefficients in the linear combination.

Computing the tangent space at the vertex

We fix the control points $b^1_{0,0} = h^1_{0,0}, b^1_{1,0} = h^1_{1,0}, b^2_{1,0} = h^2_{1,0}$ and compute the other coefficients $b^k_{1,0}$ for $k = 3..\mathfrak{v}$ in a cyclic way by using the mask in Fig. 4.7 corresponding to the relation (4.1). This will provide the value of $b^k_{0,0}$ and $b^k_{1,0}$ for $k = 1..\mathfrak{v}$ that satisfies all the relations (4.1) since the gluing data are compatible in a sense described in [21, 42].

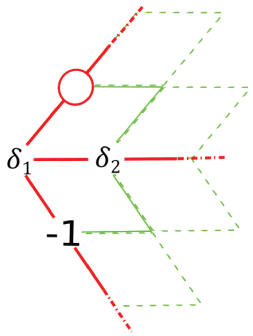

Figure 4.7: $b^{k+1}_{0,1} = \delta_1 b^k_{0,0} + \delta_2\, b^k_{0,1} - b^{k-1}_{0,1}$ with $\delta_1 = 2 - 2\mathfrak{c}$,$\delta_2 = 2\mathfrak{c}$.

Computing the second order derivative at a vertex

We compute the coefficients $b^k_{2,0}, b^k_{1,1}, b^k_{2,0}$, $k = 1, \ldots, \mathfrak{v}$ by solving the system formed by the equations (4.2) around a vertex.

We take $b^k_{2,0} = h^k_{2,0}$ and consider the linear system associated to the relations (4.2): $b^k_{1,1} + b^{k-1}_{1,1} = \frac{8\mathfrak{c}}{5} b^k_{2,0} + 2(1-\mathfrak{c}) b^k_{2,0} + \frac{2\mathfrak{c}}{5} b^k_{0,0}$ for $k = 1..\mathfrak{v}$. It is of the form

$$\begin{pmatrix} 1 & 1 & 0 & \ldots & 0 & 0 & 0 \\ 0 & 1 & 1 & \ldots & 0 & 0 & 0 \\ \ldots & & & & & & \\ \ldots & & & & & & \\ 0 & 0 & 0 & \ldots & 0 & 1 & 1 \\ 1 & 0 & 0 & \ldots & 0 & 0 & 1 \end{pmatrix} \begin{pmatrix} b^1_{1,1} \\ b^2_{1,1} \\ \vdots \\ \vdots \\ b^{\mathfrak{v}-1}_{1,1} \\ b^{\mathfrak{v}}_{1,1} \end{pmatrix} = \begin{pmatrix} RHS_1 \\ RHS_2 \\ \vdots \\ \vdots \\ \vdots \\ RHS_{\mathfrak{v}} \end{pmatrix} \tag{4.9}$$

where $RHS_i = 2/5\,\mathfrak{c}\, b^{i+1}_{0,0} + 2\,(1-\mathfrak{c})\, b^{i+1}_{1,0} + 8/5\,\mathfrak{c}\, b^{i+1}_{2,0}$. We will denote this system by $M_{\mathfrak{v}} X - RHS = 0$. The square matrix $M_{\mathfrak{v}}$ is invertible if and only if $\mathfrak{v}$ is odd and the rank of $M_{\mathfrak{v}}$ is $\mathfrak{v}$ if $\mathfrak{v}$ is odd and $\mathfrak{v} - 1$ if $\mathfrak{v}$ is even. We consider two cases depending on the parity of $\mathfrak{v}$.

The valence $\mathfrak{v}$ is odd The matrix $M_\mathfrak{v}$ is invertible and its inverse is

$$M_\mathfrak{v}^{-1} = \begin{pmatrix} \frac{1}{2} & -\frac{1}{2} & \frac{1}{2} & \cdots & \frac{1}{2} \\ \frac{1}{2} & \frac{1}{2} & -\frac{1}{2} & \cdots & -\frac{1}{2} \\ -\frac{1}{2} & \frac{1}{2} & \ddots & & \frac{1}{2} \\ \vdots & \vdots & & \ddots & \vdots \\ -\frac{1}{2} & \frac{1}{2} & -\frac{1}{2} & \cdots & \frac{1}{2} \end{pmatrix}$$

This provides the solution described in Fig. 4.8 for the odd valence.

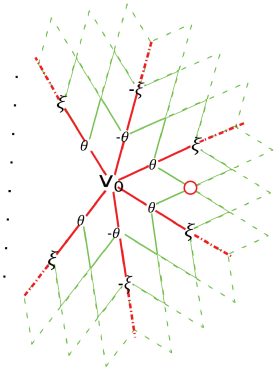

$$\begin{aligned} b^i_{1,1} &= \mathrm{v}_0\, b^1_{0,0} \\ &+ \textstyle\sum_{k=1..i-1}(-1)^{k+i+1}(\theta b^k_{1,0} + \xi b^k_{2,0}) \\ &+ \textstyle\sum_{k=i..\mathfrak{v}}(-1)^{k+i}(\theta b^k_{1,0} + \xi b^k_{2,0}) \end{aligned}$$

where $v_0 = \frac{\mathfrak{c}}{5}$, $\theta = (1-\mathfrak{c})$ and $\xi = \frac{4}{5}\,\mathfrak{c}$.

Figure 4.8: Mask of $b^k_{1,1}$ for odd valence.

The valence $\mathfrak{v}$ is even In this case, $M_\mathfrak{v}$ is not invertible and we have to guaranty the solvability of the system (4.9). This system is solvable if and only if $\sum_{i=1\ldots\mathfrak{v}} RHS_i(-1)^i = 0$. This relation is also known in the literature as the *vertex enclosing condition* [11]. This leads to the following relation:

$$\sum_{i=1,\ldots,\mathfrak{v}} b^i_{2,0}(-1)^i = \frac{5}{8\mathfrak{c}} \sum_{i=1..v} (-1)^i((2\mathfrak{c}-2)\, b^{i+1}_{1,0} - 2/5\,\mathfrak{c}\, b^{i+1}_{0,0}) \tag{4.10}$$

We compute the coefficients $b^k_{2,0}$ by the mask given in Fig. 4.9. It is obtained by orthogonal projection of the coefficients $h^k_{i,j}$ on the space of solutions of the system (4.10).

The coefficients $b^k_{1,1}$ are then computed by orthogonal projection of the vector $(h^k_{1,1})_k$ on the space of solutions of the system (4.9), which is solvable when $b^k_{2,0}$ satisfy the vertex enclosing conditions (4.10). This leads to the mask described in Fig. 4.10.

In some other smoothing algorithm the solution of the system (4.9) is derived from the second order differential of smooth objects as biquadratic parametrisation [69] or an implicit surface [70].

In the even case, both of the solutions of the systems (4.10) and (4.9) are computed by orthogonal projection of the coefficient vector $(h^k_{i,j})$ onto the corresponding linear space. To compute the projection of a point X_e onto the space of solutions of the system $AX - B$, we write X by means of the projected point X_e so that: $X = X_e + A^t d$ for some vector d, then we compute d in the system: $AA^t d - B - AX_e$, and deduce the value of $X = X_e + A^t d$.

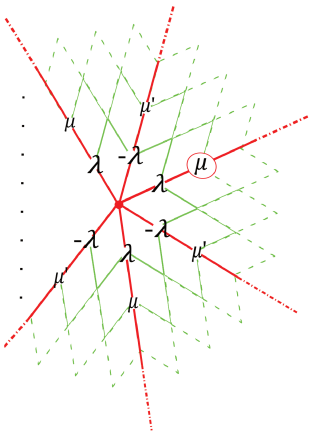

$$b^k_{2,0} = \lambda(-1)^k \sum_{i=1..\mathfrak{v}}(-1)^i b^i_{1,0} + (-1)^k \sum_{i=1..\frac{\mathfrak{v}}{2}}(\mu h^{2i+1}_{2,0} + \mu' h^{2i}_{2,0})$$

where $\lambda = \frac{5}{4\mathfrak{v}}(1-\frac{1}{\mathfrak{c}})$, $\mu = (1-\frac{1}{\mathfrak{v}})$, $\mu' = (1+\frac{1}{\mathfrak{v}})$.

Figure 4.9: Mask for $b^k_{2,0}$ in the even case.

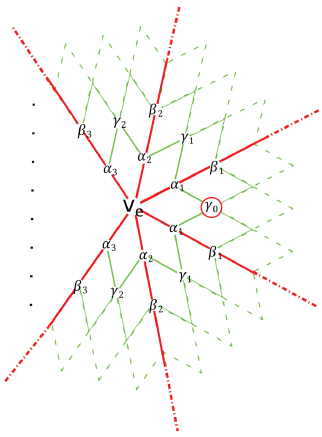

$$\begin{aligned}
b^k_{1,1} &= b^1_{0,0} v_e + \sum_{i=1..\frac{\mathfrak{v}}{2}} \alpha_i (b^{i+k}_{1,0} + b^{k-i+1}_{1,0}) \\
&\quad + \sum_{i=1..\frac{\mathfrak{v}}{2}} \beta_i (b^{i+k}_{1,0} + b^{k-i+1}_{1,0}) \\
&\quad + \gamma_0 h^k_{1,1} + \sum_{i=1..\mathfrak{v}} \gamma_i (h^k_{1,1}) \\
\alpha_k &= (-1)^{k+1}(2-2\mathfrak{c})\frac{\mathfrak{v}-k}{2\mathfrak{v}}, \\
\beta_k &= (-1)^{k+1}\frac{8\mathfrak{c}}{5}\frac{\mathfrak{v}-k}{2\mathfrak{v}}, \\
\gamma_0 &= -\frac{\mathfrak{v}-1}{\mathfrak{v}}, \\
\gamma_k &= (-1)^k \frac{1}{\mathfrak{v}}, \\
v_e &= \frac{\mathfrak{v}^2 - 2[\frac{\mathfrak{v}}{4}] - 2 + \sum_{i=0..\mathfrak{v}/2}(-1)^i}{2\mathfrak{v}}
\end{aligned}$$

Figure 4.10: Computation of $b^k_{1,1}$ for even valence.

Third and fourth order coefficients

The value of $b^k_{3,0}$ is computed by using Equation (4.5). The mask for $b^k_{3,0}$ is given in Fig. 4.11.

To compute the other coefficients, we project the coefficient vector $(h^k_{i,j})$ computed at the first step, onto the space of solutions associated to the equations (4.3) (resp. (4.4)) with unknowns $b^{k+1}_{2,1}, b^k_{2,1}$, (resp. $b^{k+1}_{3,1}, b^k_{3,1}$). The projection of the

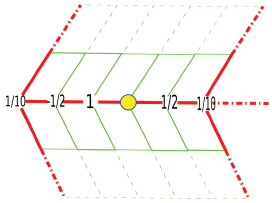

Figure 4.11: Mask for $b^k_{3,0} = \frac{1}{10}\, b^k_{0,0} - \frac{1}{2}\, b^k_{1,0} + b^k_{2,0} + \frac{1}{2}\, b^k_{4,0} - \frac{1}{10}\, b^k_{5,0}$

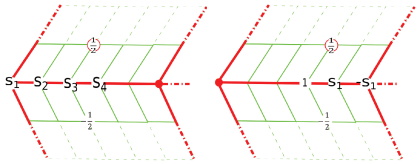

$$b^{k+1}_{2,1} = \frac{1}{2}h^{k+1}_{2,1} - \frac{1}{2}h^k_{2,1} + s_1\, b^k_{0,0} + s_2\, b^k_{1,0} + s_3 b^k_{2,0} + s_4\, b^k_{3,0}$$
$$b^{k+1}_{3,1} = \frac{1}{2}h^{k+1}_{3,1} - \frac{1}{2}h^k_{3,1} + b^k_{3,0} - s_1\, b^k_{4,0} + s_1\, b^k_{5,0}$$
$$s_1 = \frac{1}{10}\,\mathfrak{c}, s_2 = \frac{1}{2}\mathfrak{c}, s_3 = (1-\mathfrak{c})\,, s_4 = \frac{3}{5}\,\mathfrak{c}$$

Figure 4.12: Masks for $b^{k+1}_{2,1}$, $b^{k+1}_{3,1}$.

coefficients $h^k_{i,j}$ onto the spaces of G^1 coefficients yields the following relations:

$$b^{k+1}_{2,1} = \frac{1}{2}h^{k+1}_{2,1} - \frac{1}{2}h^k_{2,1} - \frac{1}{10}\,\mathfrak{c}\, b^k_{0,0} + \frac{1}{2}\mathfrak{c}\, b^k_{1,0} + (1-\mathfrak{c})\, b^k_{2,0} + \frac{3}{5}\,\mathfrak{c}\, b^k_{3,0}$$
$$b^k_{2,1} = \frac{1}{2}h^k_{2,1} - \frac{1}{2}h^{k+1}_{2,1} - \frac{1}{10}\,\mathfrak{c}\, b^k_{0,0} + \frac{1}{2}\mathfrak{c}\, b^k_{1,0} + (1-\mathfrak{c})\, b^k_{2,0} + \frac{3}{5}\,\mathfrak{c}\, b^k_{3,0}$$
$$b^{k+1}_{3,1} = \frac{1}{2}h^{k+1}_{3,1} - \frac{1}{2}h^k_{3,1} + b^k_{3,0} - \frac{1}{10}\,\mathfrak{c}\, b^k_{4,0} + \frac{1}{10}\,\mathfrak{c}\, b^k_{5,0}$$
$$b^k_{3,1} = \frac{1}{2}h^k_{3,1} - \frac{1}{2}h^{k+1}_{3,1} + b^k_{3,0} - \frac{1}{10}\,\mathfrak{c}\, b^k_{4,0} + \frac{1}{10}\,\mathfrak{c}\, b^k_{5,0}$$

The masks for the coefficients $b^{k+1}_{2,1}$, $b^{k+1}_{3,1}$ are given in Fig. 4.12. The masks for $b^k_{2,1}$, $b^k_{3,1}$ are obtained by symmetry.

3.3 Basis construction

We now describe the computation of basis functions for the space of G^1 splines on the mesh $\mathcal{M}$. Our representation of G^1 basis functions is given by vectors in $\mathbb{R}^{m^2 \times M_2}$ with $m^2 \times M_2$ entries where M_2 is the number of faces and $m = 6$ for bi-quintic b-spline patches. These entries are the coefficients of the b-spline patches associated to the faces of the mesh.

The construction of a basis of the G^1 function space over the quadrangular mesh $\mathcal{M}$ is based on the basis construction described in [21], [42], where basis functions associated to vertices, edges and faces of $\mathcal{M}$ are defined. We start by generating a set $\mathfrak{G}$ of G^0 function, representing the degrees of freedom associated to these basis functions. These degrees of freedom are given in Fig. 4.13 (yellow

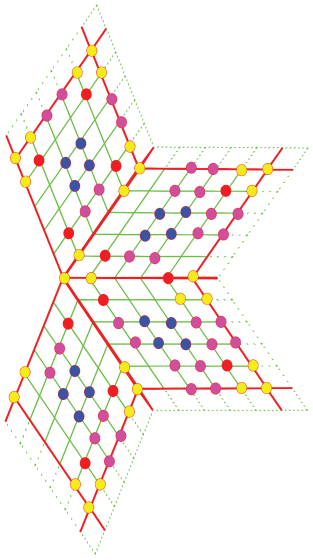

Figure 4.13: Degrees of freedom for a singular vertex

points for the vertex, red points for cross derivatives at a vertex on an adjacent face, pink points for the edges, and blue points for the faces). The G^1 basis will be obtained after applying to the elements of $\mathfrak{G}$ a smoothing process close to the one described in Section 3.2.

For a vertex $\gamma \in \mathcal{M}_0$, we denote by $g^k_{i,j}(\gamma)$ the vector in $\mathbb{R}^{m^2 \times M_2}$ with all the b-spline coefficients vanishing except the coefficient $b^k_{i,j}$ and the coefficients of the other faces equivalent to $b^k_{i,j}$ (see Fig. 4.1), which are equal to 1. If $g^k_{i,j}(\gamma)$ is interior to a face, it contains only one non-zero entry. The number of non zero entries (equal to one) of $g^k_{i,j}(\gamma)$ is the number of faces on which an equivalent coefficient appears. The set of all these vectors (removing repetitions) form a basis of the space of G^0 splines on $\mathcal{M}$.

We define:

$$\mathfrak{G} = \mathfrak{G}_0 \bigcup \mathfrak{G}_1 \bigcup \mathfrak{G}_2,$$
$$\mathfrak{G}_0 = \bigcup_{\gamma \in M_0} \mathfrak{g}^0_\gamma, \quad \mathfrak{G}_1 = \bigcup_{\tau \in M_1} \mathfrak{g}^1_\tau, \quad \mathfrak{G}_2 = \bigcup_{\sigma \in M_2} \mathfrak{g}^2_\sigma.$$

$\mathfrak{g}^0_\gamma$ will represent the degrees of freedom at the vertex γ. The elements of $\mathfrak{g}^0_\gamma$ for a given vertex γ are the following (the notation of Fig. 4.1 is used):

- If $\mathfrak{v} \neq 4$, we take
$$\mathfrak{g}^0_\gamma = \{g^1_{0,0}(\gamma), g^1_{1,0}(\gamma), g^1_{0,1}(\gamma), g^k_{1,1}(\gamma), k = 1, \ldots, \mathfrak{v}\}.$$
- If $\mathfrak{v} = 4$, we take
$$\mathfrak{g}^0_\gamma = \{g^1_{0,0}(\gamma), g^1_{1,0}(\gamma), g^1_{0,1}(\gamma), g^1_{1,1}(\gamma)\}.$$

$\mathfrak{g}^1_\tau$ represents the degrees of freedom along the edge τ. Assume that τ is the first edge emanating from γ on the face of index k. The corresponding b-spline

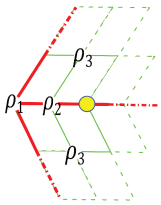

Figure 4.14: $b^k_{2,0} = \rho_1\, b^k_{0,0} + \rho_2 b^k_{1,0} + \rho_3\, b^k_{1,1} + \rho_3\, b^{k-1}_{1,1}$ where $\rho_1 = -\frac{1}{4}$, $\rho_2 = \frac{5\mathfrak{c}-5}{4\mathfrak{c}}$, $\rho_3 = \frac{5}{8\mathfrak{c}}$

coefficients are $b^k_{i,0}$, $i = 0, \ldots, 5$.
If τ emanates from a singular vertex, then we take:

$$\mathfrak{g}^1_\tau = \{g^k_{2,1}(\gamma), g^k_{3,1}(\gamma)\}$$

If τ has no singular vertex, then the set contains four elements:

$$\mathfrak{g}^1_\tau = \{g^k_{2,0}(\gamma), g^k_{3,0}(\gamma), g_{2,1}(\gamma), g_{3,1}(\gamma)\}$$

$\mathfrak{g}^2_\sigma$ represents the degrees of freedom over the face σ. If σ is the face of index k at the vertex γ, we take

$$\mathfrak{g}^2_\sigma = \{g^k_{2,2}(\gamma), g^k_{3,2}(\gamma), g^k_{2,3}(\gamma), g^k_{3,3}(\gamma)\}.$$

The next step is to smooth these elements to get the G^1 basis. Notice that the following smoothing algorithm can be also used to smooth surfaces, it will be compared in the experimentation section. We consider the (sparse) matrix associated to $\mathfrak{G}$, where each row of this matrix is the vector of an element $g \in \mathfrak{G}$. We denote by $\pi^k_{i,j}$ the column of this matrix associated to the coefficient $b^k_{i,j}$. The smoothing process operates on the columns $\pi^k_{i,j}$ of $\mathfrak{G}$ by applying the following masks:

- The first step is the adjustment of the partial derivatives of g at each vertex by using the relations: $\pi^{k+1}_{0,1} = \delta_1 \pi^k_{0,0} + \delta_2\, \pi^k_{0,1} - \pi^{k-1}_{0,1}$ with $\delta_1 = 2 - 2\mathfrak{c}$, $\delta_2 = 2\mathfrak{c}$. This step is the same as in section 3.2.

- Then we adjust the second order derivatives. For each vertex v, if v is singular we compute the vectors $\pi^k_{2,0}$ for $k \in 1..\mathfrak{v}$ at this vertex using the relation: $\pi^k_{2,0} = \rho_1\, \pi^k_{0,0} + \rho_2 \pi^k_{1,0} + \rho_3\, \pi^k_{1,1} + \rho_3\, \pi^{k-1}_{1,1}$ where $\rho_1 = -\frac{1}{4}$, $\rho_2 = \frac{5\mathfrak{c}-5}{4\mathfrak{c}}$, $\rho_3 = \frac{5}{8\mathfrak{c}}$ as in Fig. 4.14. If the vertex is ordinary, we compute using the relation $\pi^k_{1,1} = 2\pi^k_{1,0} - \pi^{k-1}_{1,1}$ for $k = 2..4$.

- For each singular vertex v, we compute $\pi^k_{3,0}$ using the relation: $\pi^k_{3,0} = \frac{1}{10}\, \pi^k_{0,0} - \frac{1}{2}\, \pi^k_{1,0} + \pi^k_{2,0} + \frac{1}{2}\, \pi^k_{4,0} - \frac{1}{10}\, \pi^k_{5,0}$ for $k = 1..\mathfrak{v}$.

- For each singular vertex v, we compute:

$$\pi^k_{2,1} = -\pi^{k+1}_{2,1} - 1/5\,\mathfrak{c}\, \pi^k_{0,0} + \mathfrak{c}\, \pi^k_{1,0} + 2\,(1-\mathfrak{c})\, \pi^k_{2,0} + 6/5\,\mathfrak{c}\, \pi^k_{3,0}$$
$$\pi^k_{3,1} = -\pi^{k+1}_{3,1} + 2\, \pi^k_{3,0} - 1/5\,\mathfrak{c}\, \pi^k_{4,0} + 1/5\,\mathfrak{c}\, \pi^k_{5,0}$$

  for $k \in 1..\mathfrak{v}$.

- For each edge τ with non singular vertex, we compute:

$$\pi_{2,1}^k = -\pi_{2,1}^{k+1} + 2\pi_{2,0}^k$$
$$\pi_{3,1}^k = -\pi_{3,1}^{k+1} + 2\pi_{3,0}^k$$

As these operations on the columns of $\mathfrak{G}$ are the one induced by the relations (4.1)-(4.7), we immediately see that the rows of $\mathfrak{G}$ represent functions that satisfy these G^1-conditions.

3.4 Algorithm

We summarize the construction of G^1 Catmull-Clark Spline surface in Algorithm 1 (this algorithm will be called GCCS). The main difference with the basis smoothing algorithm is the computation of the second order derivatives. The GCCS method projects the ACC positions onto the G^1 constraints, while the basis smoothing algorithm computes directly some specific coefficients by means of the other coefficients, using the equation in Fig. 4.14.

4 Experimentation

We present now the results of the GCCS algorithm 1 on some quadrangular meshes and analyze graphically the computed surfaces. The meshes used in Fig. 4.16, 4.17, 4.18 are taken from the web page ([1]). The mesh used in Fig. 4.19, 4.20 have been produced using the scaffolding algorithm of [71]. The model in Fig. 4.20 is coming from [72].

In Fig. 4.15, 4.16, the isophotes reveal the good quality of the surface constructed by the GCCS algorithm. In Fig. 4.17, we compare the output of GCCS method with the output of the ACC algorithm and the output of the basis smoothing algorithm described in the section 3. The Gauss curvature of the basis smoothing surface Fig. 4.17 (e) has more fluctuation than the Gauss curvature of the GCCS surface Fig. 4.17 (c). We notice that the same gluing data are used for the GCCS and the basis smoothing algorithm. The quality advantage that GCCS exhibits is due to the use of the ACC surface as guiding surface. More precisely, the b-spline coefficients obtained in the GCCS algorithm by projecting the output of the ACC method onto the G^1 constraints are closer to the ACC surface than the coefficients obtained by the basis smoothing algorithm.

5 Conclusion

We have presented a new mesh smoothing method using the ACC surface as a guiding surface, which projects it onto the space of G^1 surfaces. The use of this guide plays a major role in constructing high quality surfaces. The explicit formulas that we provide make the algorithm straightforward to implement. We present also an explicit scheme to construct basis functions of the G^1 spline space.

[1] *https://www.cise.ufl.edu/research/SurfLab/shape_gallery.shtml*

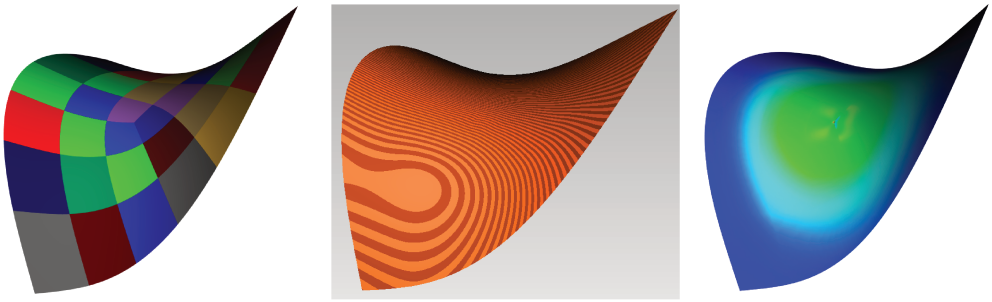

(a) B-spline patches (b) Isophotes (c) Gauss curvature

Figure 4.15: GCCS surface like a triangular saddle.

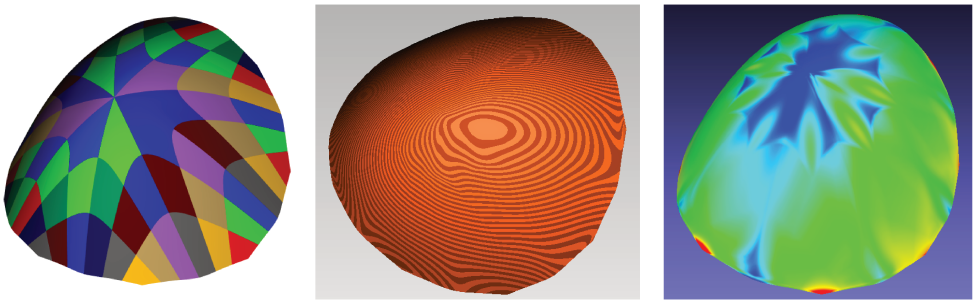

(a) B-spline patches (b) Isophotes (c) Mean curvature

Figure 4.16: GCCS surface like a dome. The curvature oscillations (c) are induced by the quadrangular mesh.

The resulting G^1 space has the maximal number of degrees of freedom for bi-quintic splines with the used gluing data. They are associated to explicit b-spline coefficients (Fig.4.13). The experimentations show the efficiency of the construction and the quality of the computed surfaces.

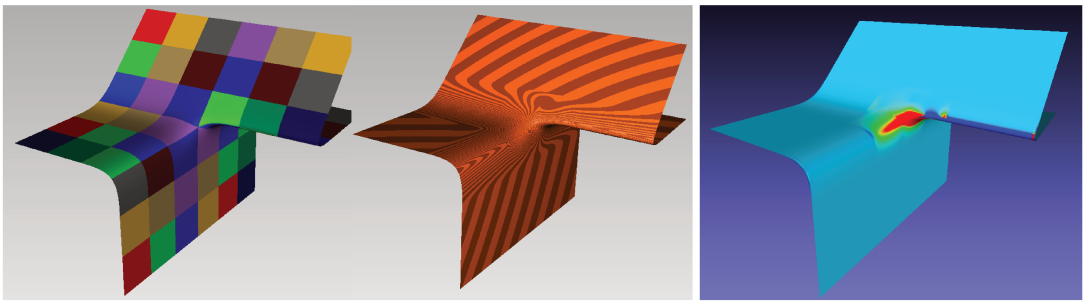

(a) B-spline patches (b) Isophotes (c) Gauss curvature

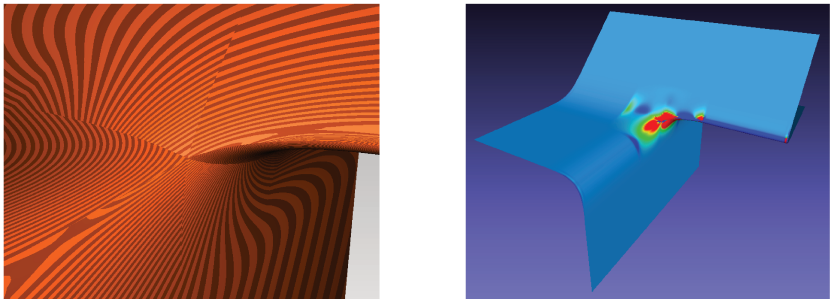

(d) Isophotes for ACC construction (e) Gauss curvature for basis smoothing

Figure 4.17: GCCS construction ((a) patches, (b) isophotes, (c) Gauss curvature). (d) Discontinuous isophotes in the ACC construction showing that the ACC surface is not G^1. (e) Oscillation of the Gauss curvature for the basis smoothing scheme.

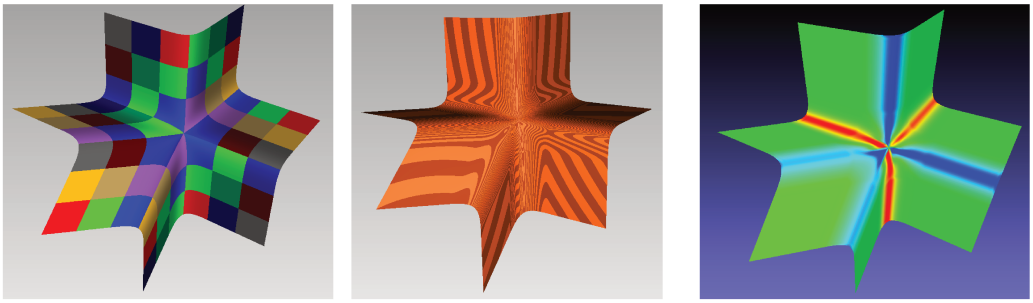

(a) B-spline patches (b) Isophotes (c) Mean curvature

Figure 4.18: GCCS surface with flat areas and smooth curved junctions.

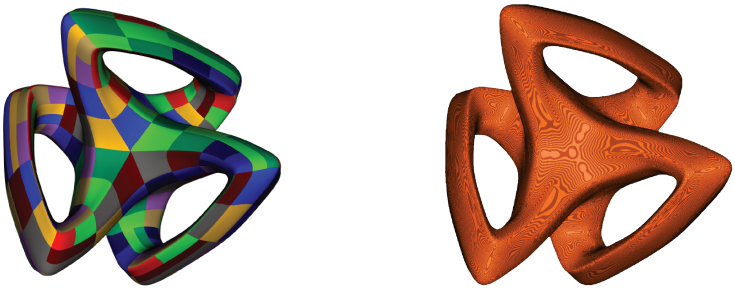

(a) B-spline patches (b) Isophotes

Figure 4.19: GCCS surface.

Algorithm 1: G^1 Catmull-Clark Spline construction

Input: Quadrilateral Mesh $\mathcal{M}$
Output: Bi-5 G^1 surface
foreach $v \in \mathcal{M}_0$ **do**
  Compute the $e_{0,0}$ using the mask;
end
foreach $E \in HE(\mathcal{M})$ **do**
  Compute $e_{1,1}$ using the mask;
  if *E is a boundary edge* **then**
    Compute $e_{1,0}$ and $e_{2,0}$ using the masks;
  end
  Compute $\mathbf{h}[0..2, 0..2]$ the degree elevation of e using the formulas in section 3.1;
end
foreach $v \in \mathcal{M}_0$ **do**
  foreach $k \in [3..\mathfrak{v}]$ **do**
    Compute $b^k_{1,0}$ around the vertex v, using the formula in section 3.2;
  end
  if *The valence is odd* **then**
    foreach $k \in [3..\mathfrak{v}]$ **do**
      Compute the coefficients $b^k_{1,1}$ around the vertex using the formulas of Fig. 4.8
  else
    foreach $k \in [3..\mathfrak{v}]$ **do**
      Compute $b^k_{2,0}$ using the formula in Fig 4.9 ;
    foreach $k \in [3..\mathfrak{v}]$ **do**
      Compute $b^k_{1,1}$ around the vertex using the formula in Fig. 4.10;
  foreach $k \in [3..\mathfrak{v}]$ **do**
    Compute $b^k_{3,0}$ using the formula in Fig 4.11;
    Compute $b^k_{2,1}$, $b^{k-1}_{1,2}$, $b^k_{3,1}$ and $b^{k-1}_{1,3}$ using the formulas in Fig. 4.12;
end

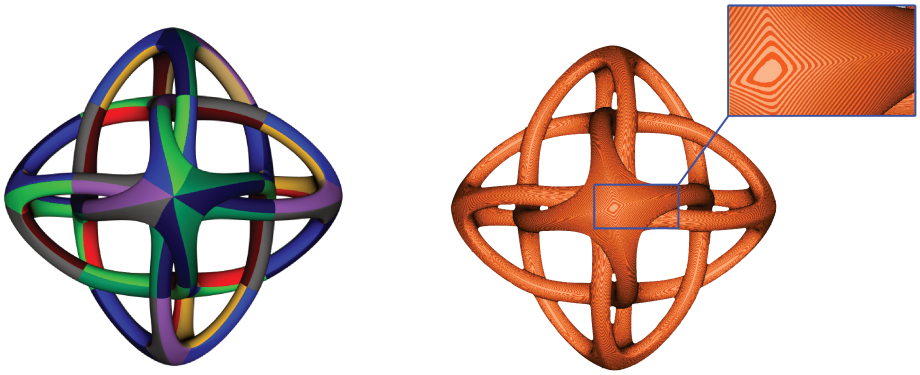

(a) B-spline patches (b) Isophotes

Figure 4.20: GCCS surface.

(a) B-spline patches (b) Isophotes

Figure 4.21: GCCS surface with 598 patches.

(a) B-spline patches (b) Isophotes

Figure 4.22: GCCS surface with 1754 patches.

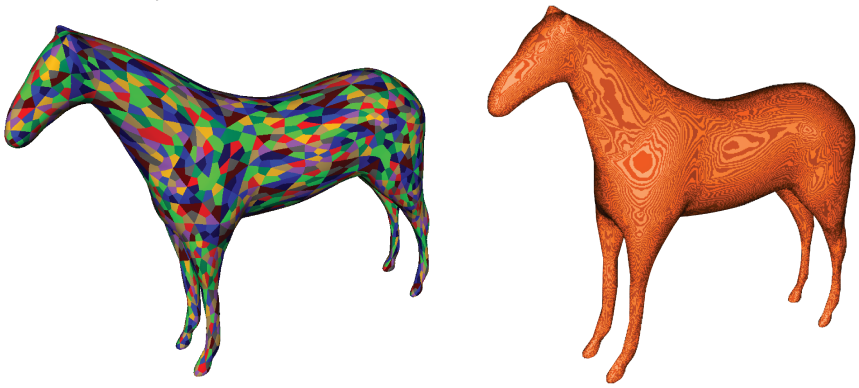

(a) B-spline patches (b) Isophotes

Figure 4.23: GCCS surface with 3000 patches.

Chapter 5

Application

We present in this chapter two applications of the space of geometrically continuous functions: In the first part we will test the G^1 basis generated earlier in this chapter on 3d point cloud approximation. Different bases are going to be compared in terms of quality using an error that we will describe later.

In the second part we use the G^1 basis to solve the diffusion equation with boundary conditions following on isogeometric approach. The tests are made using a biquintic basis.

1 Application to point cloud fitting

surface reconstruction is a major step in the digitalisation of the 3d physical objects. It consists of transforming a scanned 3d point cloud to a 3d model such as mesh or a multi-patches spline surface. A large variety of algorithms exists for that purpose, depending on the properties of the point cloud and the wanted output, the modeller have to choose which type of algorithm will give better results. What we mean by properties of the point cloud can be the type and level of imperfections driven by the 3d scan such as: noise, non uniform distribution of the sampling, missing data, density of the sampling. It can be also properties of the physical shape it self, such as global/local smoothness and piecewise smoothness constraint. Moreover, different 3d scan technologies provide additional informations besides the point clouds, such as normals or confidence of a point (that can be used to reduce noise). This additional inputs are used in some reconstruction algorithms. The paper [73] provides a detailed categorisation of the techniques in surface reconstruction field, according to the point cloud properties of the scan mentioned above as well as the wanted reconstruction output.

We distinguish two main families of surface reconstruction algorithms. The first ones are the Delaunay based methods [74, 75], where the output mesh is a subcomplex of the Delaunay triangulation. These algorithms are suitable for a modellers who wish to produce for a given cloud of points an interpolating mesh. However, these methods have very high requirement and cannot support point clouds with too many imperfections, that makes it impossible to be used for real applications. The second family of algorithms represent the surface as the zero level set of some implicit equation [76, 77], then using for instance a marching cube method for polygonization [78].

We will not give more details about this methods since it is not the subject of the thesis. In the following section we will assume that we have quad mesh that approximate the point cloud surface, issued from a polygonization pre-processing step, and see how we can use this mesh to produce a smooth approximation.

1.1 Gspline basis representation

Let $\mathcal{P} = \{p_1, \dots, p_n\}$ be a cloud of points in $\mathbb{R}^3$ and $\mathcal{N} = \{v_1, \dots, v_n\}$ their corresponding normals, representing a smooth surface that has the same topology as the topological complex $\mathcal{M}$. The goal of this section is to produce a smooth surface that is as close as possible to the cloud of points using the G^1-basis constructed from $\mathcal{M}$.

Denote by $(g_i)_{i\in I}$, $I = \{1, .., r\}$, $r \in \mathbb{N}$ the finite basis of the space $\mathcal{S}_{d,t}(\mathcal{M}, \mathfrak{g})$ of G^1 splines over $\mathcal{M}$ of degree d and with knots sequence t.

The preprocessing step consists of polygonizing the cloud of points, by producing a quad mesh that approximates the cloud of points. In this chapter we will not speak about this step since it is not the objective of the work. The functions g_i are used to parametrise 3d-surfaces, by taking linear combinations:

$$\mathfrak{s} = \sum_{i\in I} \bar{\mathbf{s}}_i g_i \tag{5.1}$$

with coefficients $\bar{\mathbf{s}}_i \in \mathbb{R}^3$ for $i \in I$.

Over each face σ of the mesh $\mathcal{M}$, the functions g_i are represented as linear combination of the b-spline basis functions with coefficients that we denote $c^{\sigma}_{k,l}(\mathfrak{s})$. Hereafter, we will also use g_i to denote the vector of all coefficients $c^{\sigma}_{k,l}(g_i)$ for all faces $\sigma \in \mathcal{M}_2$ and $\bar{G} = [g_i]_{i\in I}$ the matrix, which columns are the vectors g_i. The $N \times 3$ matrix $\bar{C} = [c^{\sigma}_{k,l}(\mathfrak{s})]$ which rows are the b-spline coefficients $c^{\sigma}_{k,l}(\mathfrak{s})$ of the surface h will be written by means of the $l \times 3$ matrix $\bar{\mathbf{s}}$ which rows are the points $\bar{\mathbf{s}}_i$:

$$\bar{C} = \bar{G} \begin{pmatrix} \bar{\mathbf{s}}_1 \\ \vdots \\ \bar{\mathbf{s}}_l \end{pmatrix} = \bar{G}\,\bar{\mathbf{s}}. \tag{5.2}$$

For simplicity, we will use the following notation:

$$\mathbf{s} = \begin{pmatrix} \bar{\mathbf{s}}[:,1] \\ \bar{\mathbf{s}}[:,2] \\ \bar{\mathbf{s}}[:,3] \end{pmatrix}, \quad C = \begin{pmatrix} \bar{C}[:,1] \\ \bar{C}[:,2] \\ \bar{C}[:,3] \end{pmatrix}, \quad G = \mathrm{diag}(\bar{G}, \bar{G}, \bar{G}),$$

where, for a matrix M, $M[:,i]$ indicates the i^{th} column of M. With this notation, we have $C = G\,\mathbf{s}$.

In order to obtain the most accurate representation of $\mathcal{P}$ by G^1 splines, we compute $\mathbf{s}$ by minimizing a weighted combination of square distance and fairing energies. We recall briefly these standard energy terms (see e.g. [79, 80]) and give their matrix formulation in terms of the coefficients in the G^1 basis.

Point-wise distance

Given a (uniform) distribution $\mathcal{U} = \{u_1, ..., u_n\}$ of parameters in $\mathcal{M}$, we define classically the point-wise distance energy as

$$E_P(\mathbf{s}) = \sum_{u \in \mathcal{U}} ||p_u - \mathfrak{s}(u)||^2 = ||D\,\mathbf{s} - P||^2$$

where the pairing between the parameters $u \in \mathcal{U}$ and points $p_u \in \mathcal{P}$ is obtained from an initial parameterisation $\mathfrak{s}_0$, by associating to $u \in \mathcal{U}$ the closest point $p_u \in \mathcal{P}$ to $\mathfrak{s}_0(u)$ (we use a kd tree algorithm to compute closest points [81]). Here $D = \text{diag}(K, K, K)$ is the block diagonal matrix formed by the matrix K which coefficients are $K_{i,j} = g_j(u_i)$, and $P = (P_1, P_2, P_3)$ where $P_1 = (p_1^1, ..., p_n^1)$, $P_2 = (p_1^2, ..., p_n^2)$, $P_3 = (p_1^2, ..., p_n^2)$ where p_i^j is the j^{th} coordinate of the vector $p_{u_i} = p_i = (p_i^1, p_i^2, p_i^3) \in \mathcal{P}$ associated to $u_i \in \mathcal{U}$.

Distance to points with normals

The energy term of the sum of square distances between the planes at the point $p_i \in \mathcal{P}$ normal to $v_i \in \mathcal{N}$ and the point $\mathfrak{s}(u_i)$ is:

$$E_T(\mathbf{s}) = \sum_{i=1,..,l} [v_i.(p_i - \mathfrak{s}(u_i))^t]^2 = ||\tilde{D}\,\mathbf{s} - \tilde{P}||^2$$

for $\mathbf{s} \in \mathcal{S}(\mathcal{M}, \mathfrak{g})$, where the matrix $\tilde{D}$ and $\tilde{P}$ are such that the k^{th} row of $\tilde{D}$ is $\tilde{D}[k,:] = (v_k^1 g(u_k), v_k^2 g(u_k), v_k^3 g(u_k))$ with $g(u_i) = (g_1(u_i), g_2(u_i), ..., g_l(u_i))$, and $\tilde{P} = (v_1^T p_1, \ldots, v_n^T p_n)$. Other distance minimizations can be used, such as the so-called Squared Distance Minimization [80], which involves the principal curvatures.

Fairing energy

To reduce oscillations in the computed surface, we use a regularization term (see e.g. [79])

$$\mathcal{F}_k(g) = \int_0^1 \int_0^1 (\partial_s^k g(s,t))^2 + (\partial_t^k g(s,t))^2 ds dt.$$

In the experimentation, we use the regularization terms $\mathcal{F}_1$ and $\mathcal{F}_2$. To avoid an explicit computation of the integrals, we further simplify them into the following expressions involving directly the b-spline coefficients:

$$\tilde{\mathcal{F}}_1(g) = \sum_{0 \leqslant i,j \leqslant n-1} ||(\Delta_1 c)_{i,j}||^2 + ||(\Delta_2 c)_{i,j}||^2$$
$$\tilde{\mathcal{F}}_2(g) = \sum_{1 \leqslant i,j \leqslant n-1} ||(\Delta_1^2 c)_{i,j}||^2 + ||(\Delta_2^2 c)_{i,j}||^2$$

with $(\Delta_1 c)_{i,j} = c_{i+1,j} - c_{i,j}$, and $(\Delta_2 c)_{i,j} = c_{i,j+1} - c_{i,j}$, $(\Delta_1^2 c)_{i,j} = c_{i,j} - \frac{(c_{i+1,j} + c_{i-1,j})}{2}$ and $(\Delta_2^2 c)_{i,j} = c_{i,j} - \frac{(c_{i,j+1} + c_{i,j-1})}{2}$. As the b-spline coefficients C of h are such that $C = G\,\mathbf{s}$, these energy terms are of the form $\mathbf{s}^T G^T A_i G\,\mathbf{s}$ where A_i is the coefficient matrix of $\tilde{\mathcal{F}}_i$ in the b-spline basis (for $i = 1, 2$).

The final formula that we minimize is of the form:

$$T_{tot}(\mathbf{s}) = w_1 E_P(\mathbf{s}) + w_2 E_T(\mathbf{s}) + w_3 \tilde{\mathcal{F}}_1(G\,\mathbf{s}) + w_4 \tilde{\mathcal{F}}_2(G\,\mathbf{s})$$

where w_i are weights, which are chosen manually depending on the type of the point cloud; the more the point cloud is noisy, the more the fairing energy weights must be large. The total energy $T_{tot}(\mathbf{s})$ is a quadratic function of $\mathbf{s}$, and its minimum(s) can be obtained by solving $\nabla T_{tot}(\mathbf{s}) = 0$, leading to the following linear system

$$(w_1 D^T D + w_2 \tilde{D}^T \tilde{D} + w_3 G^T A_1 G + w_4 G^T A_2 G)\,\mathbf{s} - w_1 \tilde{P}^T \tilde{D} - w_2 P^T D = 0$$

1.2 Illustrations

As we said in previous sections the basis $(g_i)_{i\in I}$ is precomputed. They are represented by the sparse vectors of G. This yields sparse matrices $D, \tilde{D}$ and vectors $P, \tilde{P}$. The matrices A_i for $i = 1, 2$ are diagonal by blocks of size at most 16, this can be proved by a combinatorial argument. This implies in particular that the total system is sparse.

We present in Figure 5.1 some results of fitting surfaces, the computations were made with the Julia programming language, the visualization is done with the software Axl [1], and MeshLab.

The cloud of points in Fig. 5.1 is taken from a smooth surface, made by building a scaffolding of a skeleton from [82], then by applying a Catmull-Clark subdivision algorithm for smoothing.

In Fig. 1.2 we test our basis on a lung medical scan. The input is a point cloud of 300000 point. We extract a sampling using a Poisson method [83] and an approximating mesh using the ball pivoting algorithm [24]. The basis that we use is described in Section 3 made with bi-5 Bézier patches, and the gluing data are quadratic. We notice that the approximation is smooth and has captured most of the shape, except the highly curved bottom regions where the error can be seen to be high .

2 Application in IsoGeometrics analysis

In this section[2], the proposed geometrically smooth spline bases will be applied in Isogeometric analysis (IgA) with complex geometry. IgA was created to recover some of the accuracy problems encountered in other finite element methods. We start this section by introducing finite element method and Isogeometric analysis. Then we give an example by providing a solution of the diffusion equation using IgA.

2.1 Finite element analysis

The finite element method (FEM) is a numerical method that is used to find the approximate solution of linear differential equation over a given domain Ω, that

[1] axl.inria.fr

[2] This section is a part of a forthcoming paper [43]

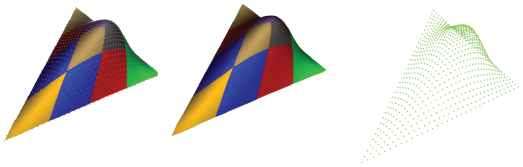

(a) Degree bi-5 Bézier patches with knots vector $\mathbf{t} = [0^6, 1^6]$ and quadratic gluing data. $F = 3$, $N = 66$, $P = 817$, $e_{ave} = 0.01004$, $e_{max} = 0.01761$.

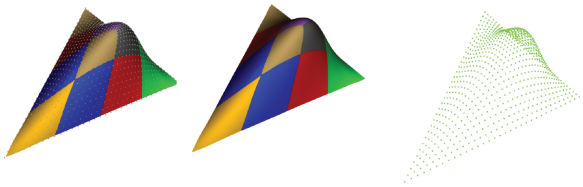

(b) Degree bi-3 bsplines patches with knots vector $\mathbf{t} = [0^4, \frac{1}{3}, \frac{2}{3}, 1^4]$ and linear gluing data. The same cloud of points as in 5.1a is used, with one level of refinement of the mesh in 5.1a using Catmull-Clark subdivision algorithm. $F = 12$, $N = 139$, $P = 817$, $e_{ave} = 0.0100075$, $e_{max} = 0.022774$.

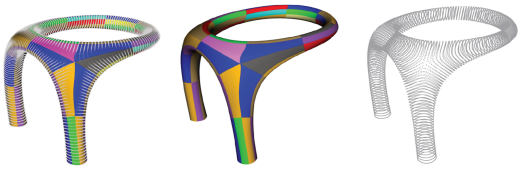

(c) Same type of splines as in 5.1a. $F = 96$, $N = 1180$, $P = 24702$, $e_{ave} = 0.0029685196$, $e_{max} = 0.00989258$.

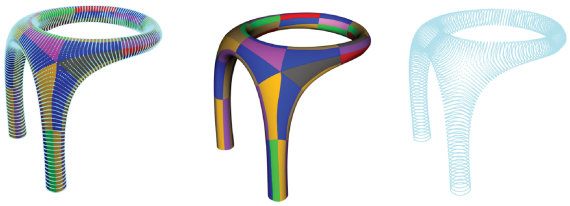

(d) Same type of splines as in 5.1b. $F = 96$, $N = 1180$, $P = 24702$, $e_{ave} = 0.0015991$, $e_{max} = 0.01391856$.

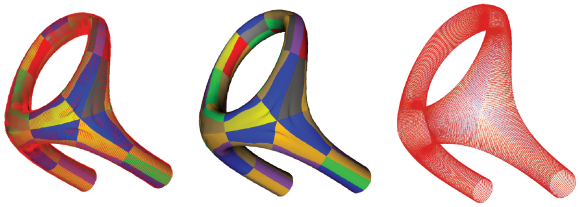

(e) Degree bi-3 bsplines patches with knots vector $[0^4, (1/3)^2, (2/3)^2, 1^4]$. This fitting exhibits a quality defect along the knots line that are close to singular vertices, because the element patches are C^1. $F = 96$, $N = 1980$, $P = 24702$, $e_{ave} = 0.00594$, $e_{max} = 0.050988$.

Figure 5.1: Comparison of fitting of 3d-geometric objects with different basis. In each example the first picture is for the cloud of points and the fitting smooth surface, the second one for the fitting surfaces, and the last one is for the cloud of points alone. F is the number of faces of the quad mesh, N is the dimension of the G^1 space, P is the number of points, e_{ave}, e_{max} are respectively the relative average error $\sum_{u \in \mathcal{U}} \frac{||p_u - \mathfrak{s}(u)||}{P\,\Delta}$ and relative maximum error $\max_{u \in \mathcal{U}} \frac{||p_u - \mathfrak{s}(u)||}{\Delta}$ where Δ is the diameter of the point cloud.

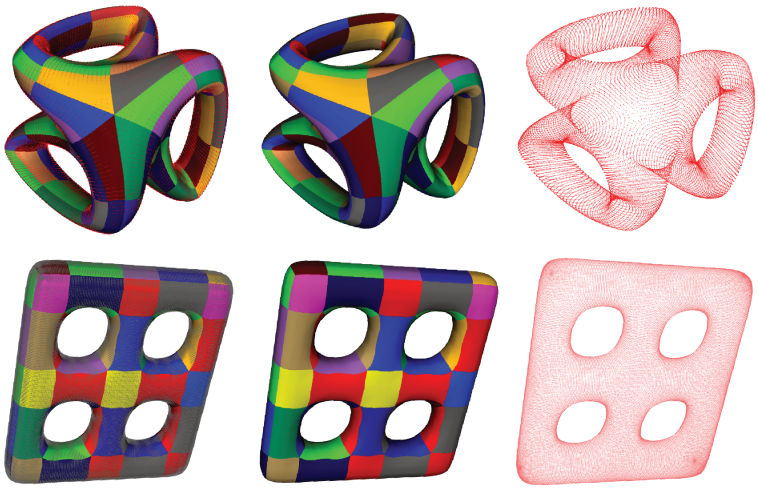

Figure 5.2: Fitting of 3d-geometric objects. The first column is for the cloud of points and the fitting smooth surface, the second one for the fitting surfaces, and the last one is for the cloud of points alone. We use the same basis types as in Fig. 5.1e, with $F = 144$, $N = 2808$, $P = 36860$, $e_{ave} = 0.00748197$, $e_{max} = 0.0324516$ for the first line example.

is defined using a differential operator A, a set of boundary conditions P and a function f in the following way:

$$Find \;\; a \; function \;\; u, defined \; over \; \Omega, verifying \; A(u) = f \tag{5.3}$$

The boundary conditions $P(u)$ are constraints that we impose on the solution function (or its derivatives) over all or a part of the domain Ω, or/and all or a part of its boundary $\partial\Omega$ [84]. We mention among the most well known boundary condition the ones that we call:

- Dirichlet conditions: when we specify the values of the solutions a over all or a part of $\partial\Omega$.
- Neumann conditions: when we specify the the valus of the derivative of the solution over all or a part of $\partial\Omega$.
- Robin condition: when we impose a a linear relation between the value and the derivative of the solution over all or a part of $\partial\Omega$.
- Mixed conditions: when the solutions is required to satisfy different boundary conditions in the same time.

The main purpose of using this boundary conditions is to ensure that the solution of the problem will be unique.

The method performs the following steps:

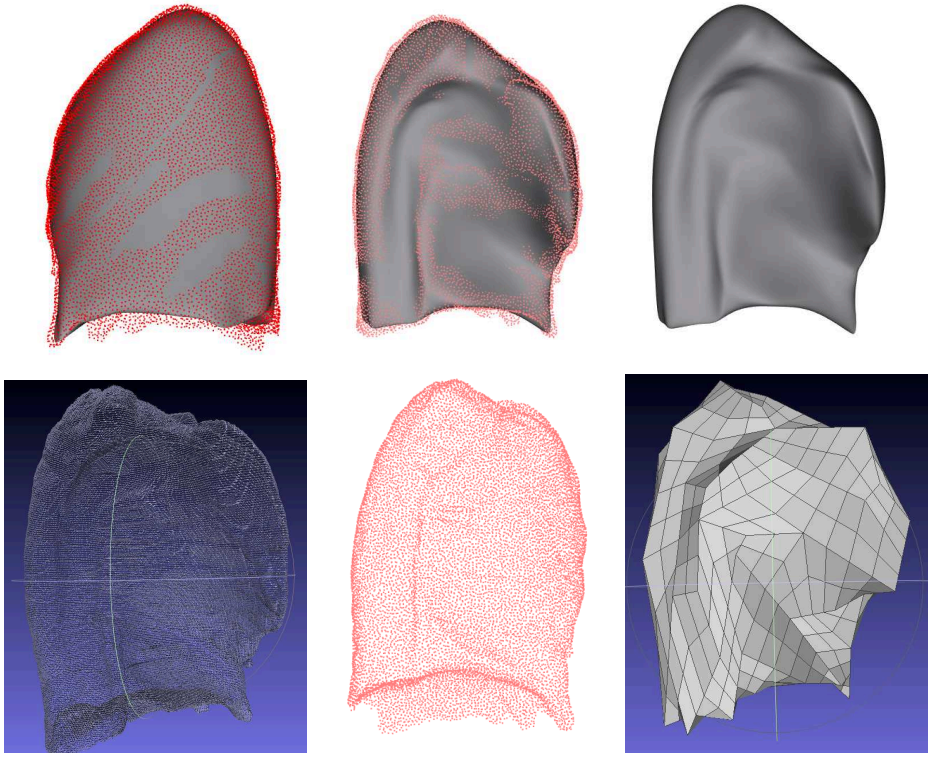

Figure 5.3: Approximation of a lung medical scan. The top left and top middle pictures represent the approximation from two different sides. The bottom left is the point cloud medical scan of the lung (we use MeshLab for visualisation), the centre bottom picture represents the sampling of the scan. The right bottom picture is an 840 face mesh approximating the point cloud, produced by a ball pivoting algorithm [24].

- First we form a subdivision Δ of the domain using a mesh. See [85] for a survey about this subject.
- The second step is to describe the space that will be used for the approximation. It is in general a space of piecewise polynomial functions $\mathcal{S}(\Delta)$ defined on the subdivision Δ. We also choose a locally supported basis $B = \{\mathcal{B}_i\}_{i=1..n}$ for it. The chapter 2 was an overview of the analyse of the dimension of such spaces. See [86] for an example of an algorithm that produces this kind of basis.
- Next we describe the weak formulation of the differential equation. We do that by multiplying the equation by "test functions" v, and integrate both sides of the equality:

  $$\textit{Find a function } u, \textit{defined over } \Omega, \textit{verifying } \int_\Omega vA(u)v\mathbf{dx} = \int_\Omega f\mathbf{dx} \quad (5.4)$$

  In general we choose the test space (ie. the space where v belongs) to be the same as the trial space.
- Then we apply the divergence theorem to reduce the maximal differential order used in the equation. The result of this operation is an equation (the weak formulation of (5.3)) with lower order differentials, it means that the space of functions $\mathcal{S}^r(\Delta)$ is used with an r as low as possible. The formulation of the problem at this level is:

  $$a(u, v) = L(v) \quad (5.5)$$

  besides of the boundary constraints $P(u)$, here a is a bilinear form, and L is a linear form on $\mathcal{S}(\Delta)$.
- The final step is to find a function $u = \sum_{i=1...n} c_i\mathcal{B}_i$ that verifies the equation(5.5) for any $v \in \mathcal{S}(\Delta)$ as well as the boundary conditions. We do that by solving the system given by: $\sum_{i=1..n} c_i a(\mathcal{B}_i, \mathcal{B}_j) = L(\mathcal{B}_j)$ for $j \in \{1, \dots n\}$. The solution of this system is an approximation of the exact solution of (5.3).

2.2 Isogeometric analysis

The main drawback of the FEM is that it is not always possible to use the output of CAD (Computer Aided Design) system, instead of that it takes a polygonal approximation of the geometry. This inherent accuracy problems [19].

In Isogeometric analysis we use a CAD piecewise polynomial geometry to represent exactly the domains. This will avoid the use of automatic remeshing algorithms that can be costly. The same space of functions used for representing the geometry will be used as a test/trial space. It is shown in [20] that the composition of a basis function from the test/trial space with the inverse of the parametrisation that are all G^k functions with respect to the same topological surface, will produce a C^k function on Ω.

In the following section we will present an example of solution of the diffusion equation using a G^1-space and IgA.

2.3 Model problem and technique details

Consider the following two-dimensional heat diffusion example as an illustrative model problem:

$$\begin{aligned} -\Delta T(\boldsymbol{x}) &= f(\boldsymbol{x}) \qquad \text{in } \Omega \subset \mathbb{R}^2 \\ T(\boldsymbol{x}) &= 0 \qquad \text{on } \partial\Omega \end{aligned} \tag{5.6}$$

where Δ is the Laplacian operator, Ω is the computational domain parameterized by the proposed geometrically smooth spline bases , $T(\boldsymbol{x})$ is the unknown heat field, and $f(\boldsymbol{x})$ is the heat source function. The trial and test spaces are defined as:

$$\begin{aligned} \mathcal{U} &= \{T \in H^1(\Omega) : T = T_D \text{ on } \partial\Omega\}, \\ \mathcal{V} &= \{\psi \in H^1(\Omega) : \psi = 0 \text{ on } \partial\Omega\}. \end{aligned} \tag{5.7}$$

where T_D Expresses the Dirichlet conditions.

The variation problem can be stated as: find the solution $T^h \in \mathcal{U}^h \subset \mathcal{U}$ such that:

$$\int_\Omega \nabla T^h(\boldsymbol{x}) \cdot \nabla \psi^h(\boldsymbol{x})\, d\Omega = \int_\Omega f(\boldsymbol{x}) \cdot \psi^h(\boldsymbol{x})\, d\Omega \qquad \forall \psi^h \in \mathcal{V}^h \subset \mathcal{V}. \tag{5.8}$$

which can be written as

$$a(T^h, \psi^h) = \langle f, \psi^h \rangle \qquad \forall \psi^h \in \mathcal{V}^h, \tag{5.9}$$

where

$$\begin{aligned} a(T^h, \psi^h) &= \int_\Omega \nabla T^h(\boldsymbol{x}) \cdot \nabla \psi^h(\boldsymbol{x})\, d\Omega, \\ \langle f, \psi^h \rangle &= \int_\Omega f(\boldsymbol{x}) \cdot \psi^h(\boldsymbol{x})\, d\Omega. \end{aligned} \tag{5.10}$$

In the isogeometric analysis framework, the solution field T^h will be represented in the proposed geometrically smooth spline bases, that is,

$$T^h = \sum_{i=1}^{N} g_i(\mathbf{u})\, T_i, \tag{5.11}$$

where T_i are unknown variables to be solved, $g_i(\mathbf{u})$ are geometrically smooth spline basis functions defined on each face σ from its b-spline coefficients $c^\sigma_{k,l}(g_i)$, $\mathbf{u}^\sigma = (\xi^\sigma, \eta^\sigma)$ are the domain parameters associated to the face σ of the parametric domain $\mathcal{P}$, N is the number of basis functions. The test function ψ^h is also defined as follows :

$$\psi^h = g_i(\mathbf{u}). \tag{5.12}$$

Then a linear system can be obtained from Eq. (5.10),

$$\boldsymbol{A}\boldsymbol{T} = \boldsymbol{b}$$

in which $\boldsymbol{T} = [T_i]$ are unknown variables. The entries in the stiffness matrix $\boldsymbol{A} = [A_{i,k}]$ and right-hand side $\boldsymbol{b} = [b_i]$ can be computed as follows,

$$A_{i,k} = \int_{\mathcal{P}} \nabla_{\mathbf{u}} g_k(\mathbf{u}) B(\mathbf{u})^T B(\mathbf{u}) \ \nabla_{\mathbf{u}} g_k(\mathbf{u}) J(\mathbf{u}) \ d\mathcal{P}$$
$$b_i = \int_{\mathcal{P}} f(\sigma(\mathbf{u})) \cdot g_k(\mathbf{u}) J(\mathbf{u}) \ d\mathcal{P}.$$

where $\sigma(\mathbf{u}) = (x(\xi,\eta), y(\xi,\eta))$ is the parametrisation defined as in Eq. (5.1), $J(\mathbf{u})$ is the Jacobian of the transformation,

$$J(\mathbf{u}) \ = \ \begin{vmatrix} x_\xi & y_\xi \\ x_\eta & y_\eta \end{vmatrix},$$

$B(\mathbf{u})$ is the transposed of the inverse of the Jacobian matrix.

2.4 Examples

In this subsection, a numerical example is presented to demonstrate the effectiveness of the proposed simulation method with geometrically smooth spline bases.

We consider a heat diffusion problem with the following exact solution

$$T(\boldsymbol{x}) = 10\sin(\frac{\pi}{30}(x+y+30))\sin(\frac{\pi}{30}(x+y-30))\sin(\frac{\pi}{30}(x-y-30))\sin(\frac{\pi}{30}(x-y+30)). \tag{5.13}$$

The computational domain is a square $[-30,30]\times[-30,30]$, which is parameterized by a quintic G^1 splines. The parametric mesh is shown in Fig. 5.4(a), and the corresponding parameterization with 52 patches is presented in Fig 5.4(b) and (c). The corresponding IGA numerical solution is shown in Fig. 5.4(d) and (e), and the corresponding error colormap is shown in Fig. 5.4(f). We can find that the proposed IGA framework with geometrically smooth splines can achieve a similar accuracy with the C^0 multi-patch method.

It should be mentioned that the IGA solution surface is also G^1 according to the property of geometrically smooth splines.

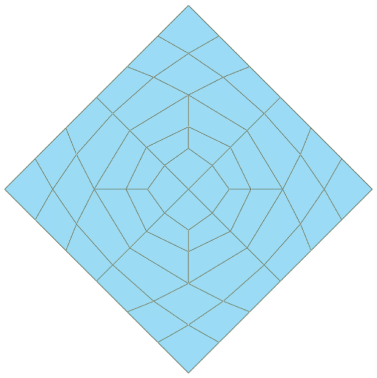

(a) parametric mesh

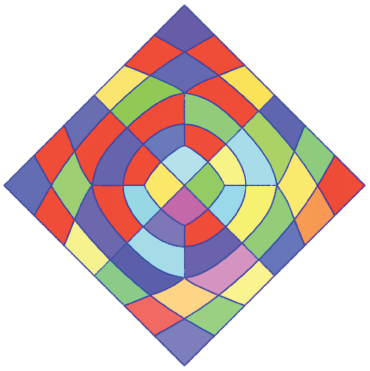

(b) parameterization with 52 Bézier patches

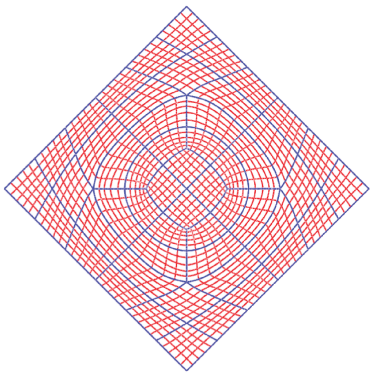

(c) parameterization with iso-parametric curves

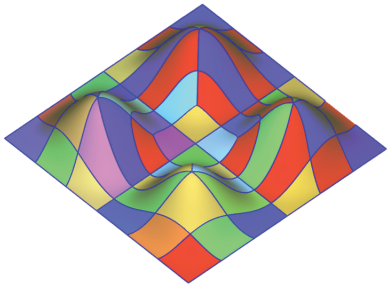

(d) G^1 IGA solution surface

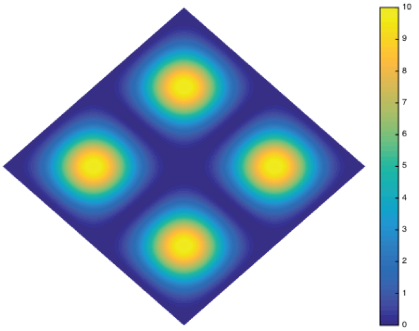

(e) IGA solution with colormap

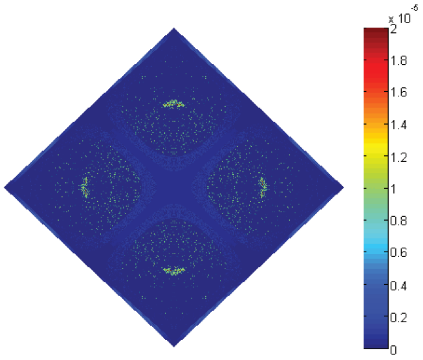

(f) Level 3 subdivision error colormap

Figure 5.4: Numerical example of IGA with geometrically smooth splines.

Level of subdivision	0	1	2	3
Dimension	529	1993	7729	30433
L^2 Error	0.00215138	0.000427664	3.14061e-005	2.90809e-006
Rate of convergence	–	2.33	3.77	3.43

Figure 5.5: Estimated rate of convergence

Chapter 6

Conclusion

The subject of this thesis was to study Geometrically Continuous splines. The main questions addressed in this manuscript are related to: basis constructions, dimension computation and shape generation. Similar to ordinary splines, G-spline functions can be seen as splines over a manifold-like topology that we called topological surface. In practice, the restrictions of our Gsplines to the patches of the topological surfaces are tensor splines or Bézier patches.

1 Gluing data

The choice of gluing data is crucial to guaranty that the space of G^1-splines that we produce have good smoothness properties around the vertices. The question of compatibility around the vertices is addressed in the Section 2 of Chapter 3. We have explained that a vertex from a topological surface is compatible if the product of the transition maps jacobians around that vertex is equal to the identity. This result corresponds exactly to the G^1 case of Theorem 7.1 in [87]. Any G^1-spline function that do not respect this condition will have a vanishing tangent space at that vertex.

2 Basis construction

A standard method of basis construction performs that task by a piecing process. This requires to know a basis of the space of Gsplines over a simple topology composed of two patches, then we choose linear combinations of that basis that can be pieced together according to the wanted topology. We keep piecing the parts of the topology until we form one base element of the space of Gsplines. By applying this piecing process on different choices of linear combinations, we end up with a base of a G^1-splines space that is suitable for Fitting and IgA.

We analyse the space of G^1-splines over a two patches topology in two different ways. The first way, by considering the G^1-continuity relation as syzygy equation as in [21]. In that context, the existing literature offers the possibility to analyse these spaces with polynomial patches. We provide a generalisation of this study by adding new homological techniques that allows to analyse the basis and the dimension of that space when the spline patches have one inserted

knot on each direction of our quads. A generalisation of the method to multiple inserted knots can be subject of future works.

A second way of analysing the space of G^1-splines over two patches is by using the tensor product spline representation of the patches. Here we will have a system of equations between the bspline coefficients of the two patches. We define the notion of separability of the space, that characterises the spaces of G^1-splines that admit a base with local support. If the chosen space doesn't admit a locally supported base, then we produce a base that span a smaller space with locally supported base elements.

Many algorithms are suitable only for a particular polynomial degree and particular gluing data type (for instance [88] construct basis for linear gluing data). We describe in this manuscript a general new piecing scheme for G^1-splines over quad meshes, that we use to produce base for many gluing data functions types.

3 Dimension computation

The commutative algebra tools that Billera have described in [25] have played a major role in understanding the impact of the geometry of a complex on the dimension of the spline space. Chapter 2 was an outline of the most important results in that direction. One of the goals of this manuscript was to show that we can use similar tools to have more precise results on the dimension of the space of Gsplines. The key ingredient of all this construction was to write an algebraic characterisation of the geometric continuity (see proposition 8.2). We succeed for instance to express the space of Gsplines as an homology group of a chain complex. Thus we can write the dimension of the space of splines by means of the dimension of other spaces.

The major obstacle of these constructions is the fact that we cannot define the space of Gsplines as graded module (at least not for the usual product by polynomials). All we can say about that space is that it is a graded vector space, so we cannot reproduce a Gspline version of the results of the Chapter 2.

4 Shape smoothing

We present in chapter 4 of the manuscript, an algorithm to generate a smooth multi-patch surface that approximate a given 3d-mesh. For this problem, the notion of guided surfaces seems to give good results (see for instance [89]). We have chosen to use approximate Catmull-Clark surface [63] as a guide for our smoothing. More precisely, after producing the approximate Catmull-Clark surface, we compute the closest G^1-surface to it by projecting onto the space of G^1-surfaces.

The vertex enclosure problem has been discussed in this chapter. We provide a solution of that problem by using explicit formulas. The two cases of odd and even valence are distinguished since the co-rank of the incidence matrix in the two cases are different.

We have explained that the same algorithm, when applied to a base of the space of one dimensional meshes will produce a set of G^1-spline functions that are

suitable for approximation. The work of [89] has used a similar basis to compute the solution of an IgA problem. We test this basis for fitting problems.

5 Fitting and IsoGeometric analysis

The base that we have produced have been tested for Fitting and isogeometric analysis. The algorithm that we have used for fitting uses a pre-processing step called ball pivoting method, that produces a coarse mesh approximating our point cloud. After that a G^1-spline space is produced using the topology of the coarse mesh. Then a regression is applied. We have tested this algorithm for many types of gluing data including Bézier bi-5 patches and bi-3 splines patches with knots. We have tested as well the basis produced in chapter 4 for medical data fitting in lung model reconstruction.

For the IgA tests, we have computed an approximation of the solution of a diffusion problem with boundary conditions using a Bi-5 Bézier patches base. We found out that the proposed IGA framework with geometrically smooth splines can achieve a similar accuracy with the C^0 multi-patch method, and with less base elements.

6 Future Works

In the continuation of this work, we see two main directions to be explored:

- **Advanced Homological technics for Geometric continuity:** After proposing the algebraic characterisation of the G^k-junctions, we have explained how to generalize some exact sequences. The next step is to compute bounds on the dimension of the co-kernel mentioned in the sequence (3.50).

- **Extension to three-variate G^1-splines:** As the reader has seen in this manuscript, to solve the vertex enclosure system at each vertex v, we consider the dual graph of the mesh formed by the patches containing v and write its incidence matrix ∂. The vertex enclosure system is written by means of the matrix ∂ and the incidence matrix has a corank that depends on the parity of the vertex valence, and more generally the corank of the incidence matrix for a random graph is equal to: $n - c_0$ where n is the number of vertices and c_0 is the number of bipartite (bicolorabel) components of the graph.

  In a planar mesh vertex enclosure problem all the incidence matrices corresponds to a cyclique graph, and these matrices have a corank equal at most to 1. A possible extension is to provide a solution of the 3d G^1 continuity problem with a scheme of solution similar to the one we have described in Chapter 4. Around an extraordinary vertex in a volumetric 3d mesh, the vertex enclosure problem takes a similar form since the incidence matrix is used to express the local system. However the corank may take different values depending on the local dual graph form, that is not a fortiori cyclic. The rest of the solution scheme is not yet clear for us.

This project has received funding from the European Union's Horizon 2020 research and innovation programme under the Marie Skłodowska-Curie grant agreement No 675789.

Bibliography

[1] SN Berstein. Démonstration du théorème de Weierstrass fondée sur le calcul des probabilities, 1912.

[2] A. R. Forrest. Interactive interpolation and approximation by Bézier polynomials. *Computer-Aided Design*, 22(9):527–537, 1990.

[3] Jean-Jacques Risler. *Méthodes mathématiques pour la CAO*. Masson, 1991.

[4] Gilbert Strang. Piecewise polynomials and the finite element method. *Bull. Amer. Math. Soc.*, 79(6):1128–1137, 1973.

[5] Peter, Alfeld and Schumaker, Larry L. The dimension of bivariate spline space of smoothness r and degree $d \geqslant 4r + 1$. *Computer Aided Geometric Design*, 4(1-2):105–123, 1987.

[6] Adel Kh. Ibrahim and Larry L. Schumaker. Super Spline Spaces of Smoothness r and Degree d $\geqslant$3r + 2. *Constructive Approximation*, pages 401–423, 1991.

[7] Louis J. Billera and Lauren L. Rose. A dimension series for multivariate splines. 128:107–128, 1991.

[8] Bernard Mourrain and Nelly Villamizar. Homological techniques for the analysis of the dimension of triangular spline spaces. *Journal of Symbolic Computation*, 50:564–577, 2013.

[9] Kestutis Karčiauskas and Jörg Peters. Refinable bi-quartics for design and analysis. *Computer-Aided Design*, 102:204–214, 2018.

[10] Georges-pierre Bonneau and Stefanie Hahmann. Flexible G^1 interpolation of quad meshes. *Graphical Models*, 76(6), 2014.

[11] Jörg Peters. Smooth interpolation of a mesh of curves. *Constructive Approximation*, 7(1):221–246, 1991.

[12] Wei-hua Tong and Tae-wan Kim. High-order approximation of implicit surfaces by triangular spline surfaces. *Computer-Aided Design*, 41(6):441–455, 2009.

[13] Chandrajit L. Bajaj, Guo Liang Xu, and Qin Zhang. Higher-order level-set method and its application in Biomolecular surfaces construction. *Journal of Computer Science and Technology*, 23(6):1026–1036, 2008.

[14] Abdulwahed Abbas, Ahmad Nasri, and Takashi Maekawa. Generating B-spline curves with points, normals and curvature constraints: A constructive approach. *Visual Computer*, 26(6-8):823–829, 2010.

[15] Catmull E and Clark J. Recursivly generated B-spline surfaceson arbitrary topological mesh.

[16] Peters Jorg and Reif Ulrich. *Subdivision surfaces*. Springer, Berlin, Heidelberg.

[17] Kestutis Karčiauskas and Jörg Peters. Fair free-form surfaces that are almost everywhere parametrically C2. *Journal of Computational and Applied Mathematics*, pages 1–13, 2018.

[18] Thomas W. Sederberg, Jianmin Zheng, Almaz Bakenov, and Ahmad Nasri. T-splines and T-NURCCs. *ACM SIGGRAPH 2003 Papers, SIGGRAPH '03*, pages 477–484, 2003.

[19] Thomas J.R. Hughes, J. Austin Cottrell, and Yuri Bazilevs. Isogeometric analysis: CAD, finite elements, NURBS, exact geometry and mesh refinement. *Computer Methods in Applied Mechanics and Engineering*, 194(39-41):4135–4195, 2005.

[20] David Groisser and Jörg Peters. Matched G^k-constructions always yield C^k-continuous isogeometric elements. *Computer Aided Geometric Design*, 34:67–72, 2015.

[21] Bernard Mourrain, Raimundas Vidunas, and Nelly Villamizar. Dimension and bases for geometrically continuous splines on surfaces of arbitrary topology. *Computer Aided Geometric Design*, 45:108–133, 2016.

[22] Mario Kapl, Florian Buchegger, Michel Bercovier, and Bert Jüttler. Isogeometric analysis with geometrically continuous functions on planar multi-patch geometries. *Computer Methods in Applied Mechanics and Engineering*, 316:209–234, 2017.

[23] Mario Kapl, Florian Buchegger, Michel Bercovier, and Bert Jüttler. Isogeometric analysis with geometrically continuous functions on planar multi-patch geometries. *Computer Methods in Applied Mechanics and Engineering*, 316:209–234, 2017.

[24] Bernardini Fausto, Joshua Mittleman, Rushmeier Holly, Silva Claudio, and Taubin Gabriel. The Ball-pivoting algorithm for surface reconstruction. *IEEE transactions on visualisation and computer graphics*, 5(4), 1999.

[25] Louis J. Billera. Homology of smooth splines: Generic triangulations and a conjecture of strang. *Transactions of the American Mathematical Society*, 310(1):325–340, 1988.

[26] Hal Schenck. A Spectral Sequence for Splines. *Advances in Applied Mathematics*, 19(2):183–199, 1997.

[27] Hal Schenck and Mike Stillman. Local cohomology of bivariate splines. *Journal of Pure and Applied Algebra*, 117-118(Supplement C):535–548, 1997.

[28] James Munkres. *Elements of Algebraic Topology*. Perseus Books, 1984.

[29] Edwin H. Spanier. *Algebraic Topology*. Springer, New York, NY.

[30] Pierre Antoine Grillet. *Abstract Algebra (Graduate Texts in Mathematics)*. Springer-Verlag, Berlin, Heidelberg, 2007.

[31] W. Whiteley. A matrix for splines. *Progress in Approximation Theory*, 1991.

[32] Louis J. Billera. The algebra of continuous piecewise polynomials. 183:170–183, 1989.

[33] Louis J. Billera and Lauren L. Rose. Modules of piecewise polynomials and their freeness. *Mathematische Zeitschrift*, 209(1):485–497, Jan 1992.

[34] Michael R. DiPasquale. Shellability and freeness of continuous splines. *Journal of Pure and Applied Algebra*, 216(11):2519–2523, 2012.

[35] Allen Hatcher. *Algebraic topology*. Cambridge University Press, Cambridge, 2002.

[36] John P Dalbec and Hal Schenck. On a conjecture of Rose. 165:151–154, 2001.

[37] John Morgan and Ridgway Scott. A Nodal Basis for C^1 Piecewise Polynomials of Degree $n \geqslant 5$. *Mathematics of Computation*, 29(131):736–740, 1975.

[38] Terry McDonald and Hal Schenck. Piecewise polynomials on polyhedral complexes. *Advances in Applied Mathematics*, 42(1):82–93, 2009.

[39] Walter Schempp Karl Zeller (eds.) Dipl.-Math. Günter Baszenski, Dr. Horst Posdorf (auth.). *Multivariate Approximation Theory: Proceedings of the Conference held at the Mathematical Research Institute at Oberwolfach Black Forest, February 4–10, 1979*. ISNM International Series of Numerical Mathematics / Internationale Schriftenreihe zur Numerischen Mathematik / Série Internationale D'Analyse Numérique 51. Birkhäuser Basel, 1 edition, 1979.

[40] Bernard Mourrain and Nelly Villamizar. Bounds on the Dimension of Trivariate Spline Spaces: A Homological Approach. *Mathematics in Computer Science*, 8(2):157–174, 2014.

[41] Anthony V Geramita and Henry K Schenck. Fat Points, Inverse Systems, and Piecewise Polynomial Functions. *Journal of Algebra*, 204(1):116–128, jun 1998.

[42] Ahmed Blidia, Bernard Mourrain, and Nelly Villamizar. G 1 -smooth splines on quad meshes with 4-split macro-patch elements. *Computer Aided Geometric Design*, 52-53:106–125, mar 2017.

[43] Blidia Ahmed, Mourrain Bernard, and Xu Gang. Geometrically smooth spline bases for data fitting and simulation. *Computer Aided Geometric Design*. Forthcoming.

[44] M.Hahn Jörg. Geometric continuous patch complexes. *Computer Aided Geometric Design*, 6(February 1987):55–67, 1989.

[45] Jörg Peters and Jianhua Fan. On the complexity of smooth spline surfaces from quad meshes. *Computer Aided Geometric Design*, 27(1):96–105, 2010.

[46] Stefanie Hahmann, Georges-Pierre Bonneau, and Baptiste Caramiaux. Bicubic G^1 interpolation of arbitrary quad meshes using a 4-split. *Advances in Geometric Modeling and Processing*, 4975(1), 2008.

[47] Jörg Peters. A characterisation of connecting maps as nonlinear roots of the identity. *Curves and Surfaces II*, pages 1–8, 1994.

[48] Mario Kapl and Vito Vitrih. Space of C^2-smooth geometrically continuous isogeometric functions on planar multi-patch geometries: Dimension and numerical experiments. *Computers and Mathematics with Applications*, 73(10):2319–2338, 2017.

[49] Annabelle Collin, Giancarlo Sangalli, and Thomas Takacs. Analysis-suitable G^1 multi-patch parametrizations for C^1 isogeometric spaces. *Computer Aided Geometric Design*, 47:93–113, 2016.

[50] Ulrich Reif. Biquadratic G-spline surfaces. *Computer Aided Geometric Design*, 8396(94), 1995.

[51] Jianhua Fan and Jörg Peters. On smooth bicubic surfaces from quad meshes. *Lecture Notes in Computer Science (including subseries Lecture Notes in Artificial Intelligence and Lecture Notes in Bioinformatics)*, 5358 LNCS(PART 1):87–96, 2008.

[52] Jorg Peters. Biquartic C1-surface splines over irregular meshes. *Computer-Aided Design*, 0010(12):895–903, 1995.

[53] Donal O'shea (auth.) David A. Cox, John Little. *Using Algebraic Geometry*. Graduate Texts in Mathematics 185. Springer-Verlag New York, 2 edition, 2005.

[54] Hartmut Prautzsch. Smoothness of subdivision surfaces at extraordinary points. *Advances in Computational Mathematics*, 9(3):377–389, 1998.

[55] Jianhua Fan and Jörg Peters. On smooth bicubic surfaces from quad meshes. In *International Symposium on Visual Computing*, pages 87–96. Springer, 2008.

[56] Stefanie Hahmann, Georges-Pierre Bonneau, and Baptiste Caramiaux. Bicubic G1 interpolation of irregular quad meshes using a 4-split. In *International Conference on Geometric Modeling and Processing*, pages 17–32. Springer, 2008.

[57] Carolina Vittoria Beccari, Daniel E. Gonsor, and Marian Neamtu. RAGS: Rational geometric splines for surfaces of arbitrary topology. *Computer Aided Geometric Design*, 31(2):97–110, 2014.

[58] Georges-Pierre Bonneau and Stefanie Hahmann. Flexible G^1 interpolation of quad meshes. *Graphical Models*, 76(6):669–681, 2014.

[59] Ruimin Wang, Ligang Liu, Zhouwang Yang, Kang Wang, Wen Shan, Jiansong Deng, and Falai Chen. Construction of Manifolds via Compatible Sparse Representations. *ACM Transactions on Graphics*, 35(2):1–10, February 2016.

[60] Michel Bercovier and Tanya Matskewich. *Smooth Bézier Surfaces over Unstructured Quadrilateral Meshes*. Lecture Notes of the Unione Matematica Italiana. Springer International Publishing, 2017.

[61] Charles Loop. Smooth spline surfaces over irregular meshes. In *Proceedings of the 21st Annual Conference on Computer Graphics and Interactive Techniques*, pages 303–310. ACM, 1994.

[62] Jörg Peters. Patching catmull-clark meshes. In *Proceedings of the 27th Annual Conference on Computer Graphics and Interactive Techniques*, pages 255–258. ACM Press/Addison-Wesley Publishing Co., 2000.

[63] Charles Loop and Scott Schaefer. Approximating Catmull-Clark subdivision surfaces with bicubic patches. *ACM Transactions on Graphics*, 27(1):1–11, 2008.

[64] Charles Loop and Scott Schaefer. G^2 Tensor Product Splines over Extraordinary Vertices. *Computer Graphics Forum*, 27(5):1373–1382, 2008.

[65] Kestutis Karčiauskas and Jörg Peters. Biquintic G^2 surfaces via functionals. *Computer Aided Geometric Design*, 33:17–29, 2015.

[66] Kestutis Karčiauskas and Jörg Peters. Improved shape for refinable surfaces with singularly parameterized irregularities. *Computer-Aided Design*, 90:191–198, 2017.

[67] C. L. Chan, C. Anitescu, and T. Rabczuk. Isogeometric analysis with strong multipatch C^1-coupling. *Computer Aided Geometric Design*, 62:294–310, 2018.

[68] Deepesh Toshniwal and Thomas J.R. Hughes. Polynomial splines of non-uniform degree on triangulations: Combinatorial bounds on the dimension. *Computer Aided Geometric Design*, 2019.

[69] Kestutis Karčiauskas and Jörg Peters. Improved shape for refinable surfaces with singularly parameterized irregularities. *CAD Computer Aided Design*, 90:191–198, 2017.

[70] Wei hua Tong and Tae wan Kim. High-order approximation of implicit surfaces by G1 triangular spline surfaces. *CAD Computer Aided Design*, 41(6):441–455, 2009.

[71] Fuentes Suárez Alvaro J. and Evelyne Hubert. Scaffolding skeletons using spherical Voronoi diagrams: Feasibility, regularity and symmetry. *CAD Computer Aided Design*, 102:83–93, 2018.

[72] Faniry Razafindrazaka and Konrad Polthier. The 6-ring. In George W Hart and Reza Sarhangi, editors, *Proceedings of Bridges 2013: Mathematics, Music, Art, Architecture, Culture*, pages 279–286, Phoenix, Arizona, 2013. Tessellations Publishing.

[73] Matthew Berger, Andrea Tagliasacchi, Lee M Seversky, Pierre Alliez, Joshua a. Levine, Andrei Sharf, Claudio T. Silva, Andrea Tagliasacchi, Lee M Seversky, Claudio T. Silva, Joshua a. Levine, and Andrei Sharf. State of the Art in Surface Reconstruction from Point Clouds. *Proceedings of the Eurographics 2014, Eurographics STARs*, 1(1):161–185, 2014.

[74] Nina Amenta, Marshall Bern, and Manolis Kamvysselis. A new voronoi-based surface reconstruction algorithm. *Proceedings of the 25th Annual Conference on Computer Graphics and Interactive Techniques, SIGGRAPH 1998*, pages 415–422, 1998.

[75] Jean-daniel Boissonnat and Frédéric Cazals. Smooth surface reconstruction via natural neighbour interpolation of distance functions. *Computational Geometry*, 22(2002):185–203, 2004.

[76] Brian Curless and Marc Levoy. A volumetric method for building complex models from range images. In *Proceedings of the 23rd Annual Conference on Computer Graphics and Interactive Techniques*, SIGGRAPH '96, pages 303–312, New York, NY, USA, 1996. ACM.

[77] Christian Mercat. Discrete Riemann surfaces and the Ising model. *Communications in Mathematical Physics*, 218(1):177–216, 2001.

[78] William E. Lorensen and E. Cline Harvey. Marching cubes: A high resolution 3D surface construction algorithm. *New Jersey medicine : the journal of the Medical Society of New Jersey*, 91(12):848–850, 1994.

[79] Günther Greiner. Variational design and fairing of spline surfaces. *Comput. Graph. Forum*, 13:143–154, 08 1994.

[80] Wenping Wang, Helmut Pottmann, and Yang Liu. Fitting B-spline Curves to Point Clouds by Curvature-based Squared Distance Minimization. *ACM Trans. Graph.*, 25(2):214–238, April 2006.

[81] Jon Louis Bentley. Multidimensional Binary Search Trees Used for Associative Searching. *ACM student award*, 18(9):555–570, 1975.

[82] Fuentes Suárez Alvaro J. and Hubert Evelyne. Scaffolding skeletons using spherical voronoi diagrams. *Electronic Notes in Discrete Mathematics*, 62:45 – 50, 2017. LAGOS'17 - IX Latin and American Algorithms, Graphs and Optimization.

[83] Massimiliano Corsini, Paolo Cignoni, and Roberto Scopigno. Efficient and flexible sampling with blue noise properties of triangular meshes. *IEEE Transactions on Visualization and Computer Graphics*, 18(6):914–924, 2012.

[84] Vincent Manet. Méthode des Éléments Finis: vulgarisation des aspects mathématiques et illustrationde la méthode. Lecture, December 2018.

[85] Pierre Alliez, Giuliana Ucelli, Craig Gotsman, and Marco Attene. Recent advances in remeshing of surfaces. *Mathematics and Visualization*, (9783540332640):53–82, 2008.

[86] Morgan John and Scott Ridgway. A nodal basis for c^1 piecewise polynomials of degree $n \geqslant 5$. *Mathematics of Computation*, 29(131):736–740, 1975.

[87] Jörg M. Hahn. Geometric continuous patch complexes. *Computer Aided Geometric Design*, 6(1):55–67, 1989.

[88] Mario Kapl, Giancarlo Sangalli, and Thomas Takacs. An isogeometric C1 subspace on unstructured multi-patch planar domains. *Computer Aided Geometric Design*, 69:55–75, 2019.

[89] K. Karčiauskas and J. Peters. Guided spline surfaces. *Computer Aided Geometric Design*, 26(1):105–116, 2009.